UAB
Universitat Autònoma de Barcelona

From mechanisms to biomarkers: the role of tumor-infiltrating NK cells in anti-HER2 antibody responses in breast cancer

Sara Raquel Santana Hernández

From mechanisms to biomarkers: the role of tumor-infiltrating NK cells in anti-HER2 antibody responses in breast cancer

Sara Raquel Santana Hernández

Thesis Supervisor: Dr. Aura Muntasell Castellví

Laboratory of Natural Killer Cells in Cancer Immunotherapy

Hospital del Mar Research Institute

Doctoral Thesis - 2025

PhD Programme in Advanced Immunology

Department of Cell Biology, Physiology and Immunology

Faculty of Medicine

Universitat Autònoma de Barcelona

UAB Universitat Autònoma de Barcelona

Hospital del Mar Research Institute Barcelona

A Marta Ridaura

Regrets, I've had a few;
But then again, too few to mention.
I did what I had to do
And saw it through without exemption.
I planned each charted course;
Each careful step along the byway,
But more, much more than this,
I did it my way.

Yes, there were times, I'm sure you knew
When I bit off more than I could chew.
But through it all, when there was doubt,
I ate it up and spit it out.
I faced it all and I stood tall;
And did it my way.

Paul Anka

ACKNOWLEDGMENTS

Aunque mi etapa como doctoranda pueda parecer breve, este camino comenzó en realidad hace mucho tiempo. Concretamente, empezó hace once años, cuando me mudé a Barcelona para ser investigadora predoctoral en otro laboratorio de inmunología. Este viaje estuvo lleno de giros inesperados y, a veces, turbulentos, pero finalmente el avión ha aterrizado. He llegado a mi destino, la tesis, y ya es seguro desabrocharse los cinturones y salir ordenadamente del avión sin dejar atrás los objetos personales. He tenido la inmensa suerte de estar muy bien acompañada en el viaje, y es a todos esos acompañantes a quienes quiero dedicar estas palabras de gratitud.

A Aura Muntasell, por tantos años de respaldo y por la insistencia en que este libro se escribiera. Aprendimos juntas durante estos años, y tengo la certeza de que todo lo que hemos construido impulsará el futuro del laboratorio.

A Miguel López-Botet, por el apoyo y la acogida que me diste desde el primer día.

Al Instituto de Investigación Hospital del Mar, a la Universitat Pompeu Fabra y a la Universitat Autònoma de Barcelona por contribuir a mi formación y al desarrollo de mi carrera profesional.

A todos los voluntarios, tanto sanos como pacientes de cáncer, ya que sin su colaboración y generosidad sería totalmente imposible realizar este tipo de estudios.

A Joan Albanell, Clara Montagut y Sonia Servitja, por los proyectos en colaboración que hemos compartido.

A Ana Rovira, por la genuina fascinación y respeto que siempre mostraste por mi trabajo, y a Carlos Vilches, por tu disposición y el invaluable apoyo en las aventuras con las PCR.

A José Yélamos y a Coral Ampurdanés, por ser unos grandes compañeros de espacio y por el constante aprecio por mi trabajo.

A Ramón Gimeno, por nuestras conversaciones inspiradoras y por hablar bien de mí a todos los estudiantes que han pasado por aquí.

A todo el personal del PRBB: seguridad, recepciones, mantenimiento, compras, cocina... Y en especial a Mari y a Montse, por ser la alegría del edificio. Creo firmemente que el avance científico es imposible sin una red de apoyo como la que tenemos aquí, donde cada persona aporta de manera importante al desarrollo del conocimiento.

Al Servicio de Genómica UPF, por las explicaciones y la búsqueda de soluciones.

A Pau Berenguer, Júlia Perera y Marcel Costa por la ayuda con la bioinformática.

A Marina Junyent, Anna Hernández y, de forma especial, a Amparo Rico, por su ayuda con las muestras de pacientes de cáncer de mama HER2-positivo en este último año.

Al servicio de Citometría del PRBB, mi espacio seguro, donde he pasado la mayoría de las horas. Gracias por ayudarme a diseñar experimentos, a resolver dudas y a aprender cada día un poco más. Y, sobre todo, gracias por ser un gran equipo humano. A Óscar Fornas, por tener un servicio tecnológicamente puntero y un ambiente que no se conseguiría sin confianza, trabajo y buenas decisiones. A Eva, por las millones de explicaciones precisas y la disponibilidad para ayudarme. A Erika, por la cercanía, la risa compartida en los días buenos y el apoyo en los días difíciles. A Àlex, por arreglarme el citómetro una y otra vez, por impulsar mi uso del catalán y por ser un gran compañero de Open Day. A Sergi, por ser esa cara amable que siempre ve el lado bueno de las cosas.

Y a la última incorporación, a Nico, por todo. Por ser el mejor fichaje para mi equipo de vóley, por las horas de conversación en las que el tiempo vuela, por hacer las cosas con el corazón, por escucharme, por darme paz mental, por compartir tu vida conmigo. Tanto tiempo en este edificio valió la pena, tenía que esperar a que llegaras tú.

Sin lugar a dudas, doy GRACIAS, enormes y en mayúsculas, a la generación de Inmunología UPF 2014-2016. Llegar a una ciudad nueva, sola y perdida, y encontrar un recibimiento así, lo hizo todo más fácil. Once años después, tengo la suerte de que sigan siendo mis amigas.

Gracias a Maria Buxadé, por ser mi inspiración, por todos los consejos de persona sabia y por confiarme a Col y a Pruneta.

A Monika, por ser mi apoyo constante, mi refugio siempre que lo necesito y por traer a mi vida a Papi Juancho.

A Sonia, por ser mi FAMILIA en Barcelona. Para todo, cualquier cosa, siempre, estás tú. Incluso ahora que tienes tu propia familia con Carlos y Valentina, yo tengo el privilegio de ser la tía loca que entra por la puerta como si estuviera en su casa. Sin ti, este camino habría sido el triple de difícil y de aburrido.

A todos mis demás compañeros de mi primer "no-doctorado", con una mención especial a Arnau, por ser la prueba de que no hay un camino único. Y por presentarme a Marc Talló.

A Marc, porque este camino lo hemos recorrido juntos de principio a fin. Estoy muy orgullosa de ti, del estudiante que fuiste y del profesional en el que te has convertido. Gracias por tus consejos, por ser un amigo excepcional y el mejor compañero para presentar entregas de premios. Que lo intenten hacer mejor, a ver si les sale.

A todos mis compañeros de los laboratorios de Inmunidad e Infección y Terapia Molecular del Cáncer. Gracias por soportar mis quejas, por entenderme en mis días malos y, sobre todo, por quererme como soy. Aprendí tanto de ciencia como de la vida con ustedes.

A Gemma, por ser mi faro y mi brújula. Sin ti, esto habría sido 100% imposible.

A Marcelinho, por tu autenticidad y tu gran corazón. Y porque *aprendí que la paciencia es madre de la ciencia y aprendí que el estrés es fabricante de canas.*

A Andrea, por enseñarme a trabajar con rigurosidad y por cuidarme siempre con chocolates y dulces ricos.

A Aldi, por acogerme con los brazos abiertos en mis inicios como Pupupartner.

A Laura Soria, por ser mi apoyo moral y por enseñarme el "Nadie Sabe Nada", mi arma secreta para los análisis de citometría.

A Mariona, por ser mi bastón en la etapa en la que fuimos compañeras y por seguir aportándome sabiduría y calma mental. Gracias por ser valiente y priorizarte.

A Mireia, por ser mi compañera de todo y por, incluso en mis peores etapas, ser mi amiga. Gracias por seguir ahí y gracias por la ayuda artística para esta portada.

A Michelle, por ese corazón enorme que tiene dentro de un cuerpo de señora despistada, y por acompañarme a darnos un baño en un río con caimanes.

A Anna Rea, que me demostró que el trabajo duro y la amabilidad pueden ir de la mano. Gracias por escucharme en mis frecuentes colapsos, por la frittattina y por abrirme tu casa.

A Jesús, por las horas codo con codo, los stickers de cuñado, los audios de Andy y Lucas, por presentarme a Álex (claramente mi favorito), y por cuidar de Irene en mi ausencia.

A Javi, por convertirse en mí, pero con una sonrisa mucho más grande.

A Eli, Bennett, Edu, Berta, Eleonora, Amparo, Marina, Eloi, Hilde, Araceli, Carlos, Marta y Èlia, por las comidas en buena compañía y por ponerme al día de las cosas de las diferentes generaciones.

A Nura, por las reflexiones, por el debate y por tener la palabra amable y reconfortante que se necesita escuchar.

A Pol Picón, por ser mi compañero de cerebro y corazón.

A David Lligé, por los ratos de fantasía y los cafés patrocinados.

A Jordi Badia, por convertirme en una orgullosa Hufflepuff y ser mi DJ favorito en la sala de cultivos.

A Víctor Herrera, por tu cariño incondicional, y por el “Furbo”.

A mi supercompañera de piso durante la tesis, a Irene, por sufrir mis mañanas y mi desorden y por haber demostrado juntas que ser diferentes no impide quererse y sostenerse.

A mis equipos de vóley playa (DrinkORG, Sorra Fina y Furbo VC) y a mi compi de capitanía Xavi, por enseñarme a disfrutar de un deporte de equipo y por los momentos post-partido.

A todos los compañeros de este edificio, que ha sido prácticamente mi casa, con los que he compartido vivencias en las “beer sessions”, las terrazas, las “Bresh” (mención especial a Florencia por ser la mejor compañera de perreos) o el campo de fútbol.

Al personal de Magatzem 03, por seguir recibiéndome con los brazos abiertos.

A mis amigas canarias, Vero, Yany y Joshua, por ser mi vía de escape, mi conexión con mi yo más auténtico y el contrapunto necesario para no perder el foco.

A mis amigas andaluzas, Nuria, Ana, Blanca, Gema y Pablo, por ayudarme a crecer cuando éramos niñas, y por seguir compartiendo vivencias ahora de adultas. Verlas felices me hace feliz.

A la danza, por ser lo que me mueve por dentro y por la energía compartida con personas especiales que encontré por el camino.

A toda mi familia, pero especialmente a mis padres, por el superpoder que me dieron: la convicción de que puedo lograr cualquier cosa que me proponga. Gracias por dejarme ser, por respetar mis decisiones y por confiar en mí al 100%. Así todo es más fácil y se enfrenta con menos miedo, sabiendo que están siempre en mi equipo.

A mi princesa Marta, por ser la fuerza incontrolable de la naturaleza que llegó a mi vida para hacerla infinitamente mejor, para enseñarme las lecciones más valiosas, y para regalarme millones de momentos especiales que atesoro en el corazón. Vivirás para siempre en todos esos recuerdos de nuestras aventuras. Esta tesis va por ti. Estoy segura de que estás orgullosa de mí, Princess.

Y, finalmente, gracias a mí misma, a Sara Raquel. Gracias a mi cuerpo por soportar el estrés continuado y el exceso de azúcar. Gracias a mi cabeza, por seguir respondiendo después de tanto tiempo. Gracias a mi ser, a mi yo, por empeñarme en hacer siempre las cosas a mi manera. Y hacerlas.

Cierro esta etapa agradecida. El trayecto se terminó, ahora toca disfrutar del destino.

And you're gonna hear me roar.

ABSTRACT

HER2-positive breast cancer remains a clinical challenge despite major advances in targeted therapies, highlighting the need for more effective and personalized strategies. Natural killer (NK) cells are emerging as central players in antibody-based treatments by linking direct cytotoxicity with immune remodeling in the tumor microenvironment.

This thesis investigates the role of tumor-infiltrating NK (TI-NK) cells and associated chemokine pathways in shaping therapeutic responses. Transcriptomic and phenotypic analyses revealed that the presence of TI-NK cells correlates with activation of the CCL5/IFN-γ-CXCL9/10 axis, driving $CD8^+$ T-cell recruitment and amplifying antitumor immunity. Functional assays confirmed that antibody-dependent NK activation triggers IFN-γ–mediated CXCL9/10 secretion by tumor cells, establishing a feed-forward loop that promotes tumor control.

We identified three NK subsets in human breast tumors, defined by CD16 and CD103 expression. $CD16^+$ NK cells showed strong cytotoxicity, $CD16^-CD103^+$ cells displayed tissue-resident, pro-inflammatory features, and $CD16^-CD103^-$ cells exhibited regulatory properties. Anti-HER2 treatment induced a shift of $CD16^+$ toward $CD16^-CD103^+$ NK cells, linking tissue residency traits with therapeutic benefit in preclinical *in vivo* models.

From a biomarker perspective, an early and coordinated increase in serum CCL5 and CXCL9 emerged as a dynamic surrogate of TI-NK activation and favorable responses to neoadjuvant therapy with anti-HER2 antibodies. In addition, the CD16A-158V/F genotype predicted relapse risk in patients that do not achieve pathological complete response (pCR).

Overall, this work supports the role of NK cells as key effectors of anti-HER2 antibody activity, mechanistically linking their activation to chemokine-driven immune remodeling, and highlights actionable biomarkers to guide personalized immunotherapy in HER2-positive breast cancer.

RESUMEN

A pesar de los avances en terapias dirigidas, el cáncer de mama HER2-positivo aún presenta desafíos terapéuticos. En este contexto, los linfocitos natural killer (NK) emergen como actores clave en los tratamientos con anticuerpos, al combinar su citotoxicidad dirigida con la capacidad para remodelar el microambiente tumoral.

Esta tesis investiga el papel tanto de las NK infiltrantes en el tumor (TI-NK) como de las quimiocinas secretadas en la modulación de la respuesta a la terapia anti-HER2. Mediante análisis transcriptómicos y funcionales, demostramos que la infiltración de linfocitos NK se asocia con la activación del eje CCL5/IFN-γ-CXCL9/10, lo que favorece el reclutamiento de células T $CD8^+$ y amplifica la respuesta inmune antitumoral. La activación de los linfocitos NK mediada por anticuerpos desencadena la secreción de IFN-γ, lo que induce la producción de CXCL9/10 en el tumor, creando un circuito de retroalimentación positiva que promueve el control tumoral.

Además, identificamos tres subpoblaciones de TI-NK en tumores de mama, definidas por la expresión de CD16 y CD103: las células NK $CD16^+$, con perfil citotóxico; las células $CD16^-CD103^+$, proinflamatorias y residentes en tejido; y la subpoblación $CD16^-CD103^-$, con propiedades reguladoras. El tratamiento con anticuerpos anti-HER2 induce la conversión de células NK $CD16^+$ a $CD16^-CD103^+$, lo que vincula la residencia tisular con una respuesta inmune antitumoral eficaz en modelos *in vivo* preclínicos.

Por otro lado, identificamos el incremento temprano y coordinado de CCL5 y CXCL9 en suero como un biomarcador dinámico que indica activación de las TI-NK y se asocia a una mejor respuesta a la terapia con anticuerpos anti-HER2. Además, evidenciamos el valor del genotipo CD16A-158V/F para predecir el riesgo de recaída en pacientes que no alcanzan una respuesta patológica completa (pCR).

En resumen, este trabajo confirma el papel de las NK como efectoras claves en la terapia anti-HER2, vinculando su activación a una remodelación inmunológica dependiente de quimiocinas, y destaca biomarcadores clave para la inmunoterapia personalizada.

RESUM

Malgrat els avenços en les teràpies dirigides, el càncer de mama HER2-positiu continua sent un desafiament clínic. En aquest context, els limfòcits natural killer (NK) emergeixen com a actors clau en els tractaments amb anticossos, ja que combinen la seva citotoxicitat dirigida amb la capacitat de remodelar el microambient tumoral.

Aquesta tesi investiga el paper tant de les cèl·lules NK infiltrants en el tumor (TI-NK) com de les quimiocines secretades en la modulació de la resposta a la teràpia anti-HER2. Mitjançant anàlisis transcriptòmiques i funcionals, demostrem que la infiltració de cèl·lules NK s'associa amb l'activació de l'eix CCL5/IFN-γ-CXCL9/10, el qual afavoreix el reclutament de cèl·lules T $CD8^+$ i amplifica la immunitat antitumoral. L'activació de les cèl·lules NK mediada per anticossos desencadena la secreció d'IFN-γ, que indueix la producció de CXCL9/10 en el tumor, creant un circuit de retroalimentació positiva que promou el control tumoral.

A més, identifiquem tres subpoblacions de cèl·lules NK en tumors de mama, definides per l'expressió de CD16 i CD103. Les cèl·lules NK $CD16^+$ tenen un perfil citotòxic; les cèl·lules $CD16^-CD103^+$ són proinflamatòries i residents en el teixit; i la subpoblació de NK $CD16^-CD103^-$ té propietats reguladores. El tractament amb anticossos anti-HER2 indueix la conversió de les cèl·lules $CD16^+$ a $CD16^-CD103^+$, vinculant la residència tissular amb una resposta immune antitumoral eficaç en models *in vivo* preclínics.

També identifiquem l'increment temprà i coordinat dels nivells de CCL5 i CXCL9 en sèrum com un biomarcador dinàmic que indica l'activació de les cèl·lules TI-NK i s'associa amb una millor resposta a la teràpia neoadjuvant amb anticossos anti-HER2. A més, evidenciem el valor del genotip CD16A-158V/F per predir el risc de recaiguda en pacients que no assoleixen una resposta patològica completa (pCR).

En resum, aquest treball recolza el rol de les cèl·lules NK com efectores claus per a l'activitat dels anticossos anti-HER2, vinculant la seva activació a una remodelació immunològica dependent de quimiocines, i destaca biomarcadors d'utilitat clínica per guiar la immunoteràpia personalitzada en el càncer de mama HER2-positiu.

TABLE OF CONTENTS

INTRODUCTION

1. Cellular innate immunity: lymphocytes

1.1 The discovery of innate lymphocytes

Innate immunity represents the evolutionarily conserved, germline-encoded arm of the immune system, providing immediate, non-antigen-specific defense against invading pathogens. While myeloid cells, including dendritic cells, macrophages, and granulocytes, are central players in innate immunity, certain lymphocyte populations also contribute significantly to this first line of defense against infected and transformed cells (1).

Natural killer (NK) cells, discovered in 1975, were the first innate lymphocytes identified. Classically, NK cells are defined as large granular lymphocytes, lacking T cell and B cell receptor complexes, endowed with cytotoxic reactivity against virally infected and transformed cells (2-4).

Twenty-two years later, lymphoid tissue inducer (LTi) cells, critical for the development and organization of secondary lymphoid organs were described (5). Subsequently, during the late 2000s and 2010s, further research revealed additional innate lymphoid cell (ILC) populations (6-11), with lower cytotoxic capacity than NK cells, but exhibiting characteristics such as cytokine production and tissue residency. These innate lymphoid cells were found mainly in the gut and categorized as ILC1, ILC2, and ILC3 (12,13). In mice, ILC are recognized as critical regulators of immune responses, playing key roles in host defense, tissue homeostasis, and inflammatory diseases (13,14). However, their tissue-resident nature presents challenges for human studies, requiring further investigation to clarify their precise functions and clinical relevance (15-17).

1.2 NK cell biology

NK cells provide rapid and efficient responses against infected and cancerous cells. In humans, NK cells are identified by the absence of the T cell marker CD3 and the expression of the neural cell adhesion molecule 1 (NCAM-1 or CD56) (18). NK cells are primarily found in circulation and make up 5–15% of the total circulating lymphocytes. Specific populations also reside in key organs such as the lungs, liver,

and uterus (19).

NK cells originate in the bone marrow from $CD34^+$ hematopoietic stem cells (HSC), which differentiate into common lymphoid progenitors (CLP), and subsequently give rise to common innate lymphoid progenitors (CILP) and NK cell precursors (NKP). This process is regulated by transcription factors including TOX, NFIL3, ID2, and ETS1. Final NK cell maturation is driven by T-bet and EOMES (13,20,21).

Human NK cells are classified into two main subsets based on their CD56 and CD16 expression: $CD56^{bright}$ and $CD56^{dim}$ NK cells. $CD56^{dim}$ NK cells, representing 90% of circulating NK cells, are characterized by the expression of CD16 (FcγRIIIA), along with cytotoxic granules containing perforin and granzymes. They possess a high cytotoxic capacity upon recognizing target cells (13) and express CXCR1, CXCR2, and CX3CR1, enabling their migration to inflamed tissues (22,23). $CD56^{bright}$ NK cells exhibit high CD56 and low to no CD16 expression, and produce cytokines, like IFN-γ, TNF-α and GM-CSF, in response to soluble factors such as IL-12, IL-15 and IL-18 (24). They express CCR7, CCR2, and the selectin CD62L, which facilitate their homing to lymph nodes (22,23).

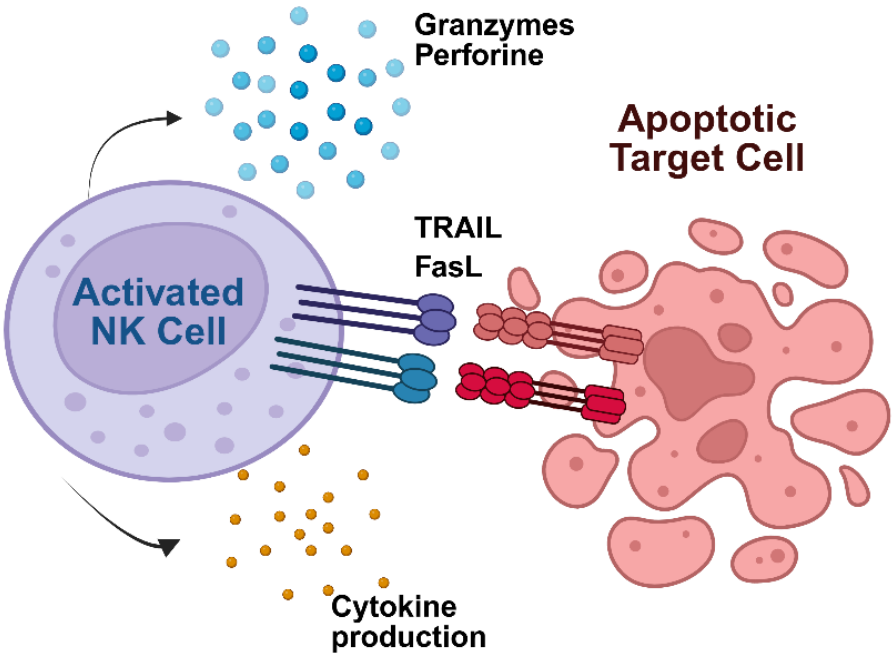

Figure 1. Effector mechanisms of NK cells. NK cell activation triggers the secretion of pre-formed granules containing granzymes and perforin, the expression of death-receptor ligands such as TRAIL or Fas Ligand (FasL), and the production of inflammatory cytokines and chemokines such as IFN-γ, TNF and CCL5. Created in https://BioRender.com.

Upon target cell recognition, NK cell activation triggers the polarized release of pre-formed cytotoxic granules. Perforin insertion into the target cell membrane facilitates granzyme entry and the initiation of a cascade of events leading to apoptosis. Additionally, activated NK cells express ligands for death receptors of the TNF receptor superfamily (TNFRSF), such as TNF-α, TRAIL, and Fas ligand, which also induce target cell death through receptor signaling (25) (Fig. 1).

1.3 Regulation of NK cell activation

NK cell activation is regulated by a balance between activating and inhibitory signals, triggered by a diverse array of germline-encoded receptors. These receptors enable NK cells to recognize specific ligands on both healthy and unhealthy surrounding cells. In a healthy state, NK cell activity is generally suppressed by the interaction of inhibitory receptors with self-major histocompatibility complex class I (MHC-I) molecules expressed on target cells (26,27). Activating receptors mostly recognize stress-induced self-molecules lowly expressed in healthy, non-stressed cells. Cellular transformation or infection are often accompanied by the downregulation of MHC-I molecules or the expression of stress-induced ligands, disrupting this inhibitory balance towards NK cell activation (28,29).

In NK cells, inhibitory signaling is typically mediated by immunoreceptor tyrosine-based inhibitory motifs (ITIM) encoded in the receptor's cytoplasmic domain. Upon ligand binding, ITIM phosphorylation facilitates the recruitment of phosphatases, which prevent downstream signaling cascades initiated by activating receptors (30). Activating receptors on NK cells lack signalling motifs and associate with adaptor molecules (i.e. CD3ζ or DAP12) to transduce their signals (28). Most of these adaptor molecules have immunoreceptor tyrosine-based activation motifs (ITAMs) in their cytoplasmic domains which upon phosphorylation by Src-family kinases, enable the recruitment and activation of Syk-family kinases, thereby regulating downstream activation signaling cascades (31,32).

1.3.1 Inhibitory receptors

NK cells constitutively express inhibitory receptors recognizing both MHC-I and non-MHC ligands (28) (Fig. 2).

MHC-I-specific receptor families include Killer-cell immunoglobulin-like receptor (KIR) family, CD94/NKG2A and LILRB1. The KIR family includes inhibitory and activating members which recognize specific epitopes shared by groups of MHC class I alleles. The KIR family is genetically diverse, varying in gene content and allelic polymorphism. It comprises 17 members: 8 inhibitory, 7 activating, and 2 non-functional pseudogenes. Human KIR haplotypes are categorized into two main groups: A and B. Haplotype A is characterized by a stable set of genes that predominantly create inhibitory receptors. In contrast, haplotype B is highly variable and includes more genes that produce activating receptors (33). In addition, KIR expression along NK cell maturation is stochastic with clonal distribution, generating diverse NK cell populations (34-36).

The inhibitory receptor CD94:NKG2A is a C-type lectin-like heterodimer that recognizes HLA-E, a non-classical MHC class I molecule presenting peptides from other MHC-I molecule leader sequences (37-39). CD94/NKG2A is one of the first inhibitory receptors expressed early along NK cell maturation. Finally, Leukocyte Immunoglobulin-Like Receptor B1 (LILRB1), or ILT2, is another MHC-I-specific inhibitory receptor on NK cells, also expressed by B and T lymphocytes and myeloid cells. LILRB1 interacts with a broad range of MHC-I molecules. In NK cells, LILRB1 is expressed across mature NK cell subsets, in addition to adaptive NK cells generated during viral infections (40,41).

In addition to prevent NK cell autoreactivity, MHC-I specific inhibitory receptors (NKG2A and KIRs) are involved in NK cell ‘education’ or ‘licensing’. During development, NK cell recognition of self MHC-I ligands results in their functional maturation while NK cell clones expressing inhibitory KIR specific for non-self MHC-I remain in a hypofunctional state (30,42,43). The inter-individual variability in the MHC and KIR genotypes determines KIR-KIR ligand availability, leading to distinct educated NK cell repertoires (44).

Beyond MHC-I-specific inhibition, several non-MHC-specific inhibitory receptors contribute to NK cell regulation. TIGIT and CD96, both members of the PVR-like protein family, are also inhibitory receptors with constitutive expression. TIGIT primarily binds to CD155 (PVR) and with lower affinity to nectins 2, 3, and 4, while CD96 ligands include CD155 and nectin-1. CD155 is important for cell adhesion and polarization and is found on antigen-presenting cells and certain tumor cells (45-47).

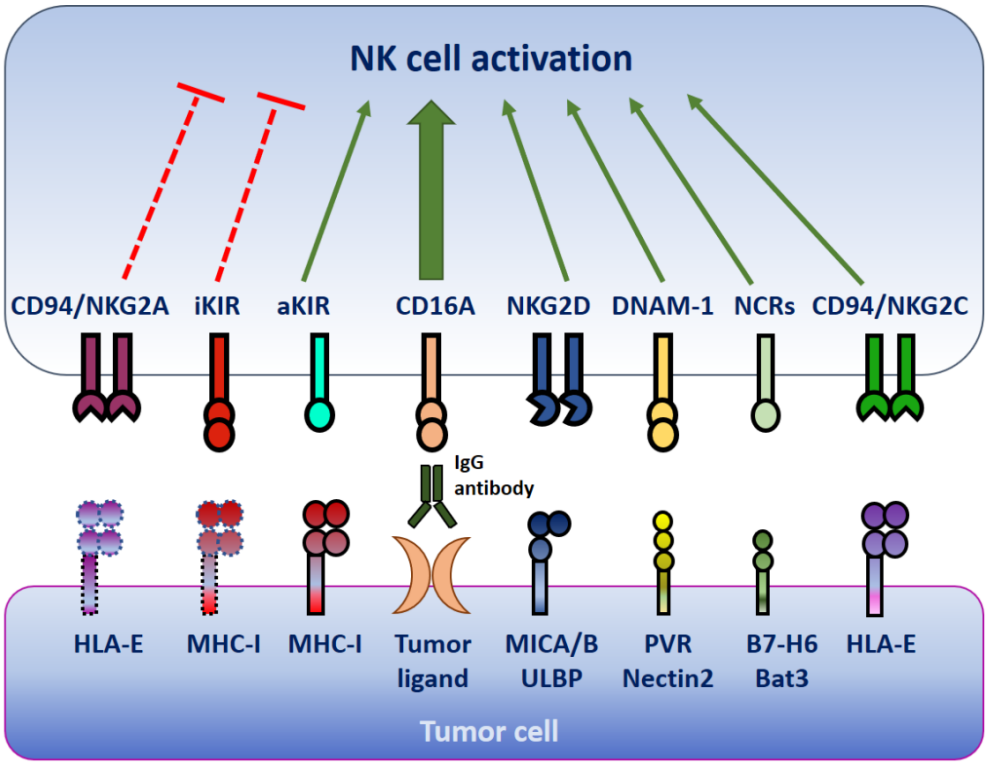

Figure 2. Main inhibitory and activating receptors on NK cells and their ligands on target cells. Green arrows label activating receptors, and red lines identify inhibitory ones. Adapted from Muntasell, 2017 (48).

Finally, in addition to constitutively expressed inhibitory receptors, NK cells can acquire additional inhibitory receptors upon activation and along maturation, including PD-1, Tim-3, CEACAM-1, KLRG1 and LAG3 which further regulate their activation threshold (49-53).

Several NK cell inhibitory receptors have an activating counterpart that shares a common ligand. In all cases, inhibitory receptors exhibit higher affinity for these shared ligands ensuring NK cell tolerance. This competitive dynamic is exemplified

by receptor systems such as inhibitory and activating KIR (54), the inhibitory CD94/NKG2A and the activating CD94/NKG2C receptor pair (37), and the inhibitory TIGIT and CD96 receptors competing with the activating receptor DNAM-1 (55).

1.3.2 Activating receptors

Most NK cell activating receptors with constitutive expression recognize stress-induced self-ligands (Fig. 2). The natural cytotoxicity receptor (NCR) family includes NKp30, NKp44 and NKp46, immunoglobulin-like type I transmembrane molecules. NKp30 and NKp46 signal through CD3ζ and/or FcεRI-γ chains, while NKp44 signals through DAP12 (56-58). Ligands for NCR include self-proteins expressed in infected or tumor cells. For example, the self-molecules B7-H6 and BAT3 are recognized by NKp30, the ecto-calreticulin expressed in ER-stressed cells is recognized by NKp46, and PCNA is the NKp44 ligand in tumors. In addition to stress-induced self-molecules, both NKp46 and NKp44 can also recognize influenza-virus derived hemagglutinin (59,60).

NKG2D, a homodimer of the C type lectin-like NKG2 receptor family, signals through the DAP10 adaptor, which uses a phosphatidylinositol 3-kinase (PI3K)- binding motif Tyr-Ile-Asn-Met (YINM) for triggering the activating signaling cascade. NKG2D ligands include MICA, MICB, and the ULBP1-6 family, and are often upregulated on stressed cells (61,62).

CD16A (FcγRIIIA) is a low-affinity receptor for the Fc region of IgG1 and IgG3 and the only receptor capable of independently triggering NK cell activation (63,64). It signals through CD3ζ or FcεRI-γ adaptors, triggering NK cell mediated cytotoxicity against antibody-coated target cells, a mechanism named antibody-dependent cellular cytotoxicity (ADCC) (65). Upon activation, CD16 is cleaved by metalloproteases, such as ADAM-17, facilitating NK cell detachment from target cells and limiting bystander damage (66,67).

A single nucleotide substitution within *FCGR3A* gene results in an allelic variation in the amino acid 158 (phenylalanine-F or valine-V) of the CD16A receptor IgG binding domain. Individuals with the V/V genotype exhibit higher affinity for IgG1 compared to those with the F/F genotype, while F/V heterozygotes show intermediate binding

levels (68) (Fig. 3).

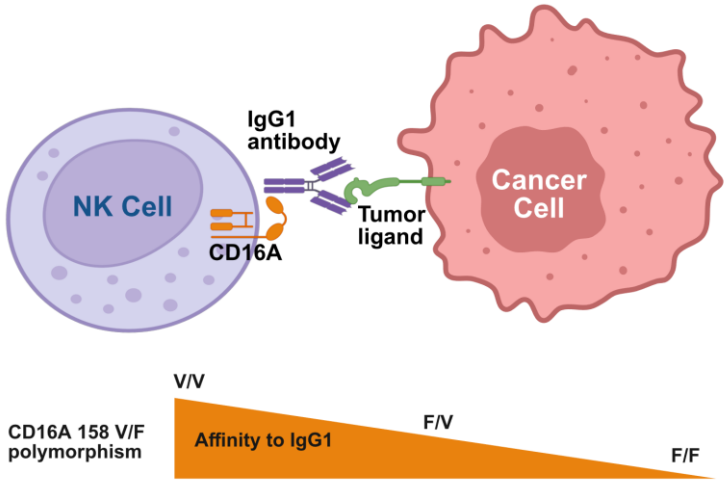

Figure 3. NK cell-mediated antibody-dependent cellular cytotoxicity (ADCC). Recognition of the Fc fraction of an IgG antibody bound to a transformed cell through CD16 receptor in NK cells. The CD16A-158 V/F polymorphism dictates the affinity of CD16 for the Fc regions of IgG1 antibodies; the VV genotype confers the highest affinity, whereas the FF genotype results in the lowest affinity. Created in https://BioRender.com.

Finally, there are receptors, like DNAM-1 or 2B4, that function as co-stimulators in NK cells, amplifying the activating signalling induced by NKG2D or NCR. DNAM-1 recognizes nectins and CD155 (69). 2B4 (CD244) is a co-stimulatory receptor that recognizes CD48, upregulated on virally infected cells (70).

1.4 Diversity of the human NK cell repertoire

The human NK cell compartment is characterized by a complex landscape of subpopulations, defined by distinct differentiation stages and unique combinations of NK receptors. This significant inter-individual variability is a consequence of both genetic determinants, such as variations in KIR and MHC-I, and environmental influences, notably human cytomegalovirus (HCMV) infection and biological aging (71,72).

$CD56^{bright}$ NK cells generally express NKG2A, and do not express KIR, whereas $CD56^{dim}$ NK cells are characterized by the acquisition of KIR expression and the loss of NKG2A. Acquisition of KIR receptors is stochastic and with clonal distribution, driving NK cell repertoire diversification (73,74). Late-stage differentiation of $CD56^{dim}$ NK cells involves the acquisition of LILRB1 and CD57.

CD57 is a carbohydrate modification related to biological age, which is associated with NK cells showing strong cytolytic activity and reduced proliferation, often considered as a marker of terminally differentiated NK cells (75-77).

Among environmental factors, HCMV infection can reshape the NK cell repertoire in some individuals, leading to the persistent expansion of adaptive NK cells. These cells are defined by high CD94/NKG2C expression in the absence of CD94/NKG2A, exhibit an oligoclonal KIR repertoire specific for self HLA-C, reduced expression of natural cytotoxicity receptors (NCR), and increased proportions of LILRB1 and CD57 expressing cells (72,73,76-79). Functionally, these adaptive NK cells are characterized by enhanced production of TNF-α and IFN-γ, elevated levels of granzyme B, and potent ADCC responses (80,81).

1.5. Regulation of NK cell function by cytokines

NK cell activity and maturation can also be regulated by cytokines present in the microenvironment, such as IL-2, IL-12, IL-15, IL-18 and type I interferons, among others (82). IL-15 is essential for NK maturation, guiding the differentiation of CLP into NK cells (21). IL-2 is important for NK cell proliferation and the production of cytolytic molecules. In combination with IL-15, they can stimulate the production of the pro-inflammatory cytokine IFN-γ (21,83). IFN-γ production can be also induced by IL-12 and IL-18 through STAT4 signaling (84) or by IFN-I through STAT1/2 (85). IL-21 and IL-2 act together to boost the levels of NKG2A, CD25, CD86, CD69, perforin, and granzyme B, which increases their cytotoxic potential (86).

On the other hand, inhibitory cytokines, such as IL-6, IL-10 or TGF-β, directly or indirectly impair NK cell function and proliferation (82, 87, 88).

1.6 Innate lymphoid cells (ILCs)

Tissue-resident ILC derive from CLP and are characterized by their rapid production of effector cytokines. The transcription factor PLZF is essential for the determination of an ILC progenitor (89). The distribution of ILC spans lymphoid and non-lymphoid tissues, with a significant accumulation at barrier surfaces, notably the mucosal

layers of the gastrointestinal and pulmonary tracts (13).

Based on their cytokine profiles, ILC are classified into three major groups: ILC1, ILC2 and ILC3 (Fig. 4). ILC1 are involved in the defense against intracellular pathogens and tumors. They are characterized by weak cytotoxicity, robust production of interferon-gamma (IFN-γ) in response to IL-2, IL-12, IL-18, and IL-21, and expression of the transcription factors T-bet, NFIL3 and RUNX3 (12,13). In contrast to NK cells, ILC1 development is independent of EOMES, although some ILC1 subsets may express it (90). IL-15 is a key cytokine regulating the function and IFN-γ production of ILC1 cells (12).

ILC2 are involved in the defense against large extracellular parasites and mediating allergic responses. They are characterized by the production of type 2 cytokines, including IL-4, IL-5 and IL-13, in response to epithelial cell-derived cytokines, such as IL-25 and IL-33. ILC2s are defined by the expression of the transcription factors RORα, Bcl11b, GATA3, and GFI1 and the characteristic surface markers CRTH2 and CD161 (12,13).

Finally, ILC3 cells play a crucial role in immunity against extracellular bacteria and fungi, particularly at mucosal surfaces. They are characterized by the production of IL-17 and IL-22, which promote neutrophil recruitment, the production of antimicrobial peptides, and the maintenance of intestinal homeostasis (91,92). ILC3 express the transcription factors RORγt, AHR, and ID2 (13). Phenotypic characterization of ILC3 is still being refined and depends on the tissue of origin. A proposed consensus for human ILC3s involves the presence of CD117 and CD127, along with the absence of CRTH2 (93).

As many cell types in the immune system, ILC display high functional plasticity with environmental signals affecting both their phenotypic and functional features (94,95). TGF-β triggers NK cell to ILC1 differentiation (96). IL-12 and IL-15 stimulation drives ILC3 to NK cell conversion in human tonsils (97), whereas IL-2 and IL-12 stimulation convert ILC3 into ILC1, upregulating T-bet and increasing IFN-γ production (98).

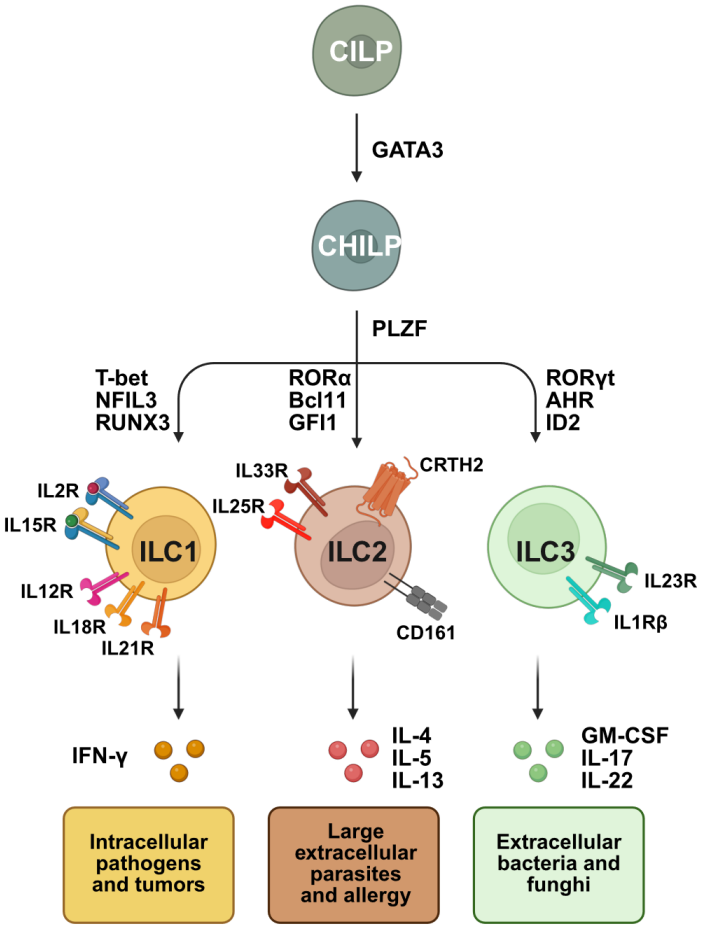

Figure 4. Innate lymphoid cell subtypes and their functions. Classification of ILC based on transcription factors, lineage receptors, cytokines produced, and functions. Created in https://BioRender.com.

This adaptability allows the ILC compartment to dynamically adjust its composition and effector functions in response to environmental cues. Further research is needed to fully understand the dynamics of ILC and NK plasticity, especially in humans.

1.7 NK/ILC cells in cancer

NK cell importance in antitumor activity has been related to their ability to eliminate tumor cells that evade $CD8^+$ T cell-mediated killing due to reduced or absent MHC-I expression. The primary activating receptors involved in tumor cell recognition by

NK cells include NCR, NKG2D, and the costimulatory molecule DNAM-1, as well as CD16, which enables the recognition of tumor cells opsonized by tumor antigen-specific antibodies (48, 60).

However, tumor can evolve several strategies to escape NK cell-mediated recognition (99). The tumor microenvironment (TME) frequently contains immunosuppressive factors such as TGF-β, indoleamine 2,3 dioxygenase (IDO) or prostaglandins, secreted by tumor cells, tumor-associated fibroblasts and several regulatory immune cells (tumor-associated macrophages, myeloid-derived suppressor cells, regulatory T cells) that suppress NK cell activation and cytotoxicity (100-102). In addition, tumor hypoxia and metabolic stress also preclude NK cell function (103). Further mechanisms of NK cell evasion include the up-regulation of ligands for inhibitory NK cell receptors (i.e. HLA-E, CD155 and CD112) (104,105) or the shedding of ligands for activating receptors (i.e. MICA/B and B7-H6) which act as decoy molecules (106,107).

Besides cytotoxicity, NK cells possess the ability to remodel the tumor microenvironment and amplify immune responses (108). TI-NK cells can produce chemokines and cytokines, like CCL5, XCL1 and XCL2, which facilitate infiltration of CD8+ T cells and cDC1, as has been observed in human and mouse melanoma and breast cancer models (109,110). Also, NK cell presence within the tumor microenvironment (TME) correlates with improved clinical outcomes across various cancers (111-113). The cooperation of different cytokines and chemokines, such as IFN-γ and CXCR3 ligands, guides the infiltration of NK cells (and T cells) into solid tumors (114,115).

The role of the other ILC subpopulations in tumors remains as an evolving area of research, with both tumor protecting and promoting roles described depending on the cancer model and the organ affected (116-123). The significant plasticity of ILC subsets, together with the lack of unique markers allowing ILC monitorization, introduces complexity in data interpretation.

2. HER2-positive breast cancer

Breast cancer is the most frequent cancer and the leading cause of cancer-related mortality among women worldwide, with 2.3 million new cases annually (124). This heterogeneous disease is classified into distinct subtypes based on the expression of estrogen receptor (ER), progesterone receptor (PR), and human epidermal growth factor receptor 2 (HER2). The resulting subtypes are luminal (ER/PR+ HER2-), HER2-positive (HER2+), and triple-negative breast cancer (TNBC, ER- PR- HER2-). Luminal tumors are further divided into luminal A (low Ki67 expression, <20%) and luminal B (high Ki67 expression, ≥20%) while HER2+ cancers are categorized as HER2+ luminal B (ER and/or PR positive) or HER2+ non-luminal (ER and PR negative) (125,126).

HER2 overexpression occurs in around 20% of breast tumors (127), leading to the constitutive activation of its tyrosine kinase activity, increased cell proliferation and survival (128). In the absence of anti-HER2 therapy, HER2-positive tumors are characterized by aggressive behavior and decreased survival in comparison with luminal tumors (127,129).

2.1 Current therapies in HER2-positive breast cancer

The standard first-line treatment for primary HER2-positive breast cancer depends on tumor size, nodal involvement, and disease stage. For localized tumors (≤20 mm diameter) without lymph node metastasis, surgical resection and radiotherapy are the conventional approaches. In the rest of the cases, patients typically undergo a neoadjuvant treatment, including chemotherapy (commonly docetaxel) and the HER2-targeted antibodies trastuzumab and pertuzumab, prior to surgery (130). Trastuzumab and pertuzumab are humanized IgG1 monoclonal antibodies that target distinct extracellular domains of the HER2 receptor, preventing HER2 dimerization and disrupting downstream signaling (131).

Upon neoadjuvant therapy, the absence of invasive cancer cells in the primary tumor area or the surrounding lymph nodes, named pathological complete response (pCR), is a significant indicator of treatment success and improved long-term

prognosis (132). For those patients that achieve pCR, post-surgery adjuvant treatment with anti-HER2 antibodies is recommended for one year, whereas those showing residual disease, receive the antibody-drug conjugate (ADC) trastuzumab-emtansine (T-DM1) as adjuvant treatment (130,133).

In metastatic HER2-positive breast cancer, the combination of trastuzumab, pertuzumab, and chemotherapy remains the standard first-line treatment, irrespective of hormone receptor (HR) status (134). This dual therapy is supported by the positive results from the CLEOPATRA and the APHINITY trials (135). Second-line therapy often involves trastuzumab-deruxtecan (T-Dxd), supported by findings from the DESTINY-Breast03 trial (136).

Beyond anti-HER2 antibodies, tyrosine kinase inhibitors have also been approved as second-line treatment in advanced disease. Lapatinib is used for advanced/metastatic HER2-positive breast cancer, significantly extending progression-free survival when combined with aromatase inhibitors. Tucatinib is combined with trastuzumab and capecitabine for advanced HER2-positive breast cancer. Lastly, neratinib serves as an intensive adjuvant therapy for high-risk, early-stage HER2-positive patients post-surgery (135,137).

Even with major treatment breakthroughs, up to 25% of patients diagnosed with early-stage HER2-positive breast cancer will relapse (138). This underscores the urgent need to enhance the efficacy of current treatments or developing novel and better therapeutic approaches.

2.2 Role of NK cells in HER2-positive breast cancer

Tumor-infiltrating lymphocytes (TILs) have been identified as indicators of good prognosis in early HER2-positive breast cancer (139). Primary HER2-positive breast tumors are usually more infiltrated by $CD8^+$ and $CD4^+$ T cells than metastatic lesions, which are essentially immune deserts (140,141). Furthermore, for trastuzumab-treated metastatic patients, the presence of tumor-infiltrating CD8+ T cells predicted a survival benefit in both early and advanced disease (139).

Beyond T cells, NK cells have also been identified as markers of good prognosis in

breast cancer (142). All anti-HER2 antibodies are immunoglobulins of the IgG1 subclass. In addition to inhibiting HER2 signaling, trastuzumab and pertuzumab can induce antibody-dependent cell-mediated cytotoxicity (ADCC) upon interacting with tumor-infiltrating CD16+ NK cells (143-146). Even in metastatic patients, those who respond to trastuzumab treatment show significantly higher NK cell activity and ADCC function compared to non-responders (147).

Previous work from our laboratory investigated the predictive and prognostic value of TI-NK cells in HER2-positive breast cancer patients treated with neoadjuvant anti-HER2 antibodies, finding that TI-NK cells were associated with the achievement of pCR and disease-free survival (DFS), independently of other clinicopathologic factors (112). Furthermore, studies on circulating NK cells showed an association between high $CD57^+$ NK cell numbers and resistance to neoadjuvant treatment with HER2-specific antibodies. This inverse correlation between peripheral blood $CD57^+$ NK cell counts and pathological complete response (pCR) was independent of age, conventional clinicopathologic factors, and the CD16A-158F/V genotype (148).

The CD16A-158V/F dimorphism has also been shown to influence the response to anti-HER2 antibodies in breast cancer patients (148). An initial retrospective study suggested an association between the high-affinity V/V genotype and enhanced trastuzumab responses in the metastatic setting (149). However, subsequent studies in larger cohorts from clinical trials evaluating trastuzumab in adjuvant setting showed conflicting results concerning the impact of this genetic variation on relapse and survival (150,151). Interestingly, margetuximab, an anti-HER2 antibody engineered for increased affinity to CD16A receptor, demonstrated clinical benefit as compared to trastuzumab in patients with F/F or F/V genotypes in the SOPHIA trial, supporting its FDA approval as a third-line treatment for metastatic breast cancer (152). Further investigation is warranted to fully elucidate the effect of the CD16A-158V/F polymorphism on the efficacy of anti-HER2 therapies.

Despite the efficacy of anti-HER2 antibodies, drug resistance frequently occurs in HER2-positive breast cancer leading to disease progression or relapse. The loss of HER2 expression (or the proliferation of HER2 negative cell clones), the appearance of HER2 mutations, or the expression of HLA-G in breast cancer cells are among several of the mechanisms described (153,154). Furthermore, tyrosine kinase

inhibitors (TKI) like lapatinib, afatinib, and neratinib can differentially alter tumor cell phenotype, impacting NK cell-mediated ADCC response to co-administered antibody therapies (155).

2.3 NK cell-based immunotherapy in HER2-positive breast cancer

Current strategies for developing NK cell-based antitumor therapies generally fit into two broad categories: potentiating the endogenous NK cell response of the patient or adoptively transfer allogeneic NK cells designed to evade host MHC-I inhibition (48,143,156). These approaches encompass everything from antibody-based therapies, which either block inhibitory checkpoint receptors or stimulate activating ones, to adoptive NK cell transfer, with genetic engineering as an optional component. Among multiple options in preclinical and clinical development, those being developed for HER2-positive breast cancer treatment will be reviewed in the following paragraphs (Fig. 5).

Monalizumab is a humanized antibody blocking the inhibitory receptor NKG2A on NK and T cells that has demonstrated a synergistic effect when combined with anti-PD1/PD-L1 antibodies, helping to reactivate the anti-tumor responses of $CD8^+$ T cells (104,157). Furthermore, it has also shown promising results in preclinical models and in a phase II clinical trial (158) against head and neck squamous cell carcinoma (HNSCC) in combination with cetuximab (anti-EGFR) (159). However, it has not improved survival in metastatic/recurrent HNSCC also combined with cetuximab (160). In metastatic HER2-positive breast cancer, the phase II clinical trial MIMOSA tested the combination of trastuzumab and monalizumab, with good safety profile despite no clinical responses were observed (161).

TIGIT blockade shows promise results in preclinical cancer models, though human trials are pending. TIGIT blockade enhances NK cell anti-tumor responses in solid tumors and boosts NK cell-mediated ADCC with trastuzumab in HER2-positive breast cancer *in vitro*, increasing IFN-γ production and degranulation (162,163).

Besides, agonist antibodies for NK cell (and T cell) co-stimulatory receptors are emerging. Stimulation of CD137, a surface TNFR family member, improves NK cell

cytotoxicity and cytokine secretion in the context of TGFβ immunosuppression. The combination of antibodies such as trastuzumab with CD137 agonists (like urelumab) promotes the activation, persistence, and antitumor functions of NK cells, increasing the secretion of IFNγ and CCL5 in preclinical models, and thereby potentially improving immunotherapy efficacy in HER2-positive tumors (164). A Phase I trial is evaluating utomilumab (anti-CD137) with trastuzumab or T-DM1 in HER2-positive advanced breast cancer (165).

Bi- and tri-specific killer cell engagers (BiKEs and TriKEs) are also being explored for boosting NK cell anti-tumor function (166,167). These engineered antibodies bridge one or two activating receptors on NK cells with antigens in the tumor cell. In breast cancer, bi/trispecific antibodies, which are designed to target HER2 and either CD16 or NKG2D at the same time, have been successfully evaluated in preclinical *in vitro* models (166). Furthermore, a triKE targeting HER2 and two more antigens (not public infomation), TriNKet DF1001, is being evaluated in patients with advanced disease with HER2 overexpressing tumors in a phase I/II clinical trial (168).

Allogeneic NK cells do not trigger graft-versus-host disease but contribute to graft-versus-leukemia effects (169,170). Adoptive transfer of NK cells, particularly allogeneic NK cells with KIR-MHC mismatch to leverage alloreactivity, represents a significant avenue for NK cell-based cancer therapy (171,172). Their safety when transferred across MHC barriers offers the potential for "off-the-shelf" therapeutic cellular strategies (173). In line with this, several phase I clinical trials for patients with HER2-positive metastatic/recurrent breast cancer have been proposed to test the infusion of allogenic NK cells in order to enhance response to treatment with anti-HER2 antibodies (174,175,176). However, a common limitation for NK cell products is their inefficient homing and functional inactivation in solid tumors (173).

Numerous strategies are being explored to boost the effectiveness of adoptively transferred NK cells against solid tumors, including genetic modifications, and combining them with agents such as checkpoint inhibitors, cytokines, and tumor-targeted antibodies (177). Genetic modifications of NK cells prior to infusion represent a promising strategy to overcome limitations and enhance anti-tumor efficacy. Chimeric antigen receptor (CAR)-engineered NK cells (CAR-NK), modified

to express a target-specific receptor, have emerged as a compelling alternative, potentially enabling them to evade immunosuppressive cells within the TME (178). HER2-specific CAR-NK cells have demonstrated efficacy in preclinical models of breast cancer (178-180). However, HER2 is also expressed in healthy tissues and these therapies could have adverse side effects. Tumor-specific HER2 variants, such as p95HER2, are being explored as a target to avoid these adverse effects (181). Despite these advances, it is necessary to optimize CAR construct designs and to develop strategies to overcome extracellular matrix barriers, which collectively are critical for enhancing both cellular penetration and overall therapeutic efficacy (182).

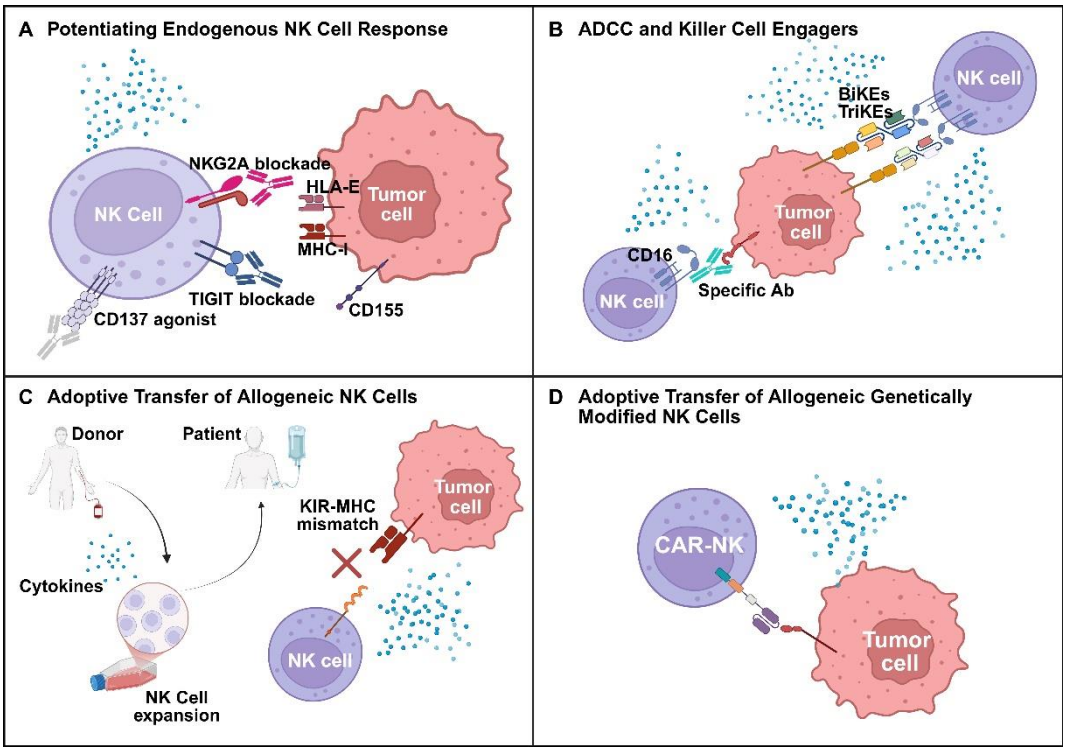

Figure 5. Potential strategies for developing NK cell-based anti-HER2-positive breast tumor therapies. A Potentiating Endogenous NK Cell Response. Immune checkpoint blockade strategies aim to disrupt inhibitory interactions, thereby promoting NK cell activation and tumor cell killing. Co-stimulation of CD137 counteracts TGF-β inhibition of NK-cell antitumor function. **B ADCC and Killer Cell Engagers.** ADCC involves tumor-specific antibodies binding to tumor cells and being recognized by the CD16 receptor on NK cells, leading to NK cell activation. Bi-specific (BiKEs) and tri-specific (TriKEs) killer cell engagers are engineered antibodies that bridge activating receptors on NK with antigens on tumor cells. **C Adoptive Transfer of Allogeneic NK Cells.** NK cells from a donor (or a cell line such as NK-92) are expanded in vitro using cytokines to pre-activate them. These expanded NK cells, often with KIR-MHC mismatch to leverage alloreactivity, are then infused into the patient to target and eliminate tumor cells. **D Adoptive Transfer of Genetically Modified NK Cells.** Chimeric antigen receptor (CAR)-NK cells are engineered to express a target-specific receptor (CAR), enabling them to recognize and kill tumor cells expressing the corresponding antigen.; BiKEs: bispecific antibodies; TriKEs: trispecific antibodies. Created in https://BioRender.com.

The landscape of HER2-positive breast cancer treatment has seen remarkable advancements, yet the challenge of metastatic relapse and treatment resistance persists, underscoring the urgent need for further innovation. Despite promising preclinical and early clinical findings, the potential of NK cell-based strategies, particularly in metastatic settings, remains to be fully realized. It is important to note that many studies in metastatic breast cancer involve patients with advanced, often overtreated disease and compromised immune systems who have exhausted other therapeutic options. This can significantly influence study outcomes.

Overall, dissecting NK cell biology in HER2-positive breast cancer is not only critical for mechanistic understanding but also for biomarker discovery/validation to stratify patients and guide personalized immunotherapy approaches.

HYPOTHESIS AND AIMS

Hypothesis

Previous work from our group demonstrated an association between the presence of tumor-infiltrating NK cells in diagnostic tumor biopsies with a higher likelihood of achieving pCR to anti-HER2 antibody therapy in primary breast cancer patients, whereas high numbers of circulating CD57+ NK cells and the CD16A-158F/F genotype correlated with a lower probability of pCR achievement.

We hypothesize that elucidating the molecular mechanism underlying the relationship between tumor-infiltrating NK cells and the efficacy of anti-HER2 antibody therapy will uncover pathways of immune activation relevant for tumor control. Moreover, validating NK cell-related biomarkers of response will facilitate personalized treatment strategies in HER2-positive breast cancer.

Aims

1- To study the molecular and immunological mechanisms underlying the association between TI-NK and response to anti-HER2 antibody therapy in HER2-positive breast cancer patients.

2- To re-evaluate the translational value of the NK cell-related biomarkers, circulating CD57+ NK cells and the CD16-158 V/F genotype, as predictors of treatment response and relapse risk in patients receiving neoadjuvant therapy with anti-HER2 antibodies

METHODS

1. Ethics statement

This study included the participation of healthy donors and patients, all of whom provided written informed consent for the analysis of peripheral blood and tumor samples for research purposes. The study protocol was approved by the local ethics committee (Clinical Research Ethics Committee, Parc de Salut Mar, No. 2018/7873/I for healthy donors and Nos. 2013/5307, 2015/6038/I and 2019/8584/I for cancer patients).

2. Patients cohorts

The analysis of breast tumor infiltrates included newly diagnosed, treatment-naive cases of primary breast cancer collected from 2017 to 2023 at Hospital del Mar, Barcelona (*n*=84). HER2-positive subtype classification was determined according to the 2013 ASCO/CAP guidelines (183).

Serum samples were obtained from newly diagnosed, previously untreated, primary HER2-positive breast cancer from Hospital del Mar, Barcelona and Hospital Clínic, Valencia, receiving neoadjuvant therapy. Serum samples were collected, at baseline (*n*=79) and after three chemotherapy cycles (*n*=32), aliquoted and stored at -80ºC until analysis. All participating patients underwent a neoadjuvant treatment consisting of standard chemotherapy in combination with anti-HER2 monoclonal antibodies. The pathological response was assessed at the time of surgery and reported according to the Miller-Payne grading system (184). Partial pathological response was defined as Miller-Payne grades 1-4, while a pathological complete response (pCR) was defined as grade 5, indicating the absence of invasive malignant cells in both the primary tumor and axillary lymph nodes, with only residual fibroelastotic stroma.

Studies on the NK cell receptor repertoire and CD16A-158V/F genotype in aim two included baseline peripheral blood samples from patients prospectively recruited between July 2017 and May 2024 at Hospital del Mar (Barcelona) and Hospital Clínic de Valencia (Valencia, prospective validation cohort *n*=74). Those patients were newly diagnosed, treatment-naive, HER2-positive breast cancer patients undergoing neoadjuvant therapy with standard chemotherapy alongside

HER2-specific antibodies. Pathologic response was evaluated at surgery and reported by the Miller-Payne grading system (184). The primary efficacy endpoints in our study were pCR, disease-free survival (DFS) and overall survival (OS). DFS and OS were calculated as the time from surgery until any breast cancer relapse or death by any cause (in months). The term ‘discovery cohort’ is used for the cohort of patients previously described in Muntasell et al (148), while ‘total cohort’ is used for those analysis combining data from both discovery and validation cohorts.

3. Isolation of human samples

Peripheral blood mononuclear cells (PBMC) were isolated from heparinized blood samples using density gradient centrifugation with Ficoll-Hypaque (Lymphoprep, StemCell, 1858). PBMC were cryopreserved on FBS supplemented with 10% DMSO until the moment of the analysis. At thawing, PBMC were incubated overnight in RPMI 1640 GlutaMAX medium (Gibco, 72400021), supplemented with penicillin and streptomycin (100 U/ml and 100 µg/ml, respectively, Gibco, 15140122), 1mM sodium pyruvate (Gibco, 11360039), 10% fetal bovine serum (FBS, Gibco, A5256701), and 200 U/ml of recombinant IL-2 (Proleukin). Following overnight incubation, NK cells were purified by negative selection using NK cell isolation kit (Miltenyi, 130-092-657) according to the manufacturer's instructions.

Fresh, treatment-naive breast tumor specimens were mechanically disrupted and subjected to enzymatically digested in RPMI with 1% FBS, 1 mg/ml collagenase type IV (Gibco, 171040-19), and 50000 U/ml DNase (New England Biolabs, M0303) for 40 minutes at 37°C. Following digestion, tissue clumps were removed by filtration through a 40 µm cell strainer. The resulting cell suspension was then stained with directly labelled antibodies.

4. Gene expression microarray analysis of FFPE breast tumor biopsies

Gene expression microarray analysis was performed on a subset of twelve HER2-positive breast tumor biopsies selected from the previously described cohort

in Muntasell et al (112). Biopsies were selected based on the presence or absence of tumor-infiltrating NK cells (TI-NK) and TIL score.

Total RNA was extracted from three consecutive 10-µm thick formalin-fixed, paraffin-embedded (FFPE) tumor sections using the RNeasy® Micro Kit (Qiagen, cat. No. 74004). RNA amplification, labeling, and hybridization were performed according to the GeneChip WT PLUS Reagent kit protocol (P/N 703174 2017) and hybridized to the Human Clariom S Array (Thermo Fisher Scientific). Presence or absence of TI-NK was validated in each biopsy using a single immunohistochemistry (IHC) staining for CD56 (anti-CD56 antibody, clone 123C3, Agilent).

Microarray data analysis was performed using R (Version 3.4.3) with Bioconductor and Comprehensive R Archive Network (CRAN, 2017) packages. Raw data were background-corrected, quantile-normalized, and summarized to the gene level using the robust multi-chip average (RMA) method. Differential gene expression between the TI-NK+ and TI-NK- biopsies was determined using an empirical Bayes moderated t-statistics model implemented in the LIMMA package, adjusting for estrogen receptor (ER) status. Genes with a *p-value* < 0.05 and a fold change >1.5 were considered differentially expressed. Heatmap data were scaled by genes using z-score normalization. Ingenuity Pathway Analysis (IPA) software (Qiagen) was used to identify enriched biological pathways and networks associated with the differentially expressed genes.

Analysis were conducted by MARGenomics core facility at the Hospital del Mar Research Institute.

5. Bioinformatic analysis of publicly available gene expression data from HER2-positive breast tumors

Gene expression microarray data from treatment-naive HER2-positive breast tumors (GSE130786) was downloaded from the Gene Expression Omnibus (GEO; https://www.ncbi.nlm.nih.gov/geo/). This dataset was generated from a Phase II randomized clinical trial of trastuzumab-based neoadjuvant treatment in breast

cancer patients. Agilent array data were quantile normalized and log2-transformed using R. A NK cell signature score, comprising 20 genes (*CD160*, *CD244*, *CTSW*, *FASLG*, *GZMA*, *GZMB*, *GZMH*, *IL18RAP*, *IL2RB*, *KIR2DL4*, *KLRB1*, *KLRC3*, *KLRD1*, *KLRF1*, *KLRK1*, *NCR1*, *NKG7*, *PRF1*, *XCL1* and *XCL2* genes) (185) was calculated using the singscore R package. Z-scores for *GZMB, IFNG, CCL5, CXCL9* and *CXCL10* transcripts were used to assess their association with pathological complete response (pCR) to trastuzumab. Odds ratios (ORs) for achieving pCR were calculated for the top and bottom quartiles of expression for each gene, as well as for the NK cell signature score (ranked sum expression).

6. Cell lines

Human HER2-positive breast cancer cell lines SKBR3 and BT474 were cultured in complete DMEM/F-12 medium (Sigma-Aldrich, D6421) supplemented with 0.5 mM of L-glutamine (Gibco, 25030-081), penicillin/streptomycin (100 U/ml and 100 µg/ml, respectively, Gibco), sodium pyruvate (1 mM, Gibco), 10% FBS (Gibco). The human HER2-positive breast cancer cell line HCC1954 and the 8866 B-LCL cell line were grown in complete RPMI 1640 Glutamax medium (Gibco), with penicillin/Streptomycin, sodium pyruvate and 10% FBS.

7. *In vitro* ADCC assays with purified NK cells

ADCC assays were done by coculturing NK cells and breast cancer cells at 1:1 effector:target (E:T) ratio with trastuzumab (210 ng/ml) for 24 hours. Cell-free culture supernatants were collected by centrifugation for cytokine/chemokine determination. Anti-IFNAR mAb (5 µg/ml, 407296, Calbiochem), anti-IFN-γ mAb (5 µg/ml, 14-7318-81, Invitrogen), anti-TNF-α mAb (infliximab, 50 µg/ml, Remicade®, Janssen) and their combinations were added along ADCC assays in blocking/neutralization experiments.

8. Treatment of breast cancer cells with recombinant cytokines

SKBR3 and HC1954 cells were treated with 10 ng/ml recombinant human (rh) IFN-γ (Preprotech, 300–02), 10 ng/ml rhTNF-α (Immunotools, 1134013), 1000 U/ ml rhIFN-β-1a (Merck, Rebif) and their combinations for 24 h prior to cell-free supernatant collection and cytokine/chemokine analysis by ELISA. Cell-free supernatants were collected by centrifugation (5 min 500 G).

9. CCL5, IFN-γ, CXCL9 and CXCL10 analysis by ELISA

CCL5, CXCL9 and CXCL10 levels were measured with commercial ELISA (DY278, DY392 and DY266, R&D, respectively) following the manufacturer's instructions. IFN-γ levels were assessed with 88–7316-88 (Invitrogen) commercial ELISA, also following the manufacturer's instructions.. Optical density was determined on an Infinite 200 Pro plate Reader (Tecan) using a microplate Reader set to 450 nm and corrected to the OD values at 570 nm.

10. Human NK cell expansion for *in vivo* ADCC model

PBMC from healthy donors were co-cultured with irradiated 8866 B-LCL feeder cells (40Gy) at a 3:1 ratio for 12 days and cryopreserved until use. Cells were subcultured every 3-4 days (from 2 to 3 wells), and NK cell expansion was monitored by flow cytometry staining with CD3 and CD56.

Prior to intratumoral injection, expanded cells were thawed and cultured overnight in complete RPMI medium supplemented with 200 U/ml recombinant IL-2 (Proleukine) prior to NK cell isolation.

11. Humanized mouse model to study in vivo NK cell-mediated ADCC

All animal experiments were conducted in compliance with ethical guidelines and protocols approved by the Barcelona Biomedical Research Park (PRBB) Animal

Facility and the Generalitat de Catalunya Animal Care and Use Committee (EARA20–0045).

Eight-week-old NOD/Scid/γc-/- (NSG) mice, obtained from Jackson Laboratories, were subcutaneously inoculated with human HCC1954 breast cancer cells (4×10^5 cells) suspended in Matrigel. Tumor growth was monitored, and tumor volume was calculated using the formula: $(\text{width}^2 \times \text{length} \times \pi)/6$.

Once tumors reached approximately 100 mm^3, mice were randomly assigned to one of four treatment groups (n = 5 mice/group):

1. Control group: Received a control human IgG1 antibody (Rituximab; 2 mg/kg).

2. Antibody therapy group: Received a combination of trastuzumab and pertuzumab (1 mg/kg each).

3. NK cell therapy group: Received expanded human NK cells (2.5×10^6 cells).

4. Combination therapy group: Received expanded human NK cells (2.5×10^6 cells) in conjunction with trastuzumab/pertuzumab (1 mg/kg each).

All antibodies were administered intraperitoneally every 3–4 days. Expanded NK cells were injected intratumorally once a week for three weeks, supported by intraperitoneal injections of recombinant human IL-2 (rhIL-2) every 3-4 days. Following three treatment cycles, mice were euthanized, and the remaining tumors were harvested and processed for analysis.

12. Analysis of *CCL5*, *IFNG*, *CXCL9* and *CXCL10* expression in tumors by RT-qPCR

Tumor cell suspensions were divided for downstream analyses: one portion was used for RNA extraction and subsequent analysis of *CCL5, IFNG, CXCL9* and *CXCL10* expression, while the other portion was used for flow cytometry analysis.

RNA from tumor cell suspensions was extracted using RNeasy Mini Kit (Qiagen,

74104). 500ng of RNA was retrotranscribed using Superscript-III (Invitrogen, 18080044), according to the manufacturer's instructions. Gene expression was analyzed using the SYBR green gene expression assay (LightCycler 480 SYBR Green I Master, 04887352001, Roche). The following primers were used for human genes (5' to 3', Table 1):

Gene	Forward	Reverse
IFNG	TGTCCACGCAAAGCAATACA	ACTCCTTTTTCGCTTCCCTGT
CCL5	GCCTGTTTCTGCTTGCTCTT	AACTGCTGCTGTGTGGTAGA
CXCL9	TTCCTGCATCAGCACCAACC	TTTCTCGCAGGAAGGGCTTC
CXCL10	AACCTCCAGTCTCAGCACCA	TGCAGGTACAGCGTACAGTTC
B2M	TTAGCTGTGCTCGCGCTACTCT	TGGTTCACACGGCAGGCATACT

Table 1. List of primers for RT-PCR.

The relative gene expression was normalized to *B2M*. qPCR reactions were performed on the Lightcycler 480 Real-Time PCR System (Roche Diagnostics) and analyzed using Lightcycler 480 SW 1.5.1 at the Genomics Core Facility, Universitat Pompeu Fabra, Barcelona. The reaction included a 30 seconds (sec) preincubation at 40ºC, followed by 40 amplification cycles (10 sec at 95ºC, 20 sec at 60ºC and 10 sec at 72ºC).

13. Analysis of the tumor-infiltrating NK cell phenotype by flow cytometry in the in vivo model

For flow cytometry analyses, cells from all tumors of the same treatment group were pulled together, pretreated with aggregated human IgG (10 µg/ml) for 20 min and subsequently stained with a combination of directly labelled antibodies (anti-CD45, anti-CD56, anti-CD3, anti-CD16, anti-CD103; Table 2). Data was acquired on a BD LSR Fortessa or BD-LSRII (BD Bioscience) and analyzed with FlowJo software (v10.0.7, Tree Star).

14. *Ex vivo* treatment with anti-HER2 antibodies of multicellular cultures derived from patient breast tumors

Multicellular suspensions obtained from fresh breast tumor digestion were culture in flat-bottom 96-well plates (Corning, 153596) at a density of 100,000 cells/well for 20–24 h with 200 U/ml of rhIL2 (Proleukine) and with or without 210 ng/ml trastuzumab (Tz, from Hospital del Mar Pharmacy). After culture, cells were stained with a combination of directly labelled antibodies (anti-CD45, anti-CD56, anti-CD3, anti-CD16, anti-CD103, anti-CD137; Table 2). Data was acquired on a BD LSR Fortessa (BD Bioscience) and analyzed with FlowJo software.

15. Characterization of human breast tumor immune lymphocyte subsets

Multicellular suspensions obtained from fresh breast tumor digestion were stained with a combination of directly labelled antibodies (anti-CD45, anti-CD56, anti-CD3, anti-CD16, anti-CD103, anti-PD1, anti-NKG2C, anti-CD8, anti-CD4; Table 2).

Eighteen randomly selected tumors were used for viSNE characterization. Tumors incorporated in the analysis comprised 5 HER2-positive, 11 luminal and 2 triple-negative breast cancer cases (TNBCs). vi-SNE was implemented for the analysis of major lymphocyte subsets (186). Raw flow cytometry data was imported into R using flowCore and openCyto packages. A compensation matrix generated in FlowJo (v10.0.7, Tree Star) was exported an applied into R. Lymphocytes were gated based on forward and side scatter within the CD45+ alive (DAPI-) gate. Data from either 10,000 gated lymphocytes or 2,000-5,000 NK cells were concatenated. Barnes-Hut t-SNE was conducted using the Rtsne package and subset identification by Phenograph. Graphics were produced using the ggplot2 and RColorBrewer packages.

16. Bulk RNAseq analyses of circulating and tumor-infiltrating NK cell subsets

Paired blood and tumor samples from three treatment-naive breast cancer patients, were processed to single-cell suspension, and stained with directly labelled antibodies (anti-CD45, anti-CD56, anti-CD3, anti-CD16, anti-CD103; Table 2). DAPI was used as a viability dye for exclusion of dead cells.

Tumor-infiltrating NK cell subsets were sorted based on the expression of CD16 and CD103 (CD16+; CD16-CD103+; CD16-CD103-) from the CD56+CD3- gate in CD45+ DAPI- lymphocytes. Circulating $CD56^{bright}$ CD16- and $CD56^{dim}$ CD16+ NK cells were sorted from PBMC. Cell sorting was conducted in a FACS Aria II SORP cell sorter (BD, 23–9641-01) at the Flow Cytometry Facility, PRBB, Barcelona.

Total RNA was isolated from each sorted NK cell subset using the RNeasy® Micro Kit (Qiagen, cat. no. 74004). RNA samples were subsequently subjected to RNA-sequencing (RNA-seq) at the Genomics UPF facility (Universitat Pompeu Fabra, Barcelona). NGS libraries were prepared using the NEBNext Ultra II Directional RNA Library Prep Kit for Illumina (New England BioLabs) with poly(A) capture. Library quality and concentration were assessed using a TapeStation D1000 (Agilent Technologies). Libraries were pooled in equimolar ratios, amplified by qPCR with specific primers, and sequenced on a NextSeq High output 2x75 cycles run (Illumina). Reads were mapped against the GRCh38 human reference genome (Ensembl release 89) using STAR (version 2.7.9a). Read counts were generated using HTSeq software for the protein-coding genes (n=19.828) and normalized to log2 counts per million (CPM) with the trimmed mean of M-values (TMM) method implemented in the edgeR package (version 3.14.0) with a prior count of 0.5. Lowly-expressed genes were filtered (mean log2(CPM)< -2), which lead to a total of 10.365 genes.

Differential expression analysis was performed using the limma package with voom transformation. Patient and surrogate variables were included in the model. Differentially expressed genes (DEG) between the three TI-NK cell populations were identified using a threshold of p-value < 0.05 and |log2(fold change)| >1.

Pre-ranked gene set enrichment analysis (GSEA) was performed with GSEA (version 4.1.0) using log(*p*-value)*sign(fold change) as the ranking metric. Gene sets tested for enrichment analysis were derived from publicly available data (GSE78897) (187) using GEO2R by performing differential expression analysis between tonsillar ILC1, ILC3, and PB CD56^{dim} NK cells (adjusted p-value > 0.005 and |log2(fold change)| > 1). 1000 permutations were performed in GSEA to assess the statistical significance of enrichment for each comparison.

17. CD16A-158 V/F genotyping

DNA was isolated from total blood using the Pure gene Blood Core kit B (Qiagen). Functional polymorphisms of *FCGR3A* (CD16A 158 V/F) were determined using a PCR with confronting two-pair primers, as described previously (188,189). Briefly, this technique uses four primers in a single reaction: allele-specific primers generate distinct amplicon lengths (230 bp for 158F and 143 bp for 158V), which are resolved via agarose gel electrophoresis, while external primers produce a control band (321 bp). The approach ensures gene specificity by targeting sequences that differentiate *FCGR3A* from its homologs, enabling efficient allele discrimination without cross-reactivity.

18. PBMC immunophenotyping from HER2-positive breast cancer patients by multiparametric flow cytometry

PBMC isolated from blood samples from HER2-positive breast cancer patients were thawed and pretreated with aggregated human IgG (10 µg/ml) for 20 min. They were subsequently stained with a combination of directly labelled antibodies (anti-CD45, anti-CD56, anti-CD3, anti-CD16, anti-CD57, anti-NKG2C; Table 2). DAPI was used as a viability dye for exclusion of dead cells. Data was acquired on a BD LSR Fortessa and analyzed with FlowJo software (v10.0.7, Tree Star).

19. Antibodies used for flow cytometry staining

Antibodies	Clone	Source	Reference
CD3-PerCP	SK7	BD Bioscience	345766
CD16-APC-eFluor 780	CB16	eBioscience	47-0168-42
CD45-Alexa Fluor 700	2D1	eBioscience	56-9459-42
CD56-APC	CMSSB	eBioscience	17-0567-42
CD103-FITC	B-Ly7	eBioscience	11-1038-42
NKG2C-PE	FAB138P	R&D systems	134591
PD-1-PE-eFluor610	610 J105	eBioscience	61-2799-42
CD45-PECy7	HI30	Thermo Fisher	25-0459-42
CD8-HV500	RPA-T8	BD Bioscience	560774
CD4-PECy7	OK-T4	Biolegend	317414
CD137-PE	4B4 (4B4-1)	eBioscience	11-1379-42
CD57-FITC	HCD57	Biolegend	322306

Table 2. List of antibodies.

20. Statistics

Statistical and correlation analysis were performed using GraphPad Prism 8.0 software. Tests performed are specified in each experiment.

Bivariate analyses by Mann–Whitney U-test were used to assess the putative association between pCR and NK cell markers as continuous variables. Chi-square analysis were used for determining the likelihood of achieving PCR for every CD16A polymorphism. Predictive effects on pCR of CD57+ NK cells and CD16A polymorphism as categorical variables were calculated by Fisher exact test. Mantel-Cox proportional hazards regression was used to estimate the hazard ratio

(HR) in DFS analysis. Kaplan-Meier curves for DFS were used to compare time to event in patients stratified by their pCR achievement or CD57+/CD16A polymorphism circulating NK cells. All P values were two-sided; P values lower than 0.05 were considered significant. For the analysis of survival of patients stratified by $CD57^+$ NK cell levels, cutoffs for classification were 65% and 164 events/µL for data expressed in percentage and absolute numbers, respectively.

Multivariate analysis was conducted with R Software. Binary logistic regression was performed by adding patient age as continuous variable in the model.

RESULTS

Aim 1

1. Study of the biological pathways enriched in NK cell-infiltrated HER2-positive breast tumors

To explore the biological mechanisms underlying the observed association between tumor-infiltrating NK cells (TI-NK) and the response to anti-HER2 antibodies (112), the gene expression profiles of HER2-positive breast tumor biopsies with (TI-NK+, *n*=6) and without (TI-NK-, *n*=6) tumor-infiltrating NK cells were compared by microarray analysis. Tumor samples were selected based on discordant TI-NK cell content, as determined by CD56 immunohistochemical staining, and paired by tumor area and tumor-infiltrating lymphocyte score (average number of TIL) (Fig. 6 A-B) to minimize the potential influence of other immune cell subsets on the results. In this tumor set, the previously reported association between TI-NK cell numbers and both pathological complete response (pCR) and disease-free survival (DFS) was also evident (Fig. 6C).

Microarray analysis adjusted by ER expression revealed a total of 130 differentially expressed genes (DEG) between TI-NK+ and TI-NK- tumors. Specifically, we identified 88 upregulated and 42 downregulated genes in TI-NK cell-rich tumors when compared to their TI-NK cell-negative counterparts (Fig. 7A). Functional enrichment analysis of these DEG pointed to the involvement of several key immune system pathways that include TLR, GP6, PKCθ, and NF-ƙB signaling, in addition to processes related to dendritic cell maturation. Conversely, genes related to IL-6 signaling showed reduced activity in TI-NK+ tumors (Fig. 7B).

The functional interactions and biological networks associated with these DEG were predicted by Ingenuity Pathway Analysis (IPA) (Fig. 7C). Among several molecular networks identified, TI-NK+ biopsies displayed an enrichment in CXCL9 and CXCL10 chemokines. This enrichment indicated that IFN-γ, type I interferons, and TNF were key upstream regulators, controlling downstream pathways like lymphocyte migration, inflammatory response, and cell activation (Fig. 7C).

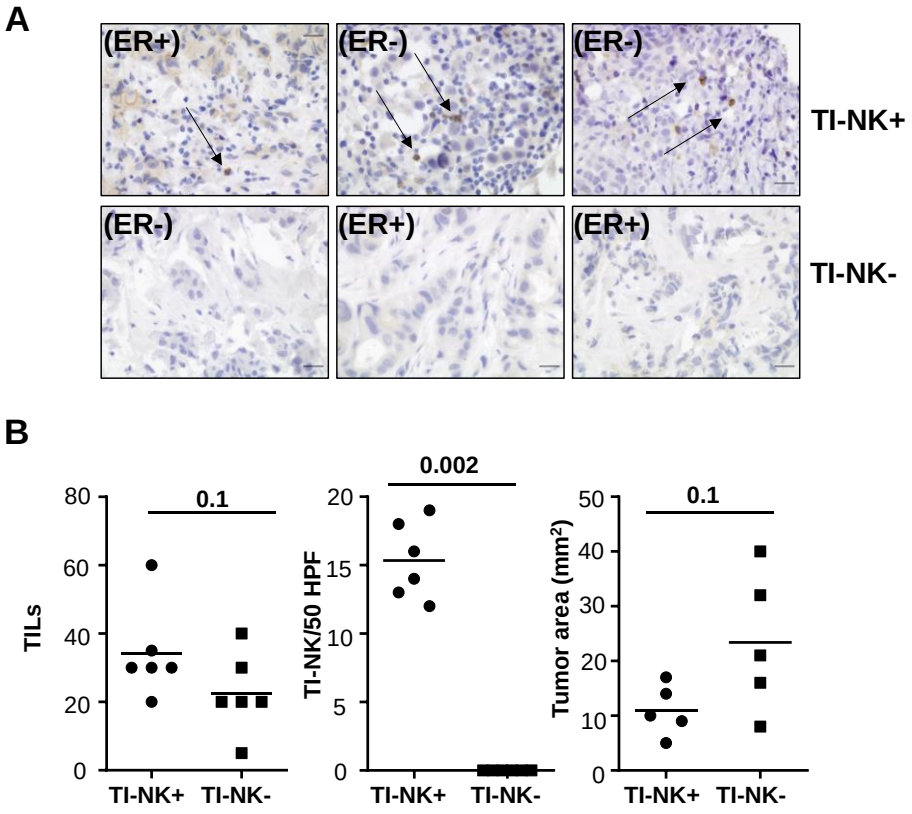

C

		TIL	TI-NK	Age	TNM	ER	Histo	pCR	RFS
TI-NK+	1	10	14	42	T2	ER+	CDI	G5	DF
	2	30	18	51	T2	ER+	CDI	G5	DF
	3	60	12	75	T4	ER-	CDI	G5	DF
	4	20	19	75	T3	ER+	CDI	G5	DF
	5	30	16	51	T2	ER-	CDI	G5	DF
	6	35	13	54	T2	ER-	CDI	G5	DF
TI-NK-	1	20	0	54	T3	ER-	CDI	G1	Relapse
	2	20	0	42	T3	ER+	CDI	G1	Relapse
	3	20	0	41		ER+	CDI	G1	
	4	5	0	58	T2	ER+	CDI	G1	
	5	10	0	36	T2	ER+		G3	Relapse
	6	30	0	40	T2	ER+	CDI	G1	DF

Figure 6. Clinicopathological characteristics of HER2-positive breast tumors included in the microarray analysis. Tumor biopsies at diagnosis from 12 patients (6 with high tumor-infiltrating NK cells [TI-NK+] and 6 with low/no TI-NK infiltration [TI-NK-]) were selected from the cohort previously characterized in Muntasell, 2019 (112). **A** Representative immunohistochemical (IHC) staining for CD56 in three representative tumor biopsies per group. Arrows indicate CD56+ lymphocytes. ER: Estrogen Receptor. **B** TIL score, TI-NK cell count, and tumor area in TI-NK+ and TI-NK- tumor biopsies (*n*=6 per group). Statistical analysis was performed using unpaired Student's t-test. **C** Clinicopathological features of HER2-positive tumor biopsies included in the microarray analysis.

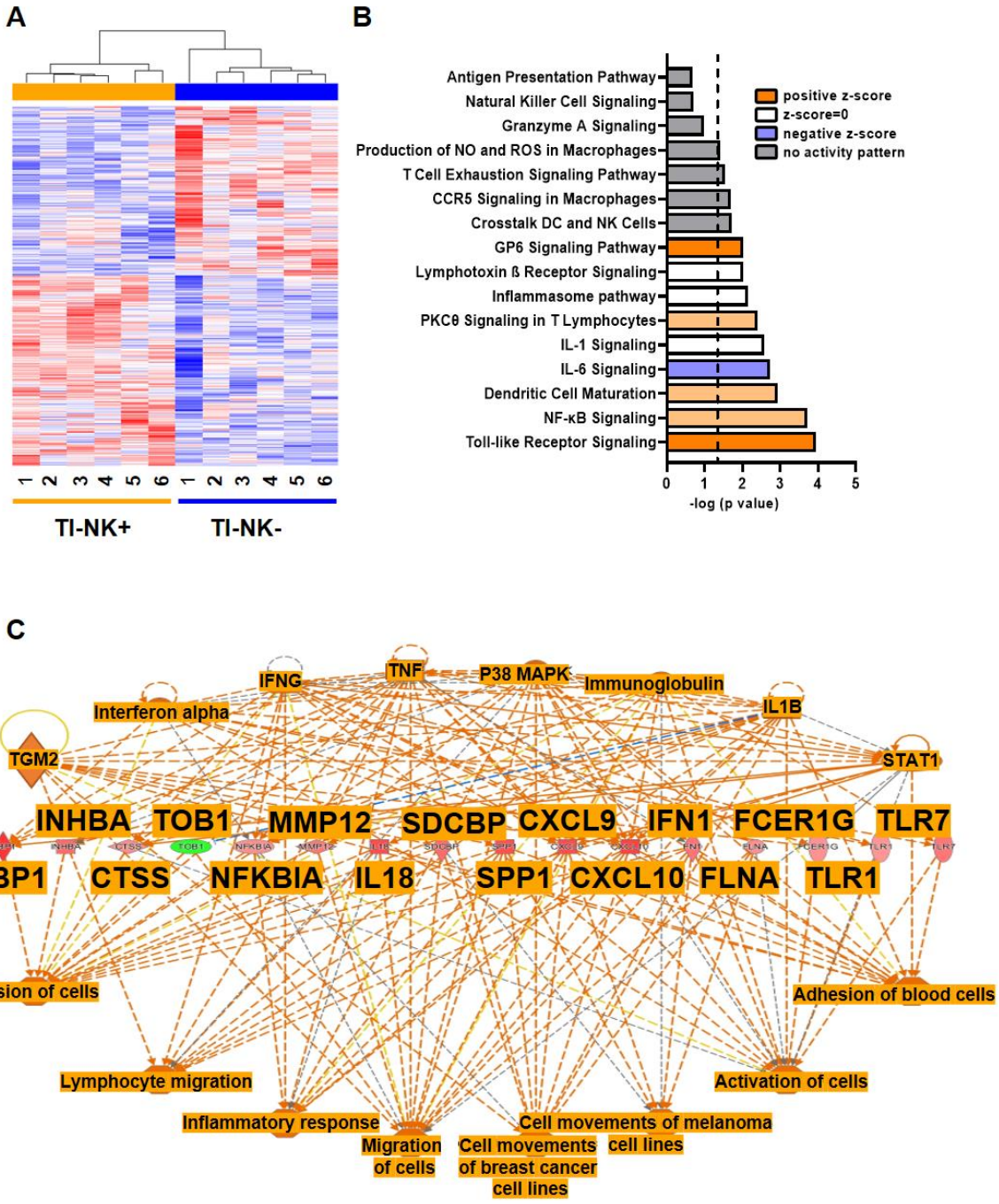

Figure 7. Biological pathways associated with NK cell infiltration in HER2-positive breast tumors. Gene expression microarray analysis was performed on total RNA extracted from FFPE tumor sections from HER2-positive breast tumor diagnostic biopsies (6 TI-NK+ and 6 TI-NK-). **A** Heatmap of differentially expressed genes (DEG, fold change >1.5 and $p < 0.05$) between TI-NK+ and TI-NK- tumors, normalized by z-score. Yellow and blue bars indicate TI-NK+ and TI-NK- groups, respectively. **B** Biological pathways enriched in TI-NK+ tumors identified using Ingenuity Pathway Analysis (IPA). The dashed line indicates a –log(p-value) of 1.3. **C** Genes differentially expressed between TI-NK-positive and negative biopsies were loaded into the Ingenuity Pathway Analysis (IPA) software. Network analysis shows major regulators (top), associated biological pathways (bottom), and differentially expressed genes (DEG) in TI-NK+ versus TI-NK- tumors (middle). Orange boxes: predicted activation; red to pink boxes: up-regulation; green boxes: down-regulation; orange arrows: activation; blue arrow: inhibition; yellow arrow: inconsistent findings; gray arrows: effect not predicted.

2. Association between CCL5/IFNG-CXCL9/10 axis, TI-NK cells and response to anti-HER2 antibodies

Microarray analysis revealed that expression of *CXCL9, CXCL10, IFNG, and CCL5* were higher in TI-NK+ tumors compared to TI-NK- tumors (Fig. 8A). These markers showed positive correlations with each other and with TI-NK cell numbers, as determined by CD56 IHC staining in the original biopsies (Fig. 8B and 8C).

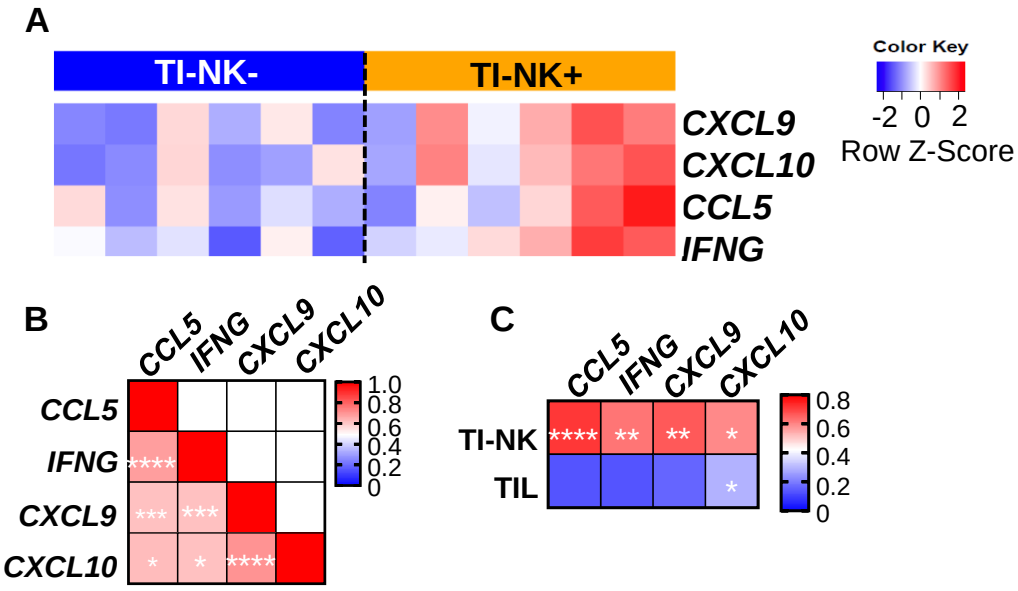

Figure 8. *CCL5*, *IFNG*, *CXCL9* and *CXCL10* expression in treatment naive HER2 positive breast tumors. *CXCL9, CXCL10, IFNG*, and *CCL5* expression in tumors with high versus low NK cell infiltration by microarray analysis. **A** Relative expression of the indicated genes in all tumors stratified by TI-NK cell content. **B** Pearson's correlation coefficient between the indicated genes. **C** Pearson's correlation coefficient between the indicated genes, TI-NK cell numbers and TIL scores in the corresponding biopsies. Asterisks indicate statistical significance (**** $p < 0.0001$; *** $p < 0.001$; ** $p < 0.01$; * $p < 0.05$).

The analysis of these four genes in an independent dataset of HER2-positive breast tumors from a Phase II clinical trial (GSE130786, *n*=81) confirmed the positive correlation among *CXCL9*, *CXCL10*, *IFNG*, and *CCL5* gene expression in baseline tumor biopsies (Fig. 9A). Remarkably, *IFNG* expression positively correlated with a TI-NK cell signature (185) (Fig. 9B) and with an increased likelihood of achieving a pathological complete response (pCR) to trastuzumab-based neoadjuvant therapy (OR 96.3, *p*=0.01) (Fig. 9C).

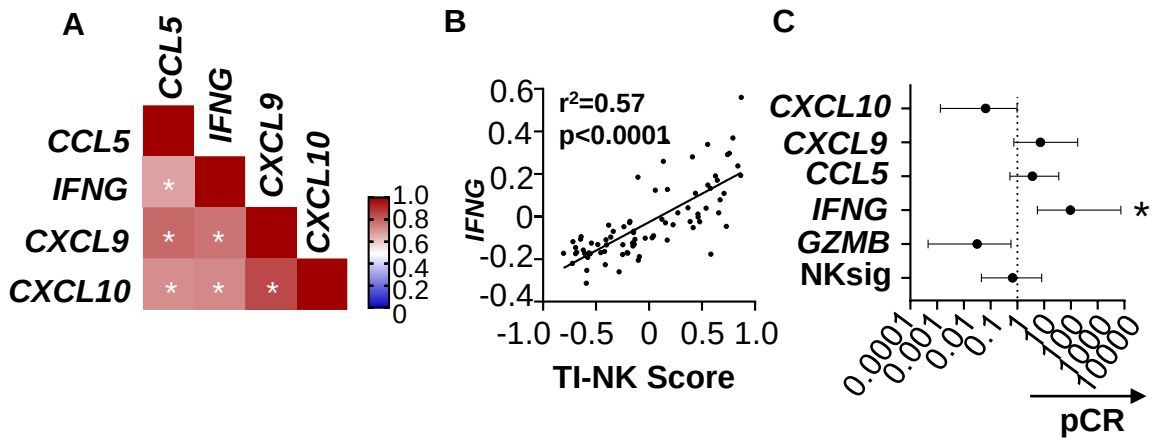

Figure 9. Bioinformatic analysis of publicly available gene expression data from HER2-positive breast tumors confirmed the association between CCL5/IFNG-CXCL9/CXCL10, TI-NK and pCR. Analysis of a public gene expression dataset from HER2-positive breast tumors generated in the context of a Phase II Randomized Trial (GSE130786, *n*=81). **A** Pearsons' correlation coefficient between the indicated genes. Asterisks indicate significant correlations. **B** Correlation between *IFNG* expression levels and a TI-NK cell score (gene signature of Cursons et al) (185). **C** Association of TI-NK cell score (NKsig), *IFNG, GZMB, CCL5, CXCL9*, and *CXCL10* expression with pCR to trastuzumab-based treatment (Odds ratios and 97.5% confidence intervals). Asterisks indicate significant associations.

These results pointed to NK cells as the primary source of IFN-γ and highlighted the importance of the CCL5/IFNG-CXCL9/10 axis for the clinical efficacy of anti-HER2 antibody-based treatment in patients with primary HER2-positive breast cancer.

3. IFN-γ produced along anti-HER2 antibody-dependent NK cell activation triggers the production of CXCL9 and CXCL10

The next step was to address whether cytokines produced during trastuzumab-dependent NK cell activation could stimulate CXCL9 and CXCL10 production from bystander breast cancer cells using *in vitro* coculture assays. Trastuzumab-induced NK cell activation against SKBR3, BT474 and HCC1954 HER2-positive breast cancer cells resulted in the secretion of CCL5, IFN-γ and the consequent production of CXCL9 and CXCL10, as analyzed by ELISA in cell-free coculture supernatants (Fig. 10).

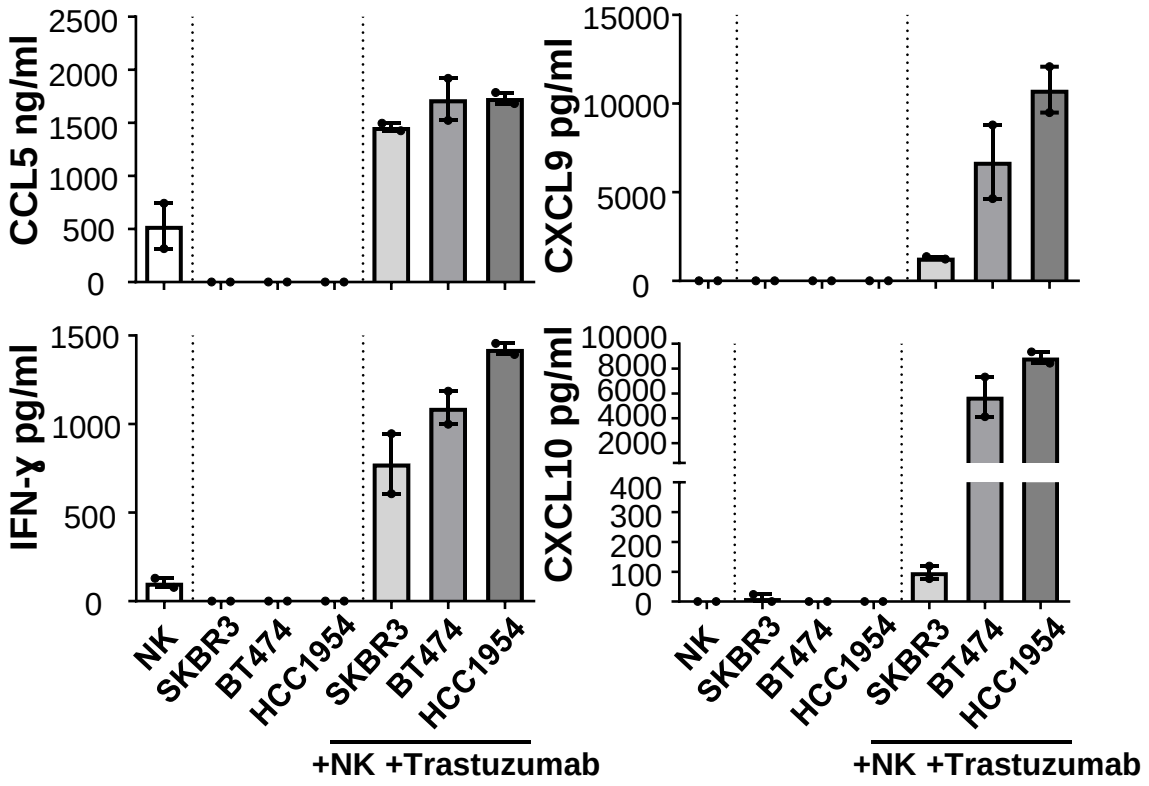

Figure 10. Anti-HER2 antibody-dependent NK cell activation triggers the production of CCL5/IFN-γ-CXCL9/10. Purified primary NK cells were co-cultured with HER2-positive breast cancer cell lines (SKBR3, BT474, and HCC1954) at a 1:1 effector:target (E:T) ratio with trastuzumab (210 ng/ml) for 24 hours. Cell-free supernatants were analyzed by ELISA to determine the concentration of the indicated cytokines/chemokines.

To dissect the specific contributions of IFN-γ, TNF-α and type-I IFN to CXCL9 and CXCL10 chemokine production, coculture experiments were repeated including blocking or neutralizing antibodies specific for IFN-γ, TNF and the receptor for type-I IFN (IFNAR). Results from blocking experiments revealed that IFN-γ was essential for CXCL9 production, while both IFN-γ and type-I IFN signaling contribute to CXCL10 expression. These effects were consistent across co-cultures of NK cells with SKBR3 and HCC1954 cells. TNF-α blockade had no impact in HCC1954 cocultures but selectively reduced CXCL10—and to a lesser extent CXCL9—in the SKBR3 model (Fig. 11A and 11B).

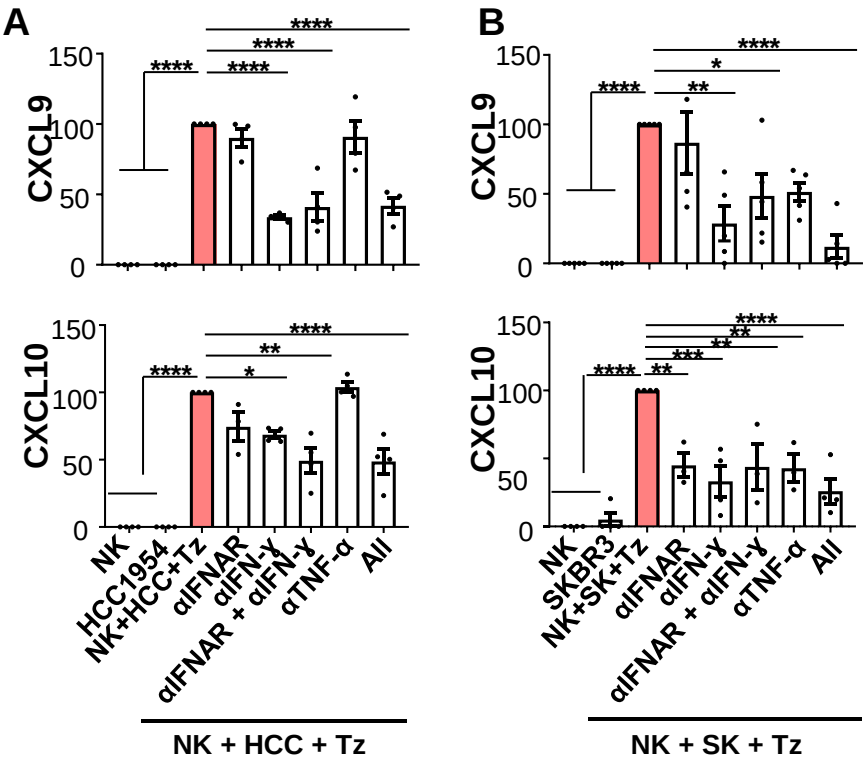

Figure 11. IFN-γ neutralization impairs CXCL9 and CXCL10 production in NK cell and HER2-positive breast cancer cell cocultures along anti-HER2 treatment. Purified primary NK cells were co-cultured with **(A)** HCC1954 (HCC) and **(B)** SKBR3 (SK) breast cancer cell lines (1:1 E:T ratio) with trastuzumab (210 ng/ml) for 24 hours. Neutralizing antibodies against IFN-γ (5 µg/ml) and TNF-α (50 µg/ml), and/or a blocking antibody for IFN-I receptor (α-IFNAR) (5 µg/ml) were added as indicated. CXCL9 and CXCL10 relative production in cell-free supernatants was measured by ELISA. Data from three independent experiments, normalized to cytokine/chemokine production without blocking antibodies. Asterisks indicate significant differences (Mann Whitney U test): **** $p < 0.0001$; *** $p < 0.001$; ** $p < 0.01$; * $p < 0.05$.

In vitro stimulation of HCC1954 and SKBR3 HER2-positive cells with recombinant cytokines confirmed that IFN-γ was the primary driver of CXCL9 and CXCL10 secretion. IFN-β had chemokine-specific effects: it synergized with IFN-γ and TNF-α to enhance CCL5 production but antagonized the induction of CXCL9. Without IFN-γ, IFN-β combined with TNF-α induced CCL5 and, to a lesser extent, CXCL10 production, but were not sufficient for inducing CXCL9 production in any cell line. IFN-γ and TNF-α together cooperatively increased CCL5 and CXCL9 levels in both cell lines (Fig. 12).

These results indicate that the interaction of NK cells with breast cancer cells along anti-HER2 antibody-dependent ADCC is sufficient for unleashing the secretion of CCL5/IFN-γ-CXCL9/10 axis.

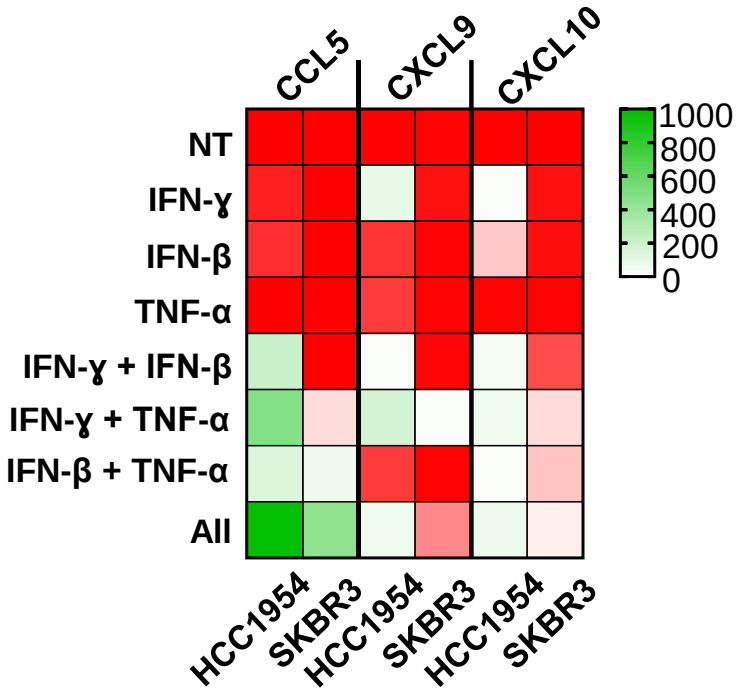

Figure 12. IFN- and TNF-induced production of CCL5, CXCL9 and CXCL10 by HER2-positive breast cancer cell lines. SKBR3 and HCC1954 cells were cultured for 24 hours with recombinant IFN-γ (10 ng/ml), IFN-β (1000 U/ml) and TNF-α (10 ng/ml) or combinations thereof. CCL5, CXCL9, and CXCL10 levels in cell-free supernatants were measured by ELISA. The heatmap shows the absolute chemokine concentrations (pg/ml for CCL5 and ng/ml for CXCL9 and CXCL10) for each condition.

4. Treatment with anti-HER2 antibodies and NK cells unleash the CCL5/IFN-γ-CXCL9/10 axis and controls tumor growth

To determine if systemic anti-HER2 antibody and NK cell combined treatment activates the CCL5/IFN-γ-CXCL9/10 axis, a humanized *in vivo* mice model was implemented. HCC1954 cells were subcutaneously injected into the right flank of NOD/Scid/γc-/- (NSG) mice. When tumors reached a volume of 100 mm^3, mice were randomized to receive: i) intraperitoneal injections of anti-HER2 antibodies (trastuzumab and pertuzumab) or control human IgG1 (Rituximab), ii) intratumoral injections of expanded human NK cells, or iii) a combination of both (Fig. 13A). Both monotherapies reduced tumor growth compared to control mice; however, the combined treatment achieved superior tumor growth control relative to either monotherapy (Fig. 13B).

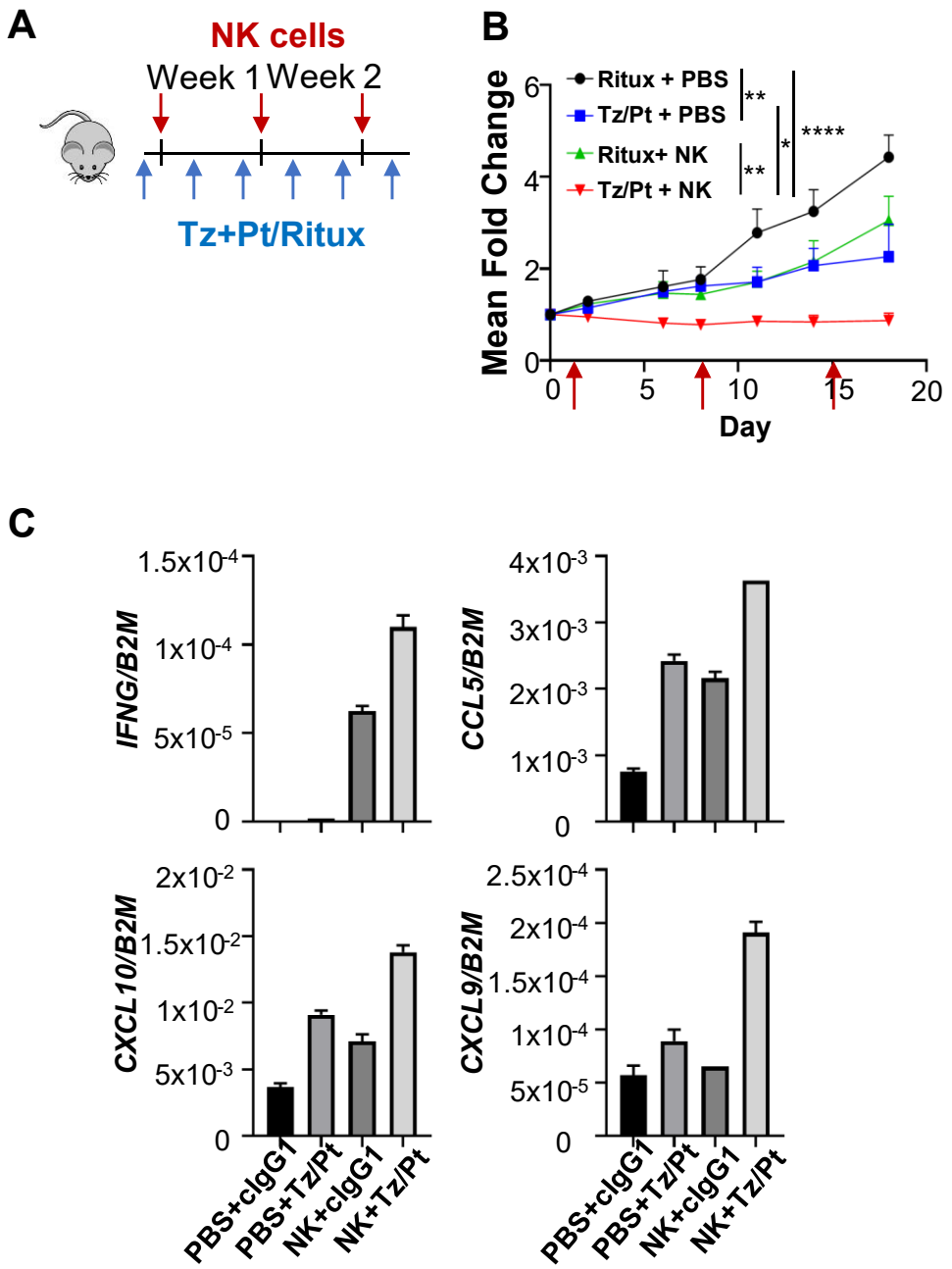

Figure 13. Combined NK cell and anti-HER2 antibody therapy controls tumor growth and activates the CCL5/IFNG-CXCL9/10 axis in a humanized mouse model of HER2-positive breast cancer. HCC1954 xenografts were implanted in NSG mice and treated with either: i) isotype control (Rituximab; 2 mg/kg, intraperitoneal); ii) trastuzumab (Tz)/pertuzumab (Pt) (1 mg/kg each, intraperitoneal); iii) expanded human NK cells (2.5 × 10^6 cells, intratumoral); or iv) Tz/Pt in combination with expanded human NK cells. Mice were sacrificed at the end of treatment. **A** Experimental design. **B** Tumor volume fold change for each treatment group (n=5 mice/group). Statistical significance was determined by two-way ANOVA: ****$p < 0.0001$; ***$p < 0.001$; **$p < 0.01$; *$p < 0.05$. **C** Tumor tissue was collected at the end of treatment, and RNA was extracted. *CCL5, IFNG, CXCL9*, and *CXCL10* expression were analyzed by RT-qPCR and normalized to *B2M* expression.

Following study completion, tumors were harvested, dissociated into single-cell suspensions, and divided: half were used for RNA extraction and subsequent RT-qPCR analysis of *IFNG*, *CCL5*, *CXCL9* and *CXCL10* (Fig. 13C); the other half, for flow cytometric phenotyping of tumor-infiltrating NK cells (Fig. 14A).

Our findings revealed that *IFNG* transcripts were detected exclusively in tumors from mice that received NK cell injections, whether these injections were administered alone or in combination with anti-HER2 antibodies. Monotherapy with either systemic anti-HER2 antibodies or intratumoral NK cells led to increased expression of *CCL5* and *CXCL10,* but not of *CXCL9*, compared to untreated tumors. A coordinated upregulation in *CCL5/IFNG-CXCL9/10* was observed only in tumors treated with the combination of NK cells and anti-HER2 antibodies, supporting the requirement of both elements for effectively triggering the CCL5/IFN-γ-CXCL9/10 axis (Fig. 13C).

These *in vivo* findings suggest that NK cell activation via ADCC during anti-HER2 antibody therapy effectively triggers the CCL5/IFN-γ-CXCL9/10 axis, contributing to improved tumor control.

Phenotypic characterization of tumor-infiltrating NK cells from resected tumors revealed a shift from the original NK cell product (primarily composed of $CD16^+$ $CD103^-$ cells) toward a phenotype characterized by the progressive acquisition of CD103 ($CD16^+CD103^+$), indicative of tissue residency, concomitant to the loss of CD16 ($CD16^-$ $CD103^+$), likely reflecting activation-induced receptor shedding (Fig. 14B). The extent of this phenotypic shift was directly proportional to the magnitude of the activating stimuli and the degree of tumor growth control (Fig. 13B).

Overall, this experiment suggests that $CD16^+$ NK cells contribute to antitumor immunity *in vivo*, particularly in the presence of anti-HER2 antibodies. Interestingly, this effect was linked to both the triggering of the CCL5/IFNγ-CXCL9/10 axis and the acquisition of a CD16-$CD103^+$ phenotype by NK cells.

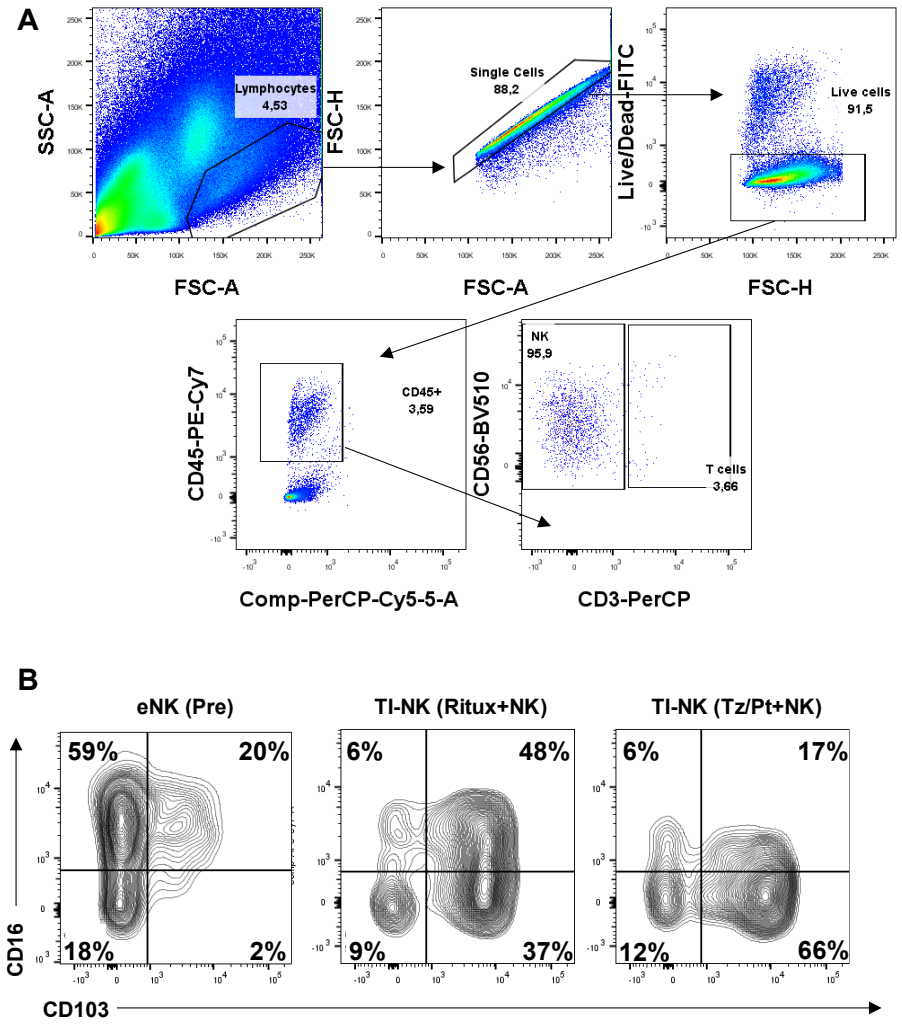

Figure 14. Expression of CD16 and CD103 in tumor-infiltrating NK cell subsets *in vivo*. HCC1954 xenografts were implanted in NSG miceand treated with either: i) isotype control (Rituximab; 2 mg/kg, intraperitoneal); ii) trastuzumab (Tz)/pertuzumab (Pt) (1 mg/kg each, intraperitoneal); iii) expanded human NK cells (2.5×10^6 cells, intratumoral); or iv) Tz/Pt in combination with expanded human NK cells. Mice were euthanized at the end of treatment. At the end of treatment, tumor-infiltrating NK cells were analyzed by flow cytometry. **A** Gating strategy used to identify NK cells. **B** CD16 and CD103 surface expression on NK cells: pre-injection, isolated from tumors treated with NK cells and control antibody (Rituximab + NK), or from tumors treated with NK cells and anti-HER2 antibodies (Tz/Pt + NK).

5. CD16 and CD103 define functionally distinct NK cell subsets in human breast tumors

Based on observations from the *in vivo* model, we studied the expression of CD16 and CD103 in TI-NK cells from fresh, treatment-naïve, human breast tumors by flow cytometry. NK cells were defined as $CD45^+$ $CD56^+$ $CD3^-$ lymphocytes (Fig. 15A).

Reminiscent of data in mice, three distinct TI-NK cells subsets were identified in human tumors based on CD16 and CD103 expression: $CD16^+$ (regardless CD103 expression), $CD16^-CD103^+$, and $CD16^-CD103^-$ (Fig. 15B).

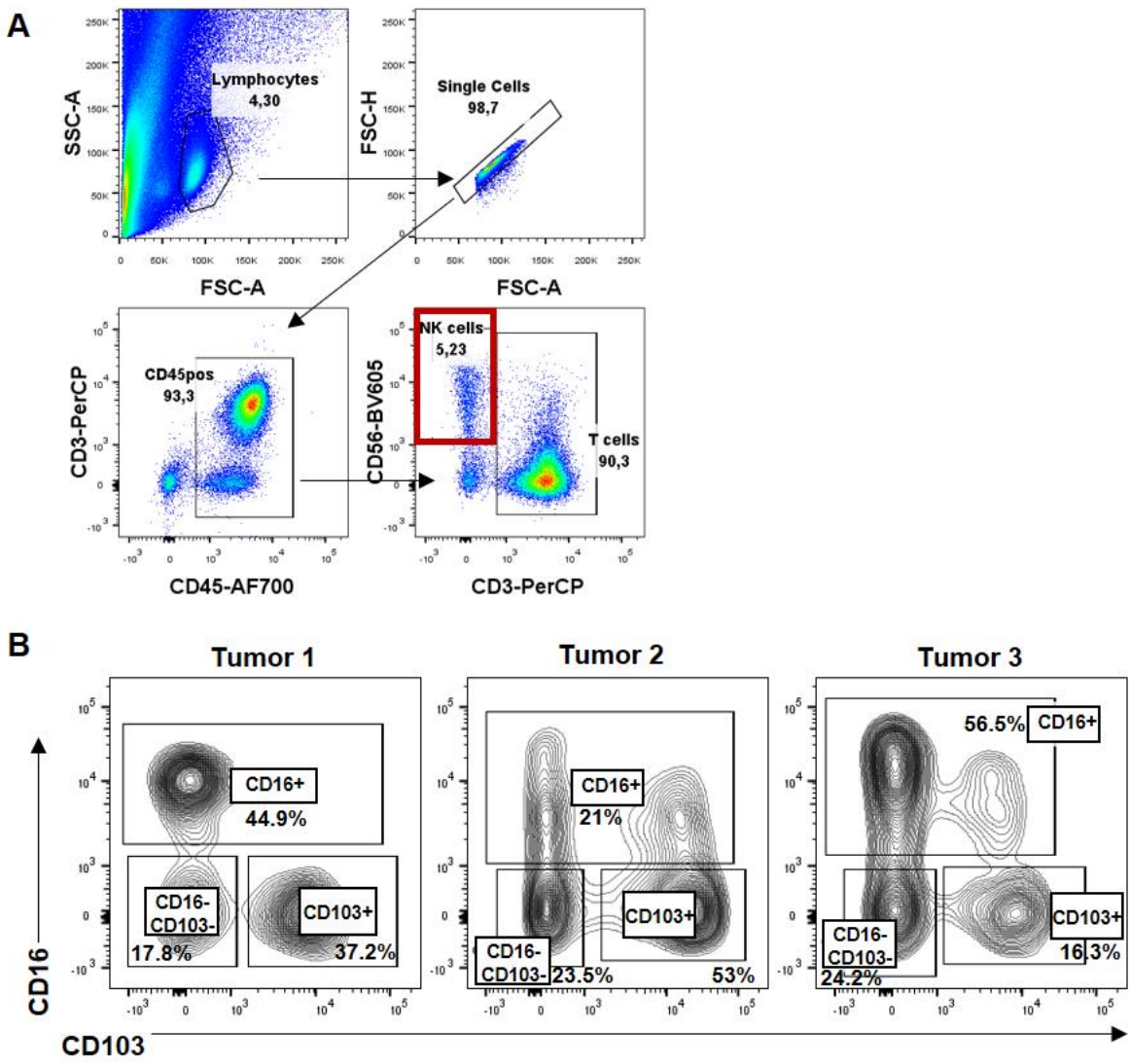

Figure 15. CD16 and CD103 expression defines distinct NK cell subsets in human, treatment-naive breast tumors. Three treatment-naive breast tumors were processed into single-cell suspensions and analyzed by flow cytometry for the expression of CD16 and CD103. **A** Gating strategy used to identify NK cells. **B** CD16 and CD103 surface expression profiles of tumor-infiltrating NK (TI-NK) cells.

To investigate the role of these three NK cell subsets in anti-HER2 therapy, multicellular cultures from digested human breast tumors were treated *in vitro* with trastuzumab, and NK cell activation was monitored by CD137 expression after 24h.

The $CD16^+$ NK cell subset was activated by trastuzumab treatment in a dose-dependent manner (Fig. 16A). Of note, CD16 shedding was also noticed in these cultures resulting in the up-regulation of CD137 in both $CD16^+$ and $CD16^-$ $CD103^-$ NK cell subsets (Fig. 16B and 16C).

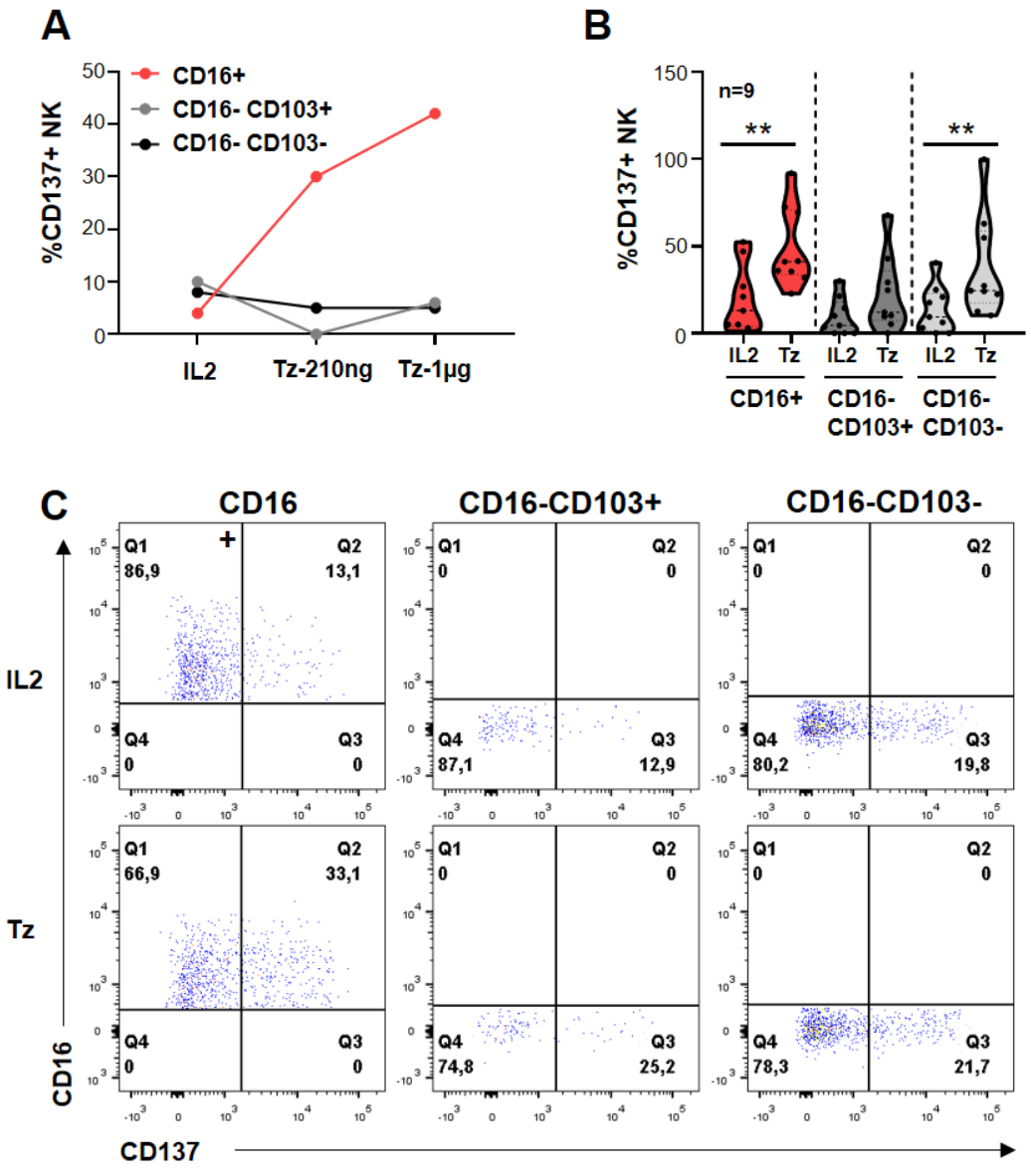

Figure 16. Trastuzumab *in vitro* treatment activates CD16+ NK cells in human breast tumor-derived multicellular cultures. Multicellular suspensions obtained after digestion of treatment-naive breast tumors were cultured with or without trastuzumab, and IL-2 (200 U/ml). After 24 hours, CD137 expression in tumor-infiltrating NK cells was measured by flow cytometry. **A** Proportions of CD137+ cells within $CD16^+$, $CD16^-CD103^+$ and $CD16^-CD103^-$ NK cell subpopulations in a representative breast tumor derived multicellular culture treated with two different doses of trastuzumab (Tz, 210 ng/ml or 1 µg/ml). **B** Proportions of CD137+ cells within CD16+, $CD16^-$ $CD103^+$ and $CD16^-$ $CD103^-$ NK subpopulations in tumor cultures treated or not with 210 ng/ml trastuzumab (*n*=9). Asterisks indicate statistical significance by one-way ANOVA test. **C** Dot plots showing CD137 expression in $CD16^+$, $CD16^+CD103^+$ and $CD16^-CD103^-$ NK cell subsets from a representative sample.

We next analyzed the functional profile of the different TI-NK subpopulations in three treatment-naïve breast tumors upon sorting and bulk RNAseq analyses (Fig. 17A). For comparative purposes, $CD56^{bright}$ and $CD56^{dim}$ NK cells were also sorted from paired blood samples (Fig. 17B). The three TI-NK cell subsets showed remarkably similar transcriptomes, with hundreds of genes differentially expressed in pair-wise comparisons (Fig. 17C) and with only 23, 51 and 68 genes uniquely expressed by $CD16^+$, $CD16^-CD103^-$ and $CD16^-CD103^+$ TI-NK cells, respectively (Fig. 17D). Biological pathways enriched in the $CD16^-$ $CD103^+$ TI-NK cells subset included cell migration and cellular defense response, whereas lymphocyte activation and NF-κB signaling were prominent in $CD16^-CD103^-$, and lymphoid and non-lymphoid cell interactions in $CD16^+$ TI-NK cell subset (Fig. 17E).

$CD16^+$ TI-NK cells showed increased expression of transcription factors involved in NK cell lineage commitment, particularly *ZEB2*, *EOMES*, and *TBX21* (T-bet), similar to circulating CD56dim NK cells. *ZNF683* (Hobit) was upregulated in $CD16^-CD103^+$ TI-NK cells, while *LEF1* was prominent in CD16-CD103- TI-NK cells and circulating $CD56^{bright}$ NK cells (Fig. 18).

Moreover, $CD16^-CD103^+$ cells showed the highest expression of *IFNG* and *CCL5* followed by $CD16^+$ TI-NK cells. Notably, $CD16^-CD103^+$ TI-NK cells also exhibited high expression of *CCL3L1, XCL1, XCL2*, *IL32*, *CSF1* and *LTA,* as far as *IL9R*, and adhesion molecules as *CD151* and *CD9.* $CD16^+$ TI-NK cells were characterized by the high expression of cytotoxic effectors such as *GZMB*, *PRF1*, *FASL*, and *TNFSF10*, KIR receptors (e.g., *KIR2DL4*, *KIR3DL2*, *KIR3DL1*, and *KIR2DL3*), and chemokine/cytokine receptors like *CXCR1* (Fig.18).

Finally, $CD16^-CD103^-$ TI-NK cells showed high expression of *IL7R, IL23R, IL2RA, CCR7,* and *CCR8*, as well as *LEF1, CSF2, CCL22*, and *TNFSF13B*, which points to the inclusion of ILC3 cells (Fig18).

A

Code	Sex	Age	Histology	ER	HER2	TNM	Ki67	Grade	TILs
Patient 1	Female	85	CLI	+	no ampl	T2N1	50	3	5%
Patient 2	Female	50	CDI	+	no ampl	T2N0	50	3	50%
Patient 3	Male	78	mucinous	+	no ampl	T3N0		2	3%

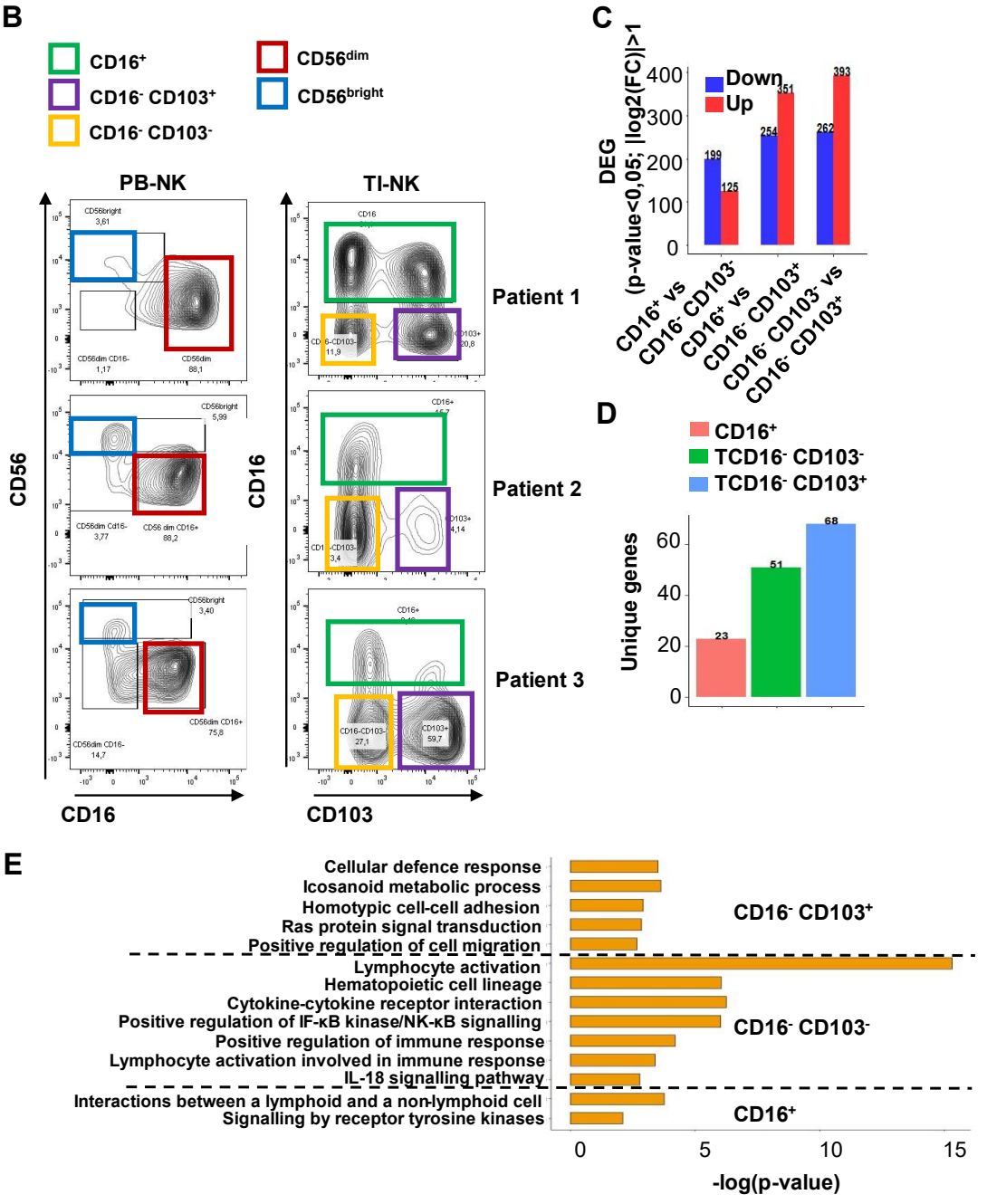

Figure 17. Transcriptomic analysis of circulating and tumor-infiltrating NK subsets. Paired blood and tumor biopsies were obtained from three breast cancer patients. RNA-seq analysis was performed on sorted NK cell subsets. **A** Patient demographics and tumor clinicopathological features. **B** Gating strategy for sorting circulating and tumor-infiltrating NK cell subsets (within DAPI- $CD45^+$ $CD56^+$ $CD3^-$ lymphocytes). **C** DEG in pairwise comparisons of the distinct tumor-infiltrating NK (TI-NK) cell subsets (p < 0.05 and |log2(fold change)|>1). **D-E)** Number of (**D**) and biological processes analysis (**E**) using unique TI-NK cell subset-specific genes (p-value < 0.05 and log2(FC) > 1 in only one of the three one-to-one comparisons).

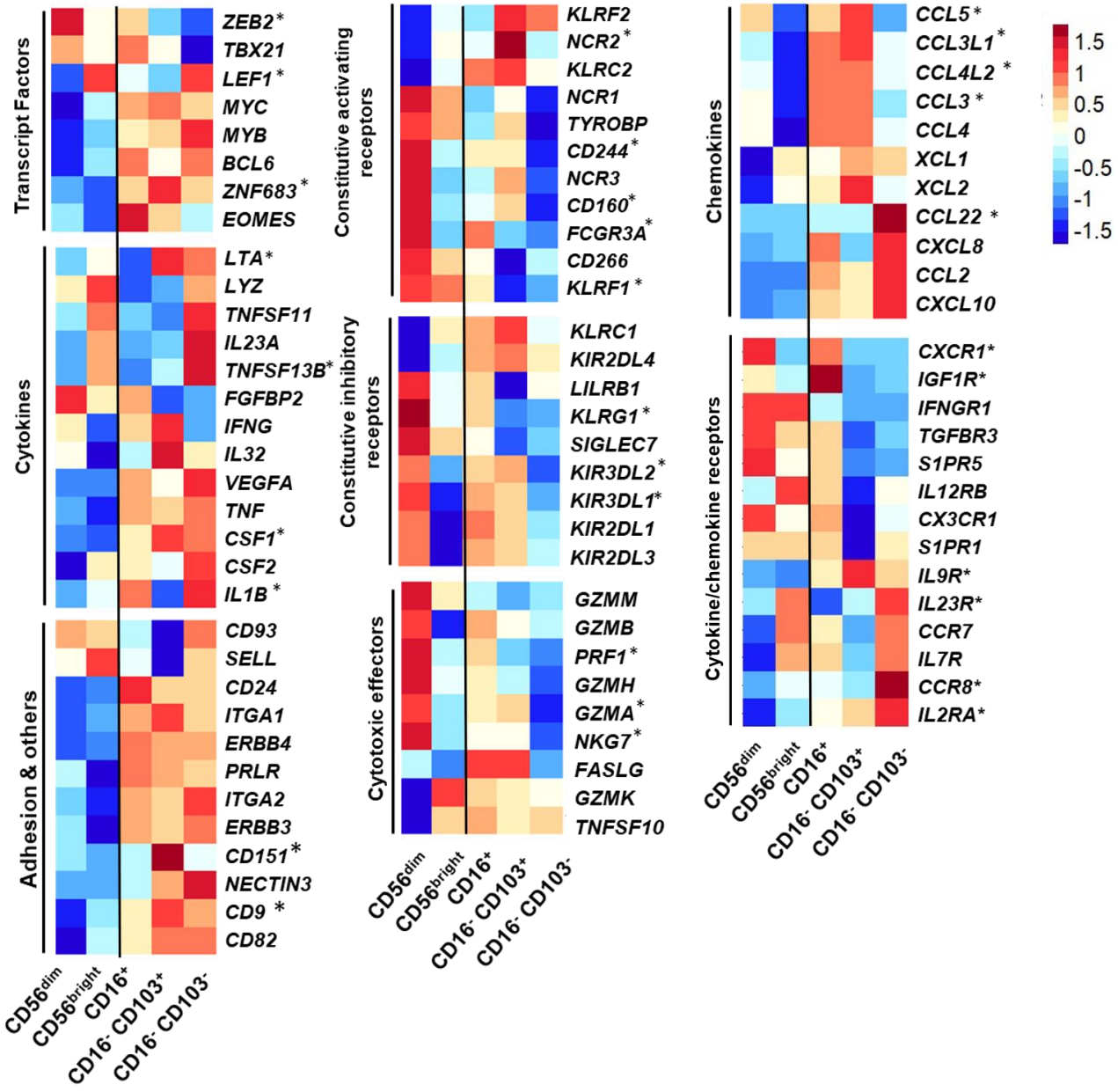

Figure 18. Transcriptomic profiling of CD16+, CD16-CD103+, and CD16-CD103- tumor-infiltrating NK (TI-NK) cell subsets and paired circulating NK cells. Total RNA was extracted from sorted $CD16^+$, $CD16^-$ $CD103^+$ and $CD16^-$ $CD103^-$ TI-NK cells (within $DAPI^-$ $CD45^+$ $CD56^+$ $CD3^-$ lymphocytes) from breast tumors as well as from $CD56^{bright}$ $CD16^-$ and $CD56^{dim}$ $CD16^+$ circulating NK cells from paired blood samples and analyzed by RNA-seq. The heatmap shows z-scores of log2 counts per million (CPM) expression of differentially expressed genes in the indicated NK cell subsets. Asterisks indicate genes differentially expressed in at least one TI-NK cell subset.

These findings were complemented by a Gene Set Enrichment Analysis (GSEA), which compared the distinct TI-NK cell transcriptomes against previously described profiles of circulating and tonsillar NK, ILC1, and ILC3 cells (187). Gene Enrichment Set Analysis (GSEA) revealed that $CD16^+$ TI-NK cell gene expression profile significantly overlapped with that of circulating $CD56^{dim}$ NK cells, $CD16^-CD103^+$ TI-NK cell aligned with ILC1 whereas $CD16^-CD103^-$ TI-NK cells resembled the immunoregulatory ILC3 population (Fig. 19).

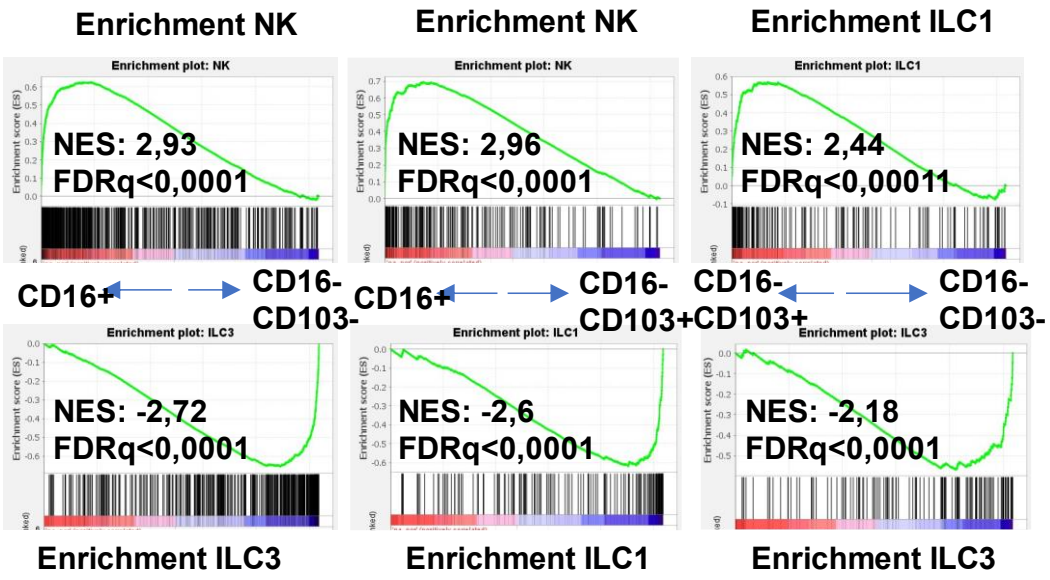

Figure 19. Gene set enrichment analysis of RNAseq data from TI-NK cell subsets compared to liver and intestinal $CD56^{dim}$ NK/ILC/ILC3 Pre-ranked gene set enrichment analysis (GSEA) was performed using RNA-seq data from the different TI-NK cell subsets and those published in (GSE78897). NES: normalized enrichment score; FDR: false discovery rate.

Altogether, these data support a lineage relationship between $CD16^+$ and $CD16^-CD103^+$ tumor-infiltrating NK cells in human breast tumors, with both subsets capable of CCL5/IFN-γ production. Furthermore, the evidence also highlighted the regulatory profile of the $CD16^-CD103^-$ subset, reminiscent of regulatory ILC3.

6. Specialized tumor-infiltrating NK cell subsets associate to distinct immune microenvironments in human breast tumors

The potential associations between the distinct tumor-infiltrating NK cell subpopulations and major T cell subsets were next evaluated by analyzing the expression of CD45, CD3, CD56, CD16, CD103, CD4, CD8, PD1, NKG2C in a prospectively collected cohort of 84 fresh breast tumor samples (Figure 20: cohort description; Figure 21: gating strategy).

Type of cohort	Prospective
Nº of patients	84
Median Age	63
Tumor size (n/%)	
T1	30 (36%)
T2	42 (50%)
T3-4	5 (6%)
NA	7 (8%)
Lymph Node status	
N0	49 (58%)
N+	27 (32%)
NA	8 (10%)
Tumor grade	
1	11 (13%)
2	36 (43%)
3	29 (35%)
NA	8 (9%)
Tumor subtype	
HRA	16 (19%)
HRB	38 (45%)
HER2	20 (24%)
TN	10 (12%)

Figure 20. Clinicopathological features of tumor specimens included in flow cytometry analysis of immune infiltrates.

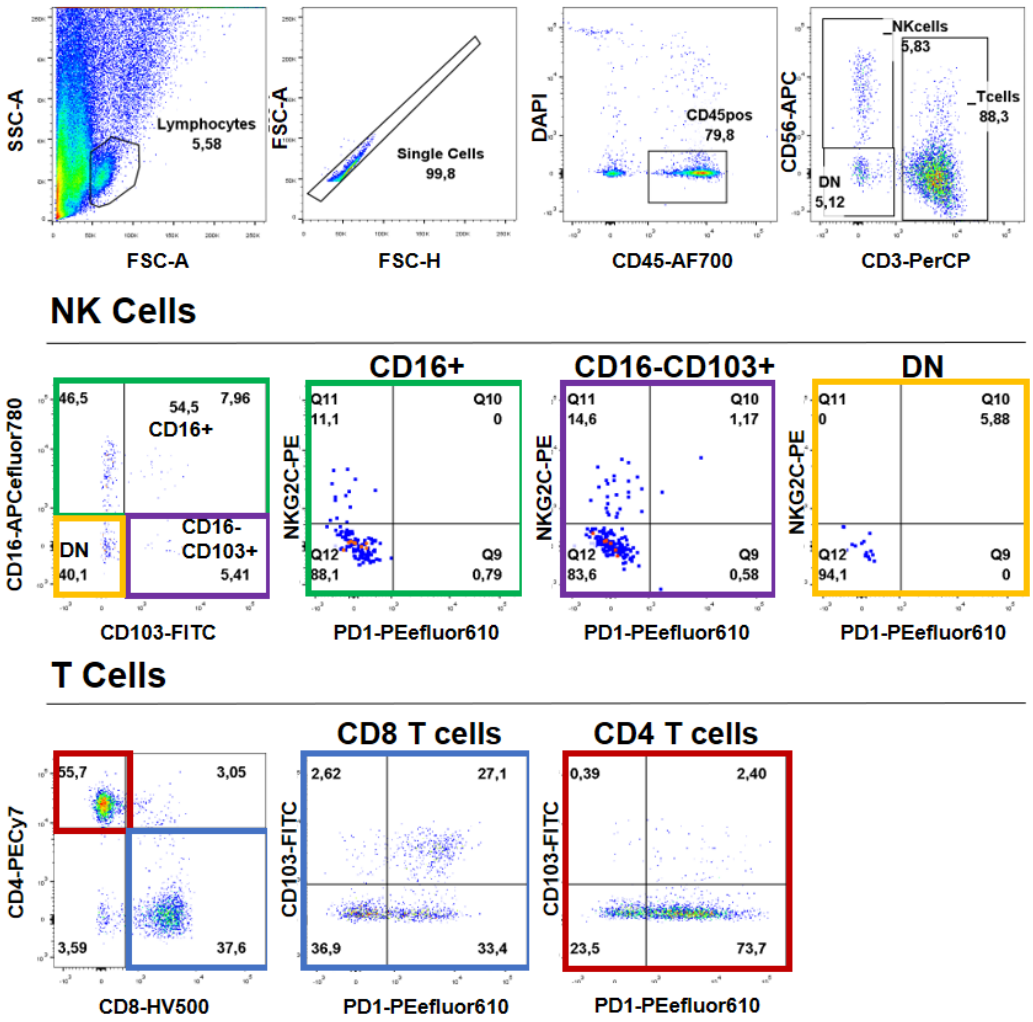

Figure 21. Gating strategy followed for analysing NK and T cell subsets in human breast tumors. Fresh breast tumor specimens (*n*=84) were processed and stained with a combination of antibodies specific for CD45, CD3, CD56, CD8, CD4, CD16, CD103, NKG2C and PD1 and analyzed by flow cytometry. DN: double negative.

Data from 18 randomly selected tumors were used for an initial t-SNE unbiased clustering analysis and PhenoGraph subsequently used for the identification of the resulting 21 clusters, which were then manually grouped into ten major lymphocyte subsets. Among NK cells, $CD16^+$ was the major subpopulation (clusters 2, 4 and 5), followed by $CD16^-CD103^-$ subset (cluster 20), and the $CD16^-CD103^+$ fraction (cluster 13). Among T cells, $CD8^+$ and $CD4^+$ T cell clusters were further subdivided into $CD103^+PD1^+$, $CD103^-PD1^+$, and $CD103^-PD1^-$ subpopulations. A significant cluster of cells was negative for all analyzed markers (cluster 3), presumably B lymphocytes (Fig. 22).

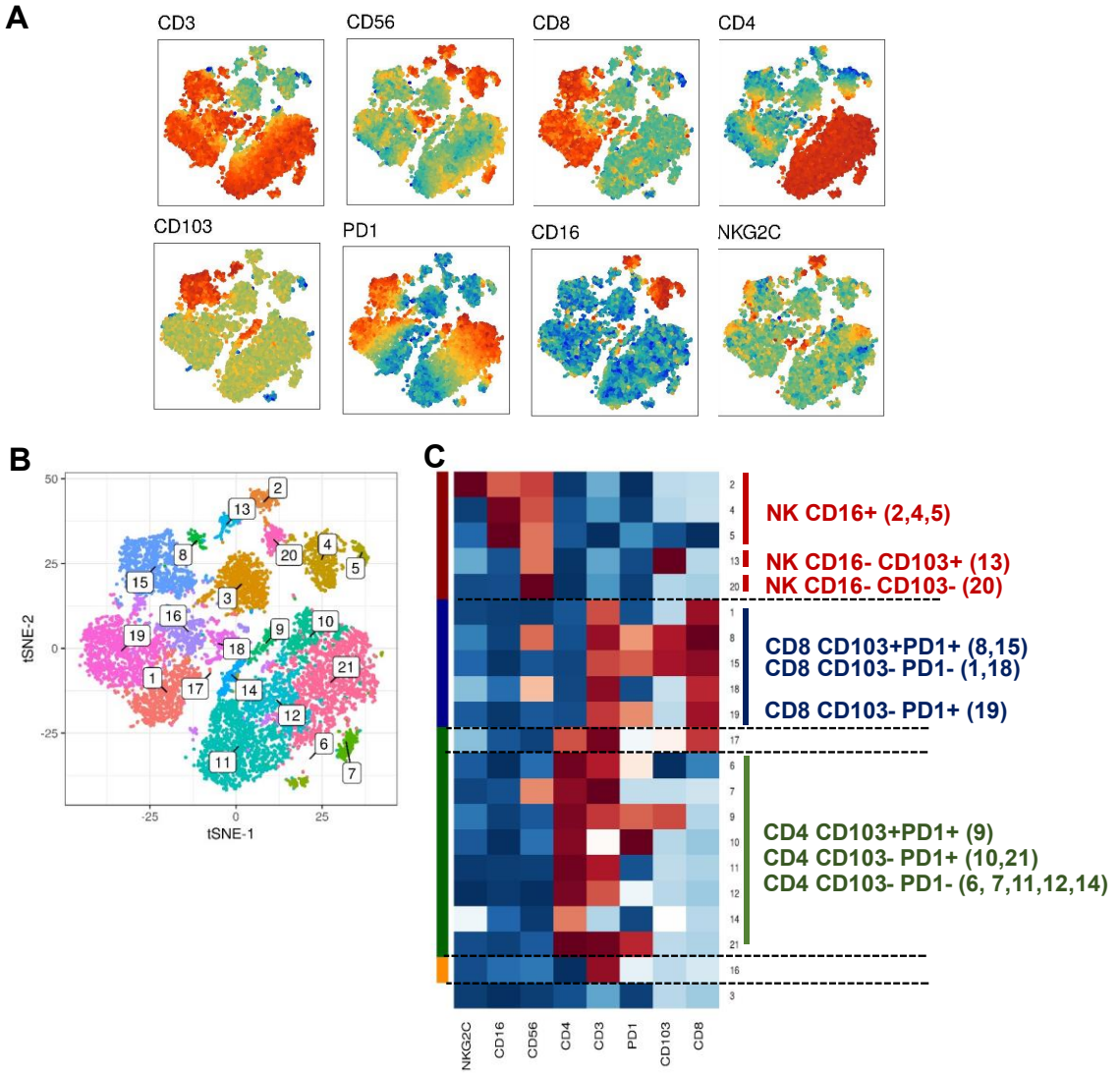

Figure 22. Unbiased identification of tumor-infiltrating lymphocyte subsets in treatment naive breast carcinomas. Fresh breast tumor specimens (*n*=18) were processed and stained with a combination of labelled antibodies specific for CD45, CD3, CD56, CD16, CD8, CD4, PD1, CD103 and NKG2C and analyzed by Flow cytometry. **A** tSNE visualization of lymphocyte subsets ($DAPI^-$ $CD45^+$) within the breast tumor immune infiltrate. **B** Phenograph clustering of lymphocyte subsets. **C** Combined phenograph and manual clustering of major lymphocyte subsets. Red and blue indicate high and low marker expression, respectively.

Data of all identified subsets were collected from the 84 analyzed tumors and the relative frequency of the three NK cell subsets was correlated with the different T cell subsets. $CD16^+$ TI-NK cells were the predominant subset (Fig. 23A) and positively correlated with total TI-NK cell abundance yet did not show any additional correlation with any other lymphocyte subset (Fig. 23B). Strong positive correlations were observed between $CD16^-CD103^+$ TI-NK cells and $CD103^+$ T cells ($CD8^+$ and $CD4^+$) (Fig. 23B). The combination of $CD16^+$ and $CD103^+$ TI-NK cells were inversely

correlated with total $CD4^+$ T cells but positively correlated with total and $CD103^+CD8^+$ T cells (Fig. 23B). In contrast, $CD16^-$ $CD103^-$ subpopulation exhibited a negative correlation with total TI-NK cells and associated with decreased CD8+, $CD103^+CD8^+$, and $CD8^+PD1^+$ T cells, and increased $CD4^+$ T cells (Fig. 23B). Similar correlations were found in the specific analysis of HER2-positive tumors (*n*=20) (Fig. 23C). Analysis by breast cancer subtypes showed no significant differences in immune subpopulation distribution across tumors (Fig. 24).

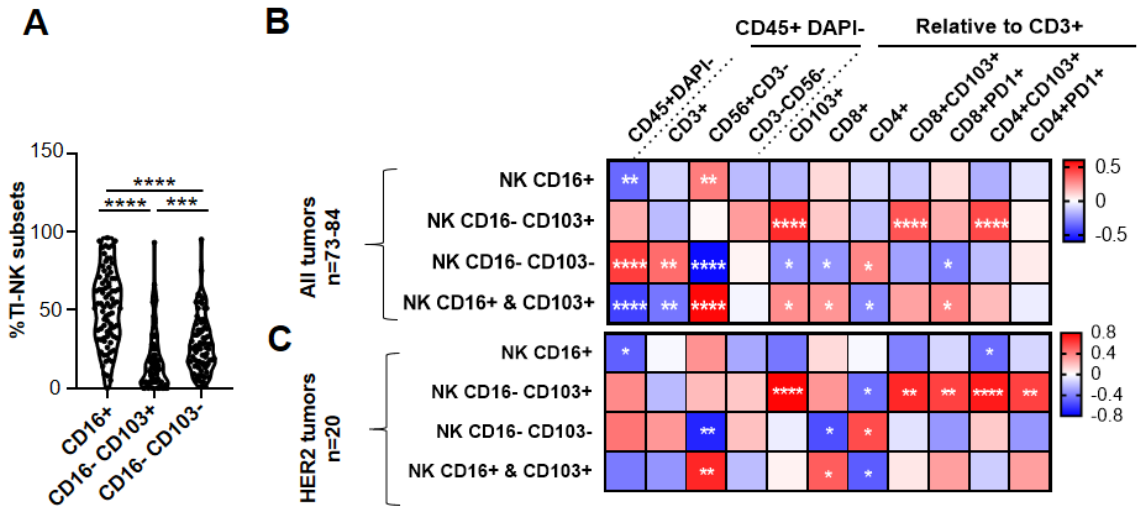

Figure 23. Association of specialized tumor-infiltrating NK cell subsets with distinct immune contexts in human breast tumors. Fresh breast tumor specimens (*n*=84) were analyzed by flow cytometry using antibodies specific for CD45, CD3, CD56, CD8, CD4, CD16, CD103, NKG2C, and PD1. **A** Frequency of $CD16^+$, $CD16^-CD103^+$, and $CD16^-CD103^-$ tumor-infiltrating NK (TI-NK) cell subsets in treatment-naive tumors. **B-C** Spearman's correlation heatmaps illustrating the correlation between TI-NK cell subsets and other major tumor-infiltrating lymphocyte subsets in **(B)** all breast tumors (*n*=73–84) and **(C)** HER2-positive tumors (*n*=20). Asterisks label significant correlations. Statistical significance is indicated as follows: ****$p < 0.0001$; ***$p < 0.001$; **$p < 0.01$; *$p < 0.05$.

In conclusion, $CD16^+$ and $CD16^-CD103^+$ TI-NK cell subsets were associated with immune infiltrates enriched in tissue-resident memory T cells, supporting their potential role in anti-tumor immunity. Conversely, the $CD16^-CD103^-$ TI-NK subset, resembling regulatory ILC3 cells, correlated with immune infiltrates characterized by elevated CD4/CD8 T cell ratios.

A

		Lum A n=16	Lum B n=38	HER 2 n=20	TN n=10	p
	CD45+ DAPI-	2.6 (0.4-6.5)	6.8 (0.3-39.6)	3.8 (0.18-17.1)	6.6 (0,4-33.3)	0.27
CD45+ DAPI-	T cells (CD3+)	75.9 (31.5-97.3)	79.7 (38.4-94.5)	80.3 (50.4-89.3)	71.3 (20.7-88.8)	0.306
	NK cells (CD56+CD3-)	7.9 (0.5-30.3)	6.2 (1.2-23.8)	8 (1.3-19.1)	8.8 (1.4-40.7)	0.583
	CD3+CD56-	10.18 (0.8-23.1)	12.15 (1.9-55.3)	9.8 (2.1-36.1)	17.6 (4-35.3)	0.164
CD56+ CD3-	CD16+ NK	68.1 (33.2-92.9)	53.9 (19.9-94.7)	46.9 (9.2-92.8)	50.5 (6.7-83.7)	**0.048**
	CD103+CD16- NK	16.3 (0-43.6)	24 (3.2-75)	28.1 (2.2-67.7)	31.5 (3.3-96.8)	0.381
	CD16-CD103- NK	23 (5.7-55.2)	28.5 (4.9-82.1)	28.4 (0-76.6)	24.5 (1.2-52.4)	0.835
	CD16+&CD103+ NK	79.2 (44.8-100)	72 (17.9-95.1)	71.8 (23.4-100)	75.5 (47.6-98.8)	0,599
CD3+	CD103+ T	24.9 (0.5-67.1)	20.6 (6.2-55)	24 (1.4-79.3)	22.2 (13.4-44.5)	0.840
	CD8+ T	43.3 (23.5-78.2)	41.9 (22.6-62.1)	42.9 (15.5-81.2)	35.1 (22.4-51.7)	0.323
	CD4+ T	49.6 (15.8-74.3)	51 (31.8-74.2)	50.6 (10.6-79)	57.4 (39.3-76)	0.417
	CD8+ CD103+ T	19.8 (0.5-66.7)	15.2 (2.5-46.5)	19.5 (2.2-76.3)	15.3 (7.2-28)	0.933
	CD8+ PD1+ T	33.8 (19.4-75.6)	28 (1.2-57.1)	31.3 (11.2-81.2)	26.5 (16-46.2)	0.753
	CD4+ CD103+ T	2.9 (0.2-6.1)	4.2 (1.1-11.9)	4 (0.8-9.8)	5 (1.5-8)	0.154
	CD4+ PD1+ T	36.1 (12.4-56.6)	38.7 (1-62.6)	36.7 (10.8-76.8)	45 (34.5-56.6)	0.126

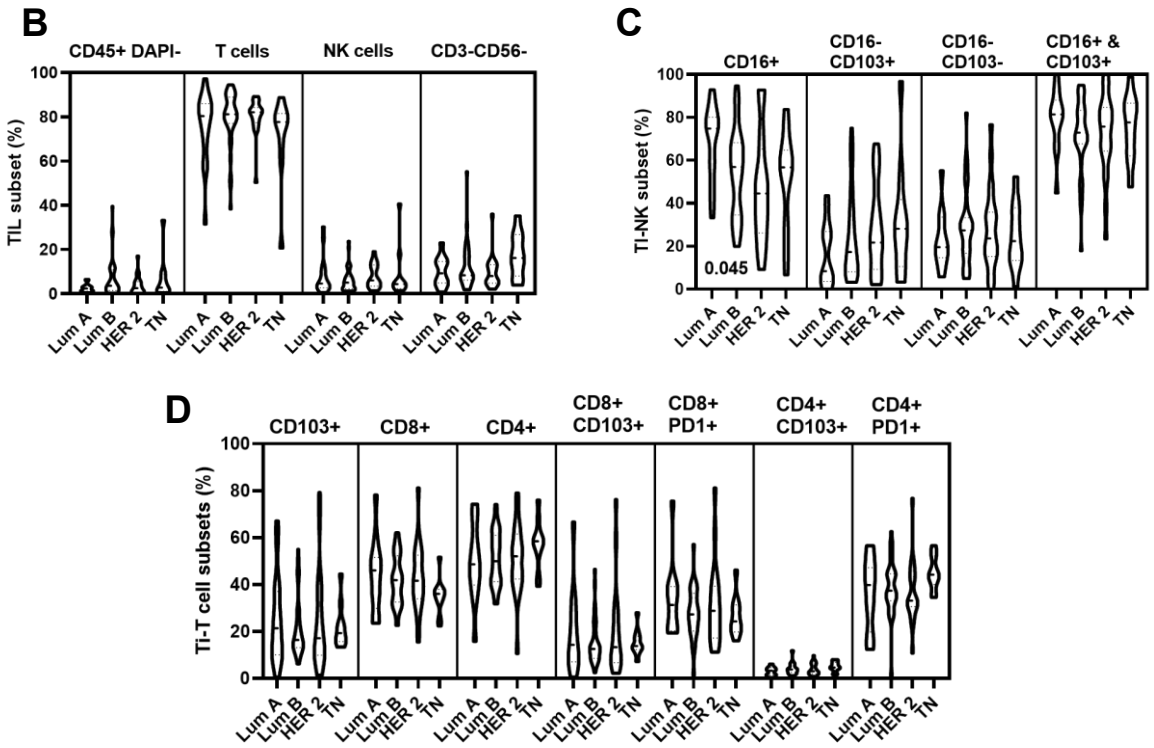

Figure 24. Immune infiltrate composition across breast cancer subtypes. Fresh breast tumor specimens (*n*=84) were processed and stained with a combination of antibodies specific for CD45, CD3, CD56, CD8, CD4, CD16, CD103, NKG2C and PD1 and analyzed by flow cytometry. **A** Median (range) percentage of the indicated lymphocyte subsets in tumors stratified by molecular subtype. Significant differences are indicated. **B-D** Distribution of the indicated lymphocyte subsets across molecular subtypes, shown as violin plots.

7. Early increase in serum CCL5/CXCL9 as an early predictor of response to neoadjuvant anti-HER2 therapy in HER2-positive breast cancer patients with NK cell-rich tumors

We next explored whether changes on CCL5/IFN-γ-CXCL9/CXCL10 cytokines could be detected at systemic level, thus serving as a potential biomarker for treatment response.

A

Type of Cohort	Baseline	Post-Chemo
Nº of patients	79	32
Mean Age	58	57
Tumor size (n/%)		
T1-2	63 (80%)	29 (91%)
T3-4	8 (10%)	3 (9%)
NA	8 (10%)	0
Lymph Node status (n/%)		
N0	30 (38%)	11 (34%)
N+	44 (56%)	21 (66%)
NA	5 (6%)	0
Histological type (n/%)		
DIC	69 (87%)	29 (91%)
Others	10 (13%)	3 (9%)
Histological Grading (n/%)		
G1-G2	38 (48%)	11 (34%)
G3-4	33 (42%)	20 (63%)
NA	8 (10%)	1 (3%)
Hormonal status		
ER+	57 (72%)	23 (72%)
ER-	22 (28%)	9 (28%)
PR+	38 (48%)	17 (53%)
PR-	41 (52%)	15 (47%)
Ki 67 index (n/%)		
<20%	9 (11%)	2 (6%)
≥20%	63 (79%)	30 (94%)
NA	8 (10%)	0
Anti-HER2 (n/%)		
Trastuzumab	38 (48%)	14 (44%)
Dual anti-HER2	41 (52%)	18 (56%)
Chemo regimen (n/%)		
Anthracyclines	43 (54%)	26 (81%)
Taxanes	9 (11%)	5 (16%)
NA	27 (34%)	1 (3%)
pathological Clinical Response		
pCR	37 (47%)	18 (56%)
no pCR	42 (53%)	14 (44%)

B

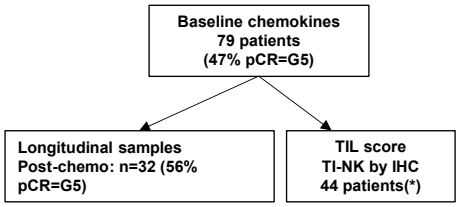

Figure 25. Clinical features of HER2-positive breast cancer patients undergoing neoadjuvant anti-HER2 therapy included in serum chemokine analysis. CCL5, CXCL9, and CXCL10 levels were measured by ELISA in longitudinal serum samples collected before treatment (baseline, *n*=79) and after 3 chemotherapy cycles (post-chemo, *n*=32). Data from TILs and TI-NK cells was available for 44 tumor biopsies. **A** Clinicopathological features of the patients included in the serum chemokine analysis. **B** Scheme indicating the number of baseline and paired longitudinal serum samples for each time point; the percentage of pathological complete response (pCR) in each patient group; and patients with TILs and TI-NK cell data available. DIC: ductal carcinoma; ER: estrogen receptor; PR: progesteron receptor.

For this purpose, serum samples from a cohort of HER2-positive breast cancer patients were prospectively collected at baseline (*n*=79) and following three cycles of neoadjuvant chemotherapy (*n*=32). Data on TIL scores and TI-NK cell numbers was available for some cases (*n*=44) (112) (Fig. 25).

CCL5, IFN-γ, CXCL9, and CXCL10 serum levels were measured by ELISA analysis. IFN-γ was not detected in any serum sample (data not shown). For assessing the reliability and reproducibility of CCL5, CXCL9, and CXCL10 ELISA assays, a subset of 34 samples was subjected to independent, duplicate testing. The results demonstrated a high degree of concordance between the replicate measurements, confirming the robustness and reproducibility of the determination (Fig. 26).

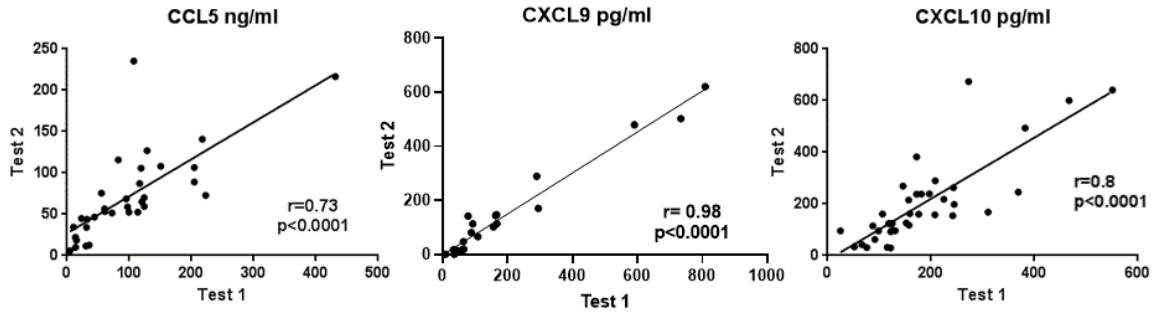

Figure 26. Inter-assay reproducibility of serum CCL5, CXCL9, and CXCL10 ELISA measurements. Chemokine levels in 34 serum samples were measured by ELISA in two independent ELISA assays. Pearson's correlation coefficients are shown for the two independent assays of each sample.

Analysis of serum CCL5, CXCL9 and CXCL10 levels revealed no statistically significant differences at baseline or after three cycles of neoadjuvant chemotherapy when comparing patients who achieved pathological complete response (pCR) (G5), those with a good response (G4), and those with poor responses (G1-G3) (Fig. 27).

	Baseline			
	G1-3 n=27	G4 n=15	G5 n=37	p
CCL5 (ng/ml)	82 (6-174)	81 (18-223)	76 (7-201)	ns
CXCL10 (pg/ml)	156 (37-626)	163 (66-363)	162 (13-1215)	ns
CXCL9 (pg/ml)	232 (0-1924)	316 (0-724)	383 (0-1489)	ns

	Post Chemotherapy			
	G1-3 n=8-9	G4 n=6	G5 n=17	p
CCL5 (ng/ml)	79 (5-137)	122 (19-217)	126 (14-265)	ns
CXCL10 (pg/ml)	159 (66-280)	154 (76-340)	191 (6-664)	ns
CXCL9 (pg/ml)	273 (60-646)	116 (0-386)	200 (0-1264)	ns

Figure 27. Serum chemokine levels in HER2-positive breast cancer patients. Systemic CCL5, CXCL9, and CXCL10 levels were measured by ELISA in serum samples collected at diagnosis (baseline) and after three months of neoadjuvant chemotherapy (post-chemotherapy). Data are stratified by response to neoadjuvant anti-HER2 therapy according to Miller-Payne criteria. Statistical analysis was performed using a Kruskal-Wallis test. Median (minimum and maximum) chemokine levels for each group are shown in parentheses.

However, patients exhibiting favorable responses to treatment (G4 and G5 groups) showed a coordinated increase in all three chemokines (CCL5, CXCL9, CXCL10) after three chemotherapy cycles as compared to those with poor responses (G1-G3) (Fig. 28).

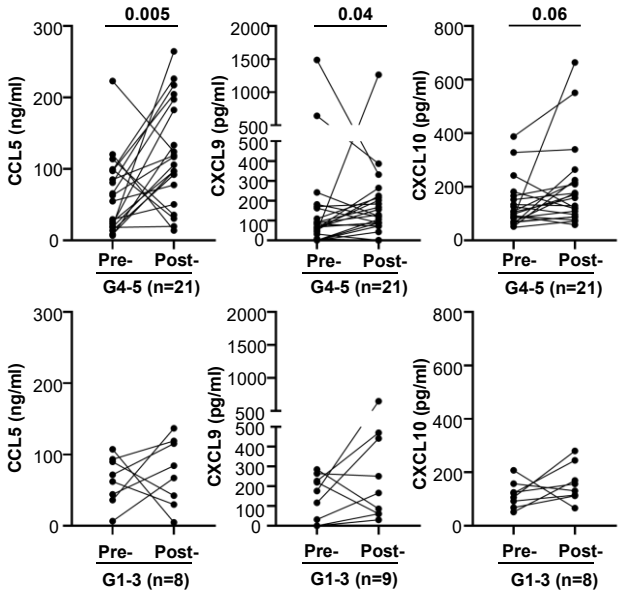

Figure 28. Early increase in serum chemokine levels as potential biomarkers of response to neoadjuvant anti-HER2 therapy in HER2-positive breast cancer. CCL5, CXCL9, and CXCL10 levels were measured by ELISA in paired baseline (pre-treatment) and post-chemotherapy serum samples from patients undergoing neoadjuvant anti-HER2 therapy. Patients were stratified as good (G4 and 5) or poor (G 1-3) responders. Statistical significance was determined by Mann-Whitney U test.

Remarkably, high numbers of TI- NK cells were present in the diagnostic tumor biopsies of patients who achieved pCR (G5 group) (Fig. 29A), positively correlating with systemic levels of CCL5 and CXCL9 post-chemotherapy (Fig. 29B).

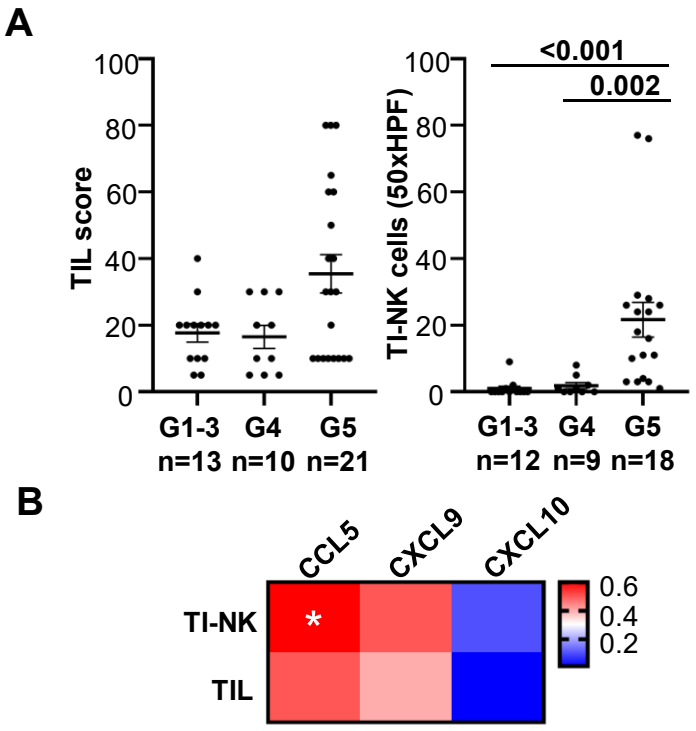

Figure 29. Correlation of systemic chemokines with tumor-infiltrating NK (TI-NK) cells. A TIL score and TI-NK cell numbers in diagnostic biopsies of the analyzed cohort, stratified by Miller-Payne response grade. Statistical significance was determined by the Mann-Whitney U test. B Spearman's correlation coefficient between baseline TIL score and TI-NK cell numbers, and post-chemotherapy CCL5, CXCL9, and CXCL10 levels. Significant correlations are indicated by an asterisk.

Collectively, these results underscore the pivotal role of TI-NK cell activation by anti-HER2 antibodies as a key driver of CCL5/IFNG-CXCL9/10 axis and the subsequent recruitment of additional immune effectors, ultimately contributing to the therapeutic benefits of anti-HER2 antibodies.

Aim 2

1. Association between the CD16A-158V/F genotype and clinical response to neoadjuvant anti-HER2 antibody treatment

We have previously described two potential biomarkers for response to neoadjuvant treatment with anti-HER2 antibodies in HER2-positive breast cancer patients: the CD16A-158 V/F polymorphism and the percentage/numbers of $CD57^{+}$ NK cells (148). In this work, the described biomarkers were reassessed by analyzing a new cohort of HER2-positive breast cancer (BC) patients (*n*=74) undergoing neoadjuvant treatment with anti-HER2 antibodies as a validation cohort. The combined data from the originally described cohort (148) and the one here presented, showing similar clinicopathological characteristics (Fig. 30), was also analyzed to increase the overall cohort size.

	Discovery	Validation	Total
Patients (n)			
	66	74	140
Age mean (years)			
	58	60	59
Tumor size (n)			
T1-T2	51 (77%)	47 (64%)	94 (67%)
T3-T4	15 (23%)	22 (30%)	37 (27%)
Lymph node status (n (%))			
N0	25 (38%)	37 (50%)	62 (45%)
N+	41 (61%)	35 (47%)	75 (54%)
Ki67 index (n (%))			
<20%	8 (12%)	10 (14%)	18 (13%)
≥20%	57 (86%)	59 (80%)	115 (82%)
pCR (n (%))			
Yes	27 (41%)	32 (43%)	59 (42%)
No	37 (56%)	39 (53%)	78 (56%)
DFS			
Median (IQR)	92.7 (85-101)	60.2 (35-68)	79.2 (56-96)

Fig. 30. Characteristics of the HER2-positive breast cancer patient cohorts included in the study. A Discovery cohort as previously described in Muntasell et al (148). The validation cohort includes new patients prospectively recruited. Total cohort is the combination of both.

The distribution of the CD16A-158V/F genotype conformed to the Hardy–Weinberg equilibrium in all cohorts (Fig 31), even though the F/V:F/F ratio was higher in the validation cohort compared to the discovery cohort.

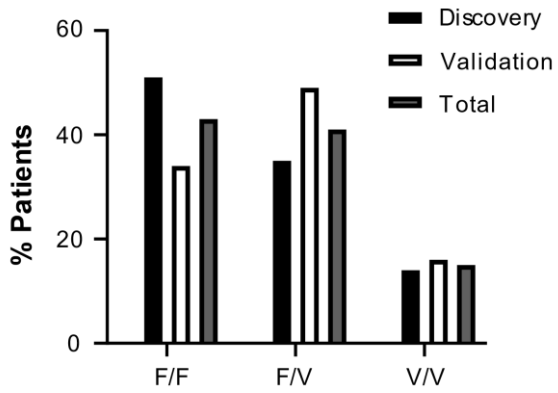

Fig. 31. Distribution of CD16 158 V/F genotypes in the three cohorts evaluated. Discovery cohort: *n*=61 MAF:0.33; Validation cohort: *n*=61 MAF:0.38; Total cohort: *n*=122 MAF:0.34. (MAF: minor allele frequency).

Patients with the F/F genotype from the discovery cohort showed a lower likelihood of achieving pCR in comparison with those with the F/V genotype. However, no difference was observed between F/F and V/V genotypes, likely due to the small number of V/V patients analyzed (n=8) (Fig. 32A). In contrast, in the validation cohort, V/V homozygous patients showed a significantly higher likelihood of achieving pCR compared to both F/V and F/F genotypes (Fig. 32B), a finding confirmed in the combined analysis of both cohorts (Fig. 32C).

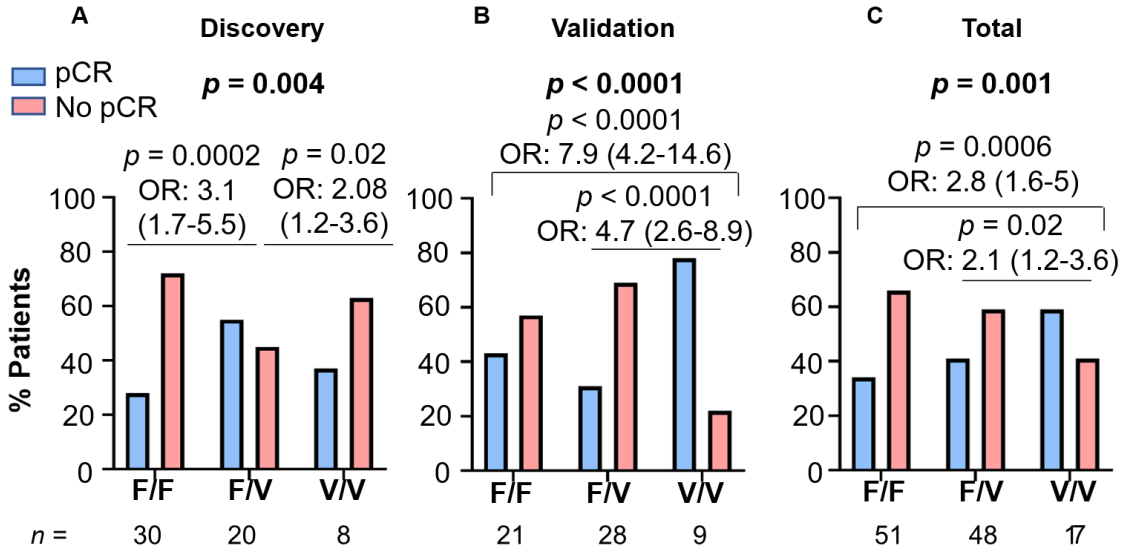

Fig. 32. Association between CD16A-158V/F genotype and pCR achievement. Proportion of patients grouped according to their CD16A-158V/F genotype and stratified based on pCR achievement. Significant *p*-values, Odds Ratios (OR) and 95% Confidence Interval (in parenthesis) are indicated by Fisher's exact test. Bold *p*-values correspond to the overall significance according to Chi-square. **A** Discovery cohort. **B** Validation cohort. **C** Total cohort.In all graphs n indicate the absolute number of patients for each genotype.

The influence of the CD16A-158V/F genotype on disease-free survival (DFS) and overall survival (OS) was also investigated by comparing DFS and OS across all three genotypes and by grouping patients carrying at least one copy of the CD16A-158V allele. Patients with the low affinity F/F genotype showed higher risk of relapse compared to those with F/V or V/V genotypes (Fig. 33). While similar trends were observed in both cohorts individually, statistical significance was reached when data from both cohorts were combined, with F/F genotype associated with 7.24-fold increased risk of relapse than patients carrying the V allele (Fig. 33C). The lower number of relapses observed in the validation cohort compared with the discovery cohort is likely influenced by the clinical shift in adjuvant therapy, as from 2019 non-pCR patients received trastuzumab-emtansine (T-DM1) instead of trastuzumab, following the results of the KATHERINE trial (135).

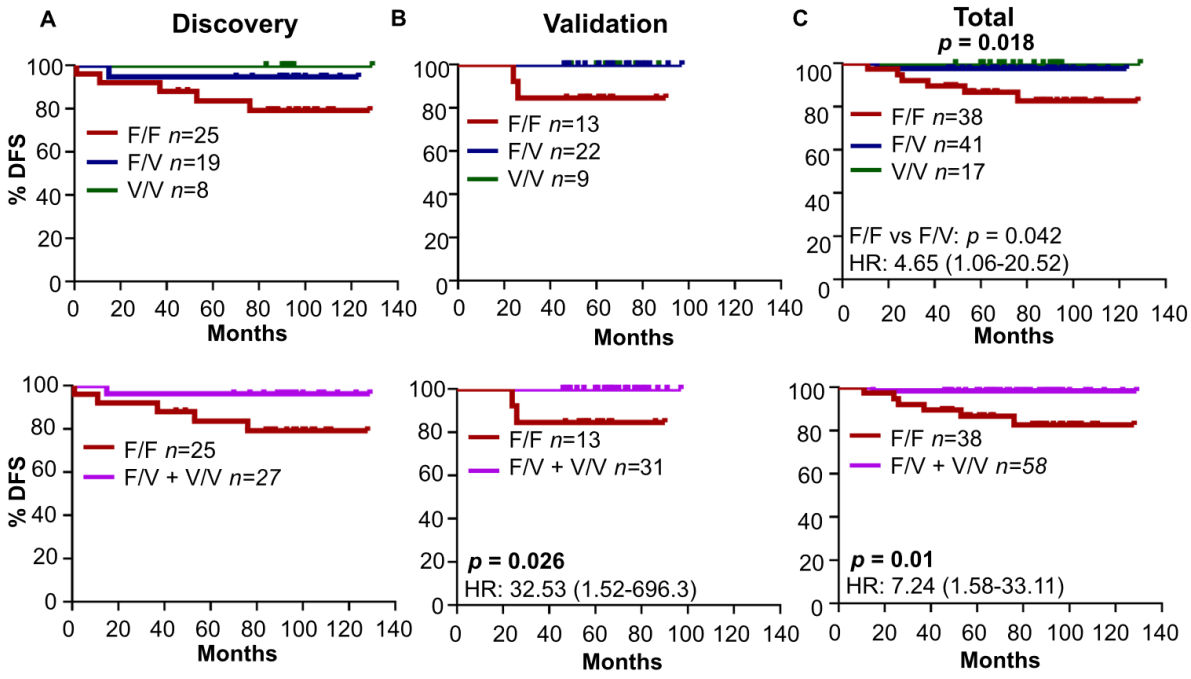

Fig. 33. Association between CD16A-158V/F genotype and DFS. Patients were grouped according to their CD16A-158V/F genotype and by grouping patients carrying at least one V allele. Log-rank test for trend was used for statistical analysis in three group comparisons. Log-rank test (Mantel-Cox) was used in two group comparisons. Statistically significant *P* values, Hazard Ratios (HR) and 95% Confidence Interval (in parenthesis) are indicated. **A** Discovery cohort. **B** Validation cohort. **C** Total cohort.

The association of CD16A-158 V/F genotype with OS showed similar results (Fig. 34). Altogether, these results indicate that patients with primary HER2-positive breast cancer who carry the CD16A-158V allele display higher rates of pCR and lower risk of relapse after neoadjuvant treatment with anti-HER2 antibodies, compared to patients with the F/F genotype.

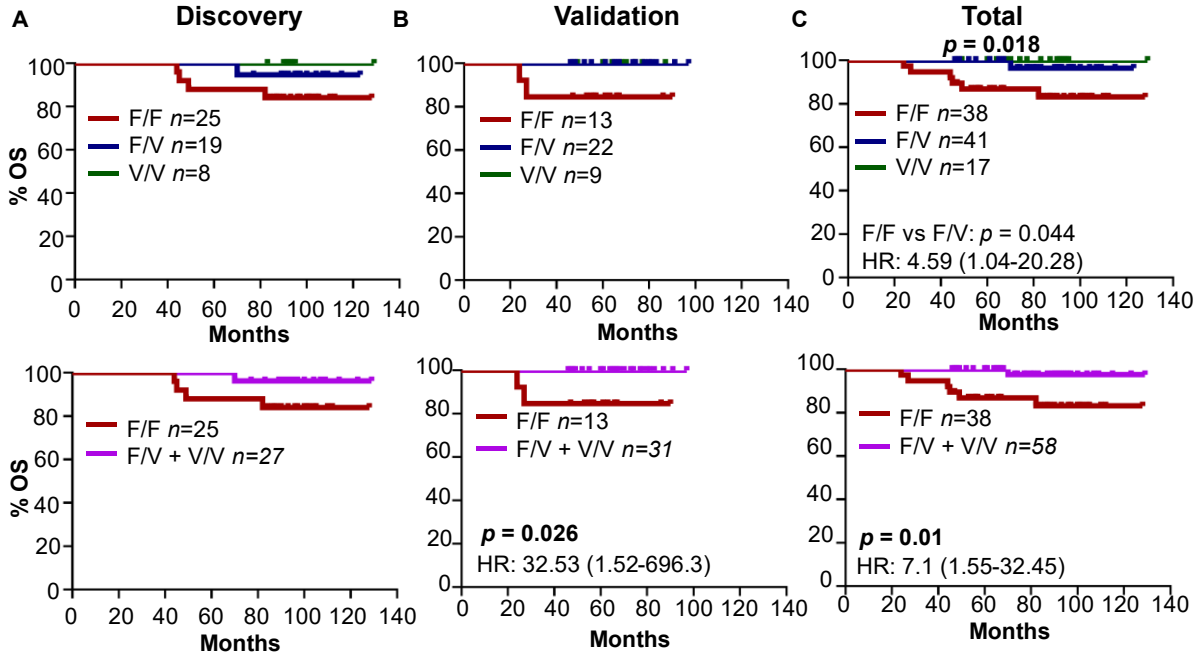

Fig. 34. Association between CD16A-158V/F genotype and OS. Patients were grouped according to their CD16A-158V/F genotype and by grouping patients carrying at least one V allele. Log-rank test for trend was used for statistical analysis in three group comparisons. Log-rank test (Mantel-Cox) was used in two group comparisons. Statistically significant *P* values, Hazard Ratios (HR) and 95% Confidence Interval (in parenthesis) are indicated. **A** Discovery cohort. **B** Validation cohort. **C** Total cohort

2. Reassessment of circulating CD57⁺ NK cells as a biomarker of resistance to neoadjuvant anti-HER2 antibody treatment

The second set of biomarkers previously described included the proportion and absolute numbers of circulating CD57⁺ NK cells, which showed an inverse association with pCR achievement (148). With the objetive of validating both biomarkers of primary resistance to anti-HER2 antibodies, percentages and absolute numbers of CD57⁺ NK cells were analyzed in the validation cohort, together with NKG2C and NKG2A receptors by multiparametric flow cytometry (Fig.35).

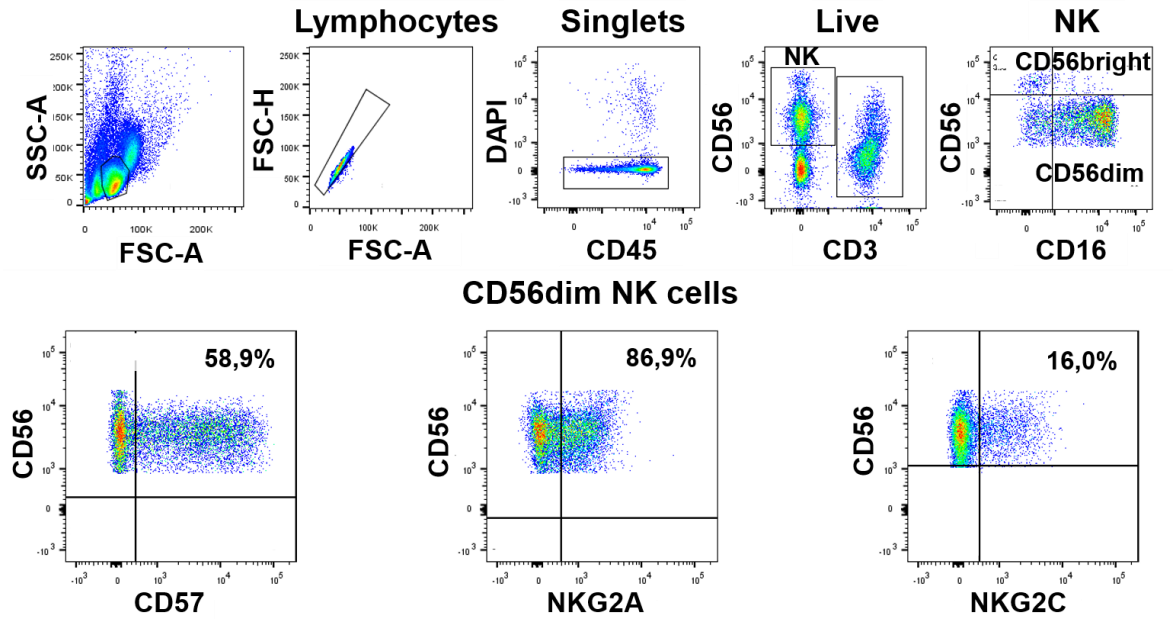

Fig. 35. Gating strategy for the characterization of circulating NK cell repertoire in HER2-positive breast cancer. PBMC were isolated from blood of HER2-positive breast cancer patients, stained for CD45, CD56, CD3, CD16, CD57, NKG2A and NKG2C and analyzed by flow cytometry. Every marker was analyzed in the CD56dim NK cell population following the indicated strategy.

As for the CD16A-158F/V genotype, the analysis of the NK cell repertoire and clinical outcomes was performed in each patient cohort by separate and upon combination. In agreement with our original report, no differences in the percentage and absolute number of circulating NK and T cells nor in the distribution of the circulating $CD56^{bright}$ and $CD56^{dim}$, $CD16^{+}$, $NKG2C^{+}$ and $NKG2A^{+}$ NK cell subsets were detected between patients achieving or not pCR (Fig.36 and data not shown).

		Discovery			Validation			Total		
	Marker	pCR	No pCR	*p*	pCR	No pCR	*p*	pCR	No pCR	*p*
	% NK	12,5 (4-37)	16,5 (4-47)	0.07	12,1 (3-40)	12,3 (3-40)	0.70	12,3 (3-37)	14 (3-47)	0.23
	% CD56dim NK	93,6 (67-99)	94,7 (80-98)	0.15	93,4 (86-100)	91,6 (70-98)	0.07	93,4 (67-100)	93,3 (70-98)	0.80
	% CD56bright NK	6,2 (1-33)	5,1 (1-19)	0.16	6,6 (0-14)	8,4 (2-26)	0.06	6,6 (0-33)	6,7 (1-26)	0.89
CD56dim NK	%CD16	91,7 (31-99)	93,3 (75-99)	0.28	92,1 (66-98)	89,8 (54-96)	0.25	91,9 (31-99)	91,9 (54-99)	0.99
CD56dim NK	%NKG2A	44,8 (14-70)	40,6 (13-75)	0.33	28,9 (1-62)	43,5 (2-98)	0.07	41,6 (1-70)	41,9 (2-98)	0.40
CD56dim NK	%NKG2C	17,1 (0-66)	11,4 (0-73)	0.47	9,9 (0-76)	9,9 (0-91)	0.90	12,1 (0-76)	11 (0-91)	0.87

Fig. 36. Association between between NK markers and pCR achievement. The mean percentage of each marker is indicated (minimum-maximum). Patients were grouped by pCR achievement. No comparison was statistically significant using the Mann-Whitney U test (*p* is indicated).

Analyses of the validation cohort did not confirm the association between the frequency and absolute numbers of CD57⁺ NK cells and the rate of pCR (Fig. 37B), observed in the discovery cohort (Fig.37A). However, when both cohorts were combined, the significant association between a high percentage of CD57⁺ NK cells and lower pCR rates persisted (Fig. 37C).

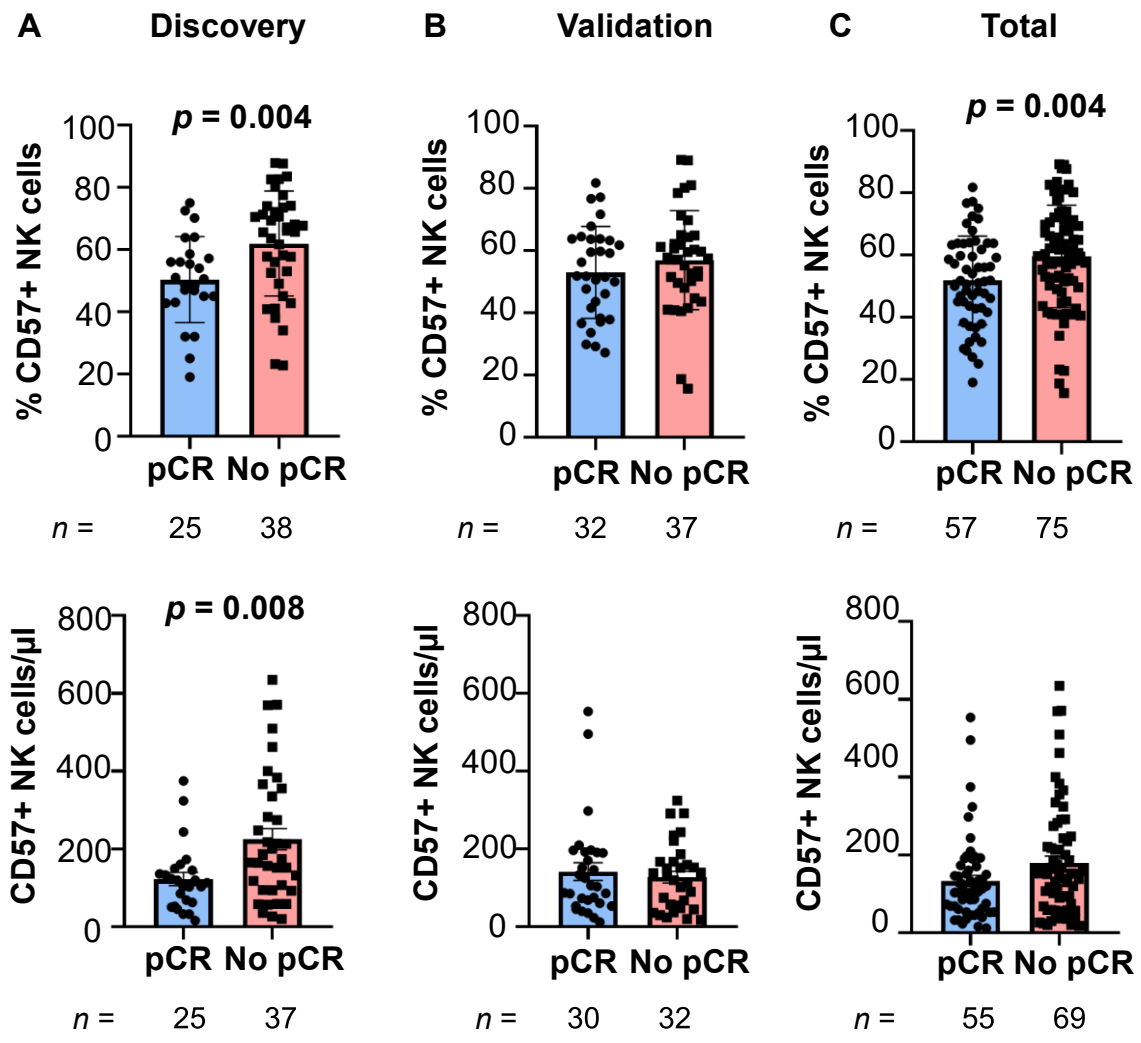

Fig. 37. Association between CD57⁺ NK cell numbers and pCR achievement. Patients were grouped according to their $CD56^{dim}$ CD57⁺ percentage or absolute numbers and divided in two groups depending on the achievement of pCR. Statistical significance by Mann-Whitney test is indicated. **A** Discovery cohort. **B** Validation cohort. **C** Total cohort.

For the analysis of the potential impact of CD57$^+$ NK cells on long-term clinical outcomes (DFS and OS), the clinical follow-up for all patients was updated and patients were stratified based on high and low CD57$^+$ NK cells, based on the previously described thresholds (148). An association between high numbers and percentages of CD57$^+$ NK cells and increased risk of relapse was observed in the discovery cohort (Fig. 38A) yet not supported by data from the validation cohort (Fig. 38B). In the combined analysis, frequencies of CD57$^+$ NK cells but not their absolute numbers showed a significant impact on the probability of DFS (38C).

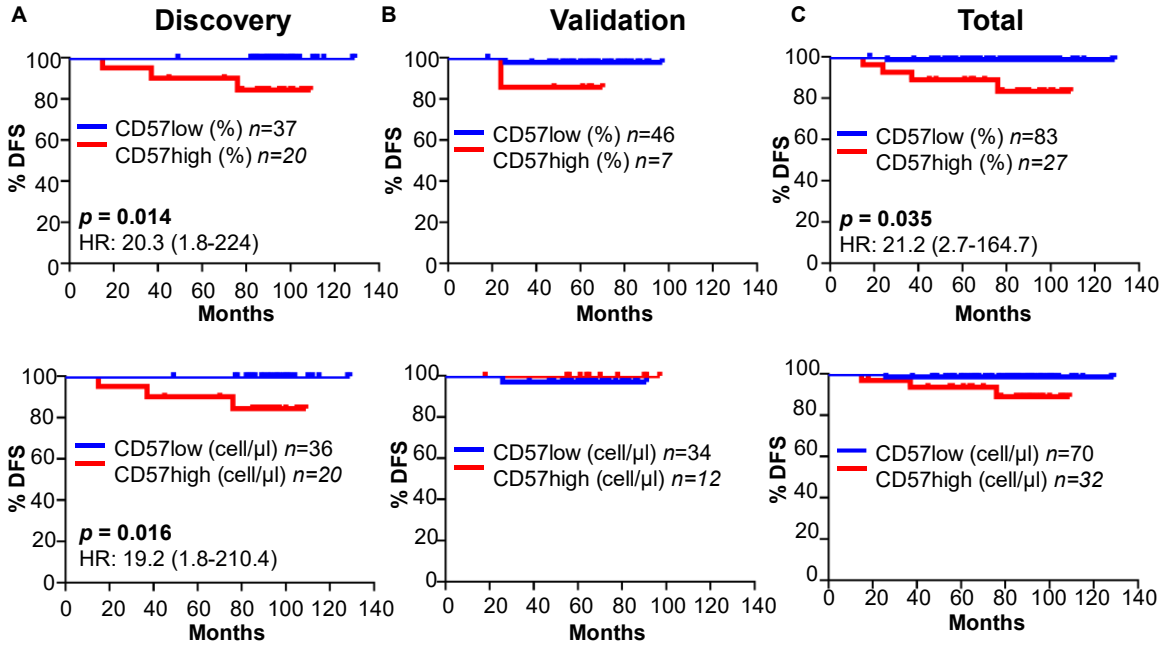

Fig. 38. Association between CD57$^+$ NK cell frequency and numbers and DFS. Patients were stratified based on either the 65% of CD57$^+$CD56^{dim} NK cell (top) or 164 CD57$^+$ CD56^{dim} NK cells/ul (bottom) thresholds or (left). **A** Discovery cohort. **B** Validation cohort. **C** Total cohort.

The analysis of overall survival (OS) largely mirrored the results for DFS (Fig. 39). Statistical significance for the association between the frequency of CD57$^+$ NK cells and OS was observed in the discovery cohort (Fig. 39A) and in the combined cohort analysis (Fig. 39C), but not in the validation cohort (Fig. 39B).

The lack of significance of the association in the validation cohort may be attributed to the low number of relapse events in the validation cohort (*n*=2).

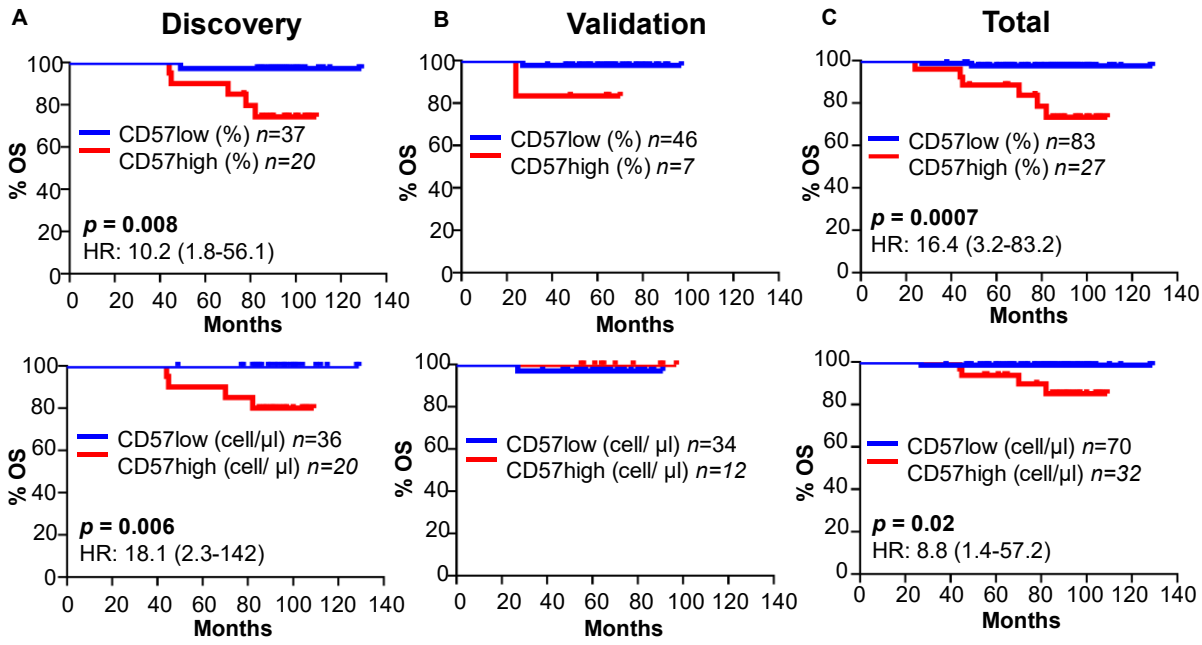

Fig. 39. Association between CD57+ NK cell frequency and numbers and OS. Patients were stratified based on either the 65% of $CD57^{+}CD56^{dim}$ NK cell (left) or 164 $CD57^{+}$ $CD56^{dim}$ NK cells/ul (top) thresholds or (bottom). **A** Discovery cohort. **B** Validation cohort. **C** Total cohort.

3. CD16A-158F/F genotype and high $CD57^{+}$ NK cells as biomarkers of relapse among patients failing to achieve pCR

On a patient level, pCR is strongly correlated with improved long-term outcomes (132,190) (Fig. 40). This was sustained in both patient cohorts, where there as an association between pCR and DFS (Fig. 40). In the validation cohort, the association did not reach statistical significance, but the two relapses documented occurred in patients failing to achieve pCR (Fig. 40).

We next investigated whether the CD16A-158F/V genotype and the frequency of $CD57^{+}$ NK cells could help identifying patients at increased risk of relapse among those who did not achieve pCR following neoadjuvant therapy. DFS data were first analyzed by stratifying patients according to pCR status and CD16A-158V/F genotype. Remarkably, within the No pCR group, patients with the low affinity F/F genotype had a higher risk of relapse than carriers of the V allele in the total cohort

[*p*=0.03, HR: 7.3 (95%CI: 1.7-32.5)]. Conversely, carriers of the V allele displayed a lower relapse risk regardless of pCR status (Fig. 41A). Indeed, no relapses occurred among patients with the V/V genotype during follow-up (data not shown). A similar analysis stratifying patient by pCR status and $CD57^+$ NK cells showed that among non-pCR patients, those with high $CD57^+$ NK cell frequencies had an increased risk of relapse, reaching statistical significance only in the combined cohort [p=0.03, HR:7.4 (95%CI: 1.2-46.5)] (Fig. 41B).

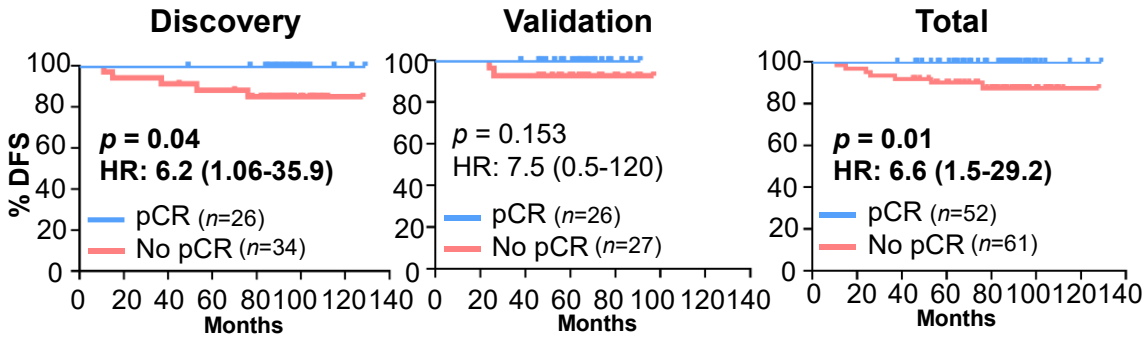

Fig. 40. Association of pCR and DFS. DFS was analyzed in patients stratified by pCR achievement. Log-rank test (Mantel-Cox) was used for statistical analysis. *P* values, Hazard Ratios (HR) and 95% Confidence Interval (in parenthesis) are indicated.

These findings strongly support the value of CD16A-158V/F dimorphism as a prognostic biomarker for long-term outcomes in HER2-positive BC patients treated with anti-HER2 antibodies, particularly among those who do not achieve pCR following neoadjuvant treatment. Additionally, the frequency of $CD57^+$ NK cells may further refine risk stratification within this high-risk patient subgroup.

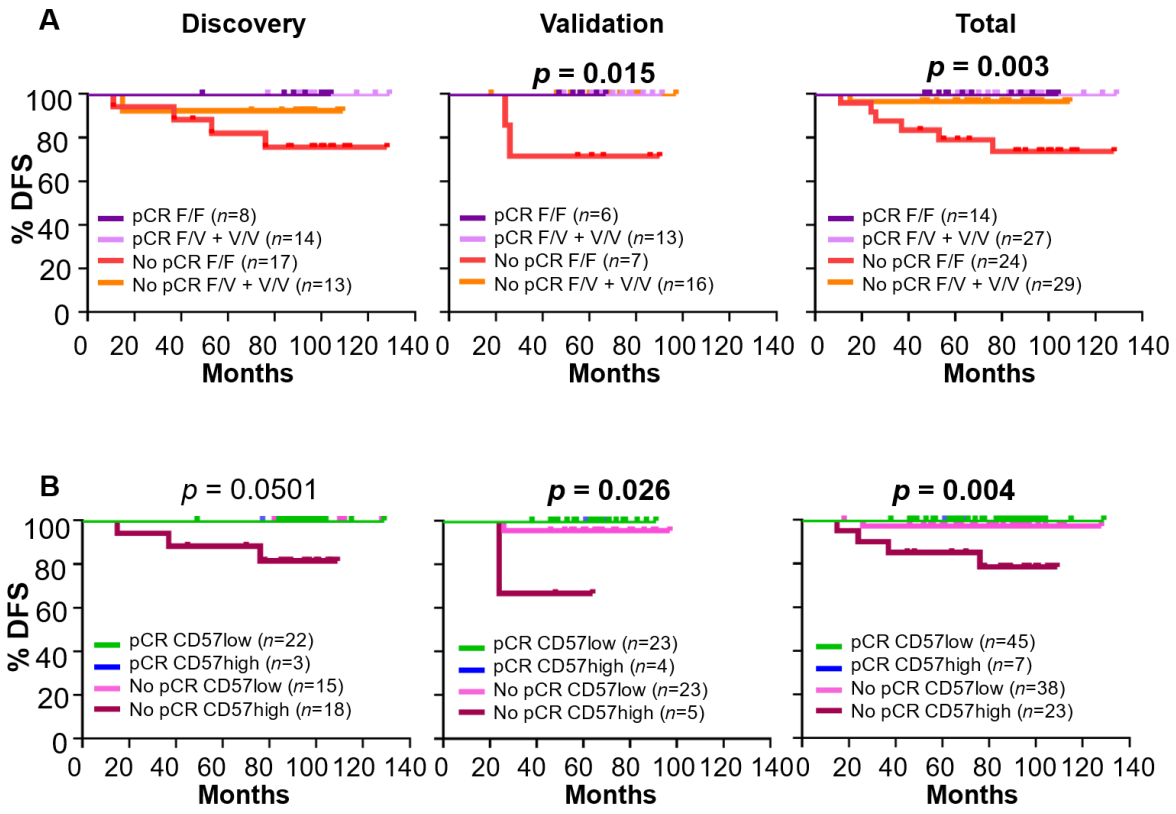

Fig. 41. Combined analysis of CD16A-158F/V genotype, CD57+ NK cell frequencies and pCR in relation with DFS. Log-rank test (Mantel-Cox) was used for statistical analysis. P values were indicated when the analysis reached statistical significance. **A** Samples were stratified by pCR achievement and CD16A genotype **B** Samples were stratified by pCR achievement and CD57 levels (according to $CD57^+$ NK percentages).

4. Analysis of potential confounding factors influencing the association between $CD57^+$ NK cell levels and pCR achievement

Factors that possibly influence the association between CD57 expression in peripheral NK cells and pCR achievement in HER2-positive breast cancer patients treated with anti-HER2 monoclonal antibody therapy were next analyzed (Fig. 42). While both the CD16A-158F allele and a high number of $CD57^+$ NK cells were independently linked to a poor treatment response, no significant relationship was found between CD57 expression and CD16A genotype (data not shown).

The CD57 epitope is a sulfated carbohydrate post-translationally added to glycoproteins and glycolipids (75). Acknowledging that CD57 expression can be influenced by biological age (76), our study confirmed a correlation between CD57

levels and patient age within our cohorts (Fig. 42A). Despite the positive correlation between CD57⁺ NK cells and age, percentages of CD57⁺ NK cells independently associated with lower likelihood of response to HER2-specific antibodies in multivariate analysis when adjusting by age in the discovery and the total cohort, and remained without statistical significancy in the validation cohort [Discovery cohort: p = 0.05, OR 1.04 (95% CI, 1.001–1.08); Validation cohort p = 0.37; Total cohort p = 0.037, OR 1.03 (95% CI, 1.002-1.05)].

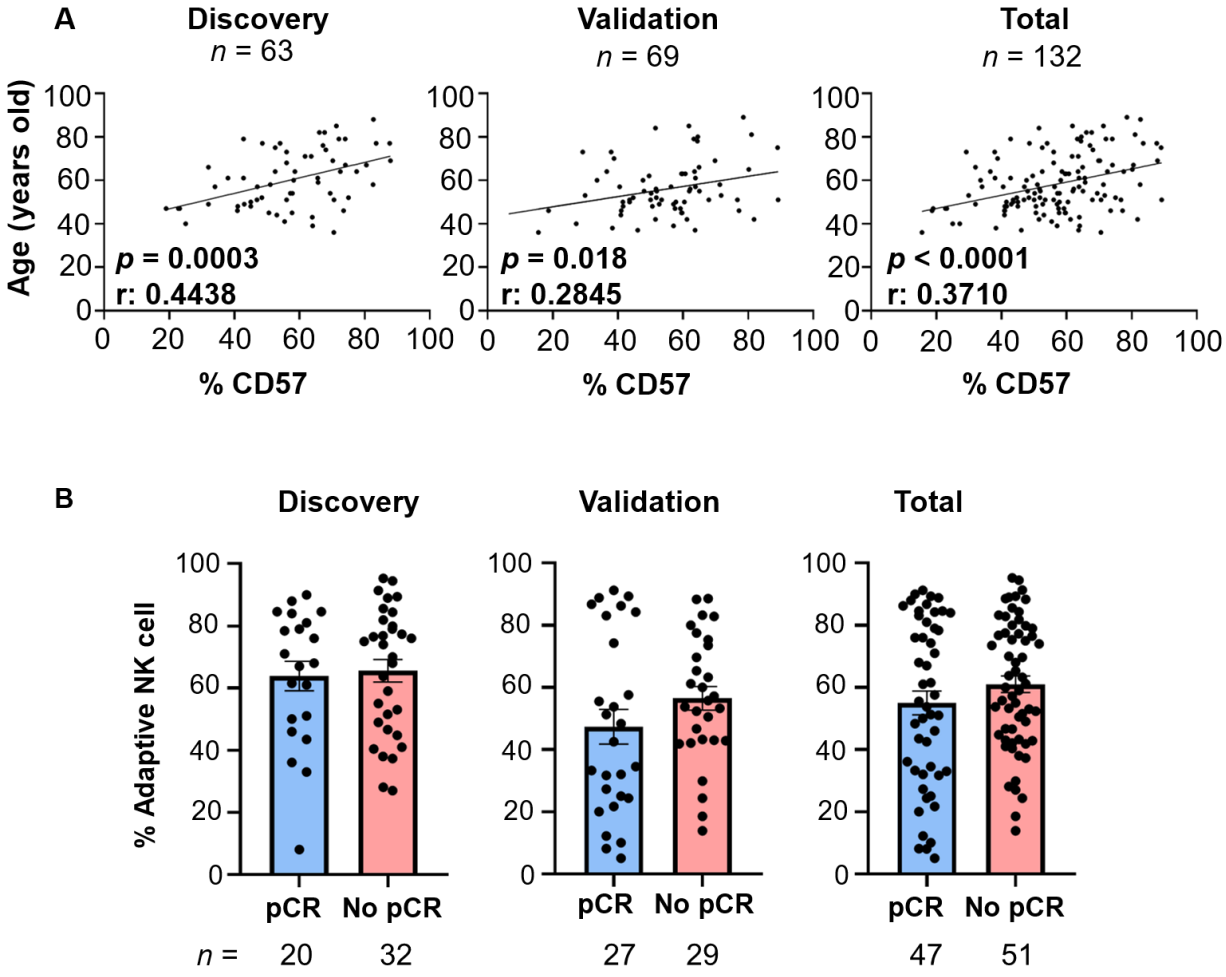

Fig. 42. Analysis of potential confounding factors influencing the association between CD57⁺ NK cell levels and pCR achievement. A Linear correlation of CD57⁺ NK cells (%) and patient age. Statistics for the linear correlation are noted on each graph**. B** Association of adaptive (NKG2C⁺CD57⁺) NK cell counts (%) and pathological response (no pCR and pCR).

CD57, along with the activating receptor NKG2C, also marks a subset of NK cells with adaptative features that expands during chronic viral infections, particularly HCMV (73). To determine if this subset may be responsible for the observed associations, the potential association between the percentage of $CD57^{+}NKG2C^{+}$ NK cells and pCR was analysed. No differences in pCR were found according to the proportions of $CD57^{+}$ adaptive (NKG2C+) NK cells (Fig. 42B).

Taken together, these findings show that the influence of circulating $CD57^{+}$ NK cells on the response to neoadjuvant anti-HER2 mAb-based treatment in patients with primary HER2-positive breast cancer appears to be independent of both HCMV infection status and CD16A genotype.

In summary, our results suggest that the CD16A-158V/F genotype refine prediction of therapeutic benefit and relapse risk in HER2-positive breast cancer, whereas circulating $CD57^{+}$ NK cells show limited and cohort-dependent value, underscoring the need for further validation of their role as biomarkers.

DISCUSSION

1. The CCL5/IFN-γ-CXCL9/10 axis: integrating innate and adaptive immunity

The TME of HER2-positive breast cancer constitutes a complex ecosystem where immune cells interact with tumor cells, influencing disease progression and therapeutic response. Our previous research reinforced the prognostic significance of TI-NK in HER2-positive breast cancer, demonstrating a predictive power that surpasses that of TILs. Notably, the absolute number of TI-NK cells within tumors is frequently low, suggesting their antitumor effects may extend beyond direct cytotoxic killing of malignant cells, possibly through modulation of the TME (110-112,191,192). This thesis aimed to elucidate the biological pathways and mechanisms underlying the prognostic and therapeutic significance of TI-NK in HER2-positive breast cancer. Our data support a pivotal role for the CCL5/IFN-γ-CXCL9/10 chemokine axis in mediating NK cell-driven anti-tumor responses and point to their potential value for optimizing the efficacy of anti-HER2 monoclonal antibodies.

By comparing the transcriptomes of HER2-positive breast tumors with high versus low NK cell infiltration, we identified immune pathways that were significantly associated with NK cell infiltration. The NF-κB and PKCθ signalling pathways, together with cytokines such as IL-12 produced by mature dendritic cells, are essential for IFN-γ production by NK cells. The upregulation of these pathways suggests that TI-NK+ tumors possess a more immunologically active microenvironment (193-196).

Beyond the role of IFN-γ, our data reveal that TI-NK cells orchestrate the coordinated production of a specific chemokine axis within the TME responsible for recruiting other immune effectors. Mechanistically, we observed that anti-HER2 antibody-dependent activation of NK cells triggers the release of CCL5, IFN-γ and TNF-α, which collectively induce subsequent production of CXCL9 and CXCL10—potentially by other cells within the TME—establishing a positive feedback loop that may further recruit and activate effector cells (114).

Our data also highlight the heterogeneity of breast cancer cell lines in their responsiveness to IFN-γ, IFN-β and TNF-α, indicating that intrinsic differences in

signalling or epigenetic states may influence tumor cell participation in chemokine-mediated immune recruitment. Additionally, the impact of NK/ILC repertoire in different tumor models may vary depending on the TME and its complex regulation (197). This underlines the importance of understanding patient-to-patient response variability

While the dependency of CXCL9 and CXCL10 production on IFN-γ is well established (198-200), this work provides novel evidence for a cooperative effect between IFN-γ and TNF-α. Furthermore, our results demonstrate that type-I interferons can exert a context-dependent, dual effect on this axis: synergizing with IFN-γ and TNF-α to boost CCL5 and CXCL10 release, yet simultaneously repressing CXCL9 production. This finding suggests that the delicate balance of CCL5, CXCL9, and CXCL10 levels can become dysregulated under specific conditions, potentially depending on TI-NK paracrine effects (201). An imbalance of these cytokines and chemokines may promote tumor growth via autocrine signalling (202-206).

Remarkably, both preclinical cancer models and studies in patients have shown that CXCL9/10 blockade, via epigenetic silencing or soluble inhibitors, promotes tumor progression (207,208), whereas coordinated secretion of this chemokine axis, as seen in our *in vivo* model, significantly improves tumor control. Collectively, our findings suggest that NK cell activation through ADCC during anti-HER2 therapy initiates a coordinated chemokine cascade that enhances immune cell recruitment and tumor clearance.

2. Functional diversity of TI-NK cell subsets

This study provides novel insights into the phenotypic and functional heterogeneity of TI-NK cells. Three distinct TI-NK cell subsets were identified, characterized by differential surface expression of CD16 and CD103. The different transcriptional profiles of these populations suggest that each subset may have specific roles in the TME.

The $CD16^{+}$ subset displayed a robust cytotoxic profile, supporting its role in

mediating antitumor immunity *in vivo* (209). In contrast, the $CD16^{-}CD103^{+}$ subpopulation exhibited a gene expression profile reminiscent of pro-inflammatory ILC1s. This transcriptional signature suggests that these cells play a key role in orchestrating antitumor immune responses within the TME. Additionally, this subset expressed high levels of adhesion molecules, such as CD151 and CD9, which may facilitate tissue residency, cell adhesion and migration, as well as interactions with other immune and stromal cells in the TME (173, 210-212).

Importantly, both $CD16^{+}$ and $CD16^{-}CD103^{+}$ subsets retain the capacity to produce CCL5 and IFN-γ, key mediators of antitumor immunity. The coordinated production of these molecules by distinct NK cell subsets underscores their potential contribution to the activation of the CCL5/IFN-γ–CXCL9/10 chemokine axis. The observed lineage relationship between $CD16^{+}$ and $CD16^{-}CD103^{+}$ TI-NK cells, supported by transcriptional and functional similarities, suggests a model of sequential differentiation within the TME. Notably, anti-HER2 antibody therapy induced the phenotypic remodelling in TI-NK cells in the in vivo murine model, marked by increased CD103, concomitant with a decrease in surface CD16. Circulating and TI-NK cells also displayed distinct different gene expression profiles, indicating phenotypic plasticity as an adaptation to local cues within the TME. Our data support a model in which circulating $CD16^{+}$ NK cells infiltrate the tumor and become activated upon ADCC. After activation, a subset of NK cells downregulates CD16. TGF-β present in the TME promotes the upregulation of CD103, promoting these cells to acquire features of tissue residency and enhanced cytokine production (notably CCL5 and IFN-γ). This transition may be critical for sustaining local immune responses, facilitating the recruitment of additional effector cells, and orchestrating tumor immunity by promoting the antigen presentation and the differentiation of macrophages and T cells to M1 and Th1 phenotypes (21) (Fig.43).

Furthermore, the abundance of $CD16^{+}$ and $CD16^{-}CD103^{+}$ subsets correlated positively with the presence of $CD8^{+}$ $CD103^{+}$ T cells within the TME. This finding supports the hypothesis that tissue residency programs are co-regulated across lymphocyte lineages, potentially through shared exposure to local cytokines such as TGF-β and IL-15, or through common transcriptional regulators (213). The spatial and functional proximity of both populations may facilitate coordinated antitumor

responses. The interplay between ILC1-like cells, NK cells and CD8$^+$ T cells may be central to effective antitumor immunity, particularly in the context of antibody-based therapies.

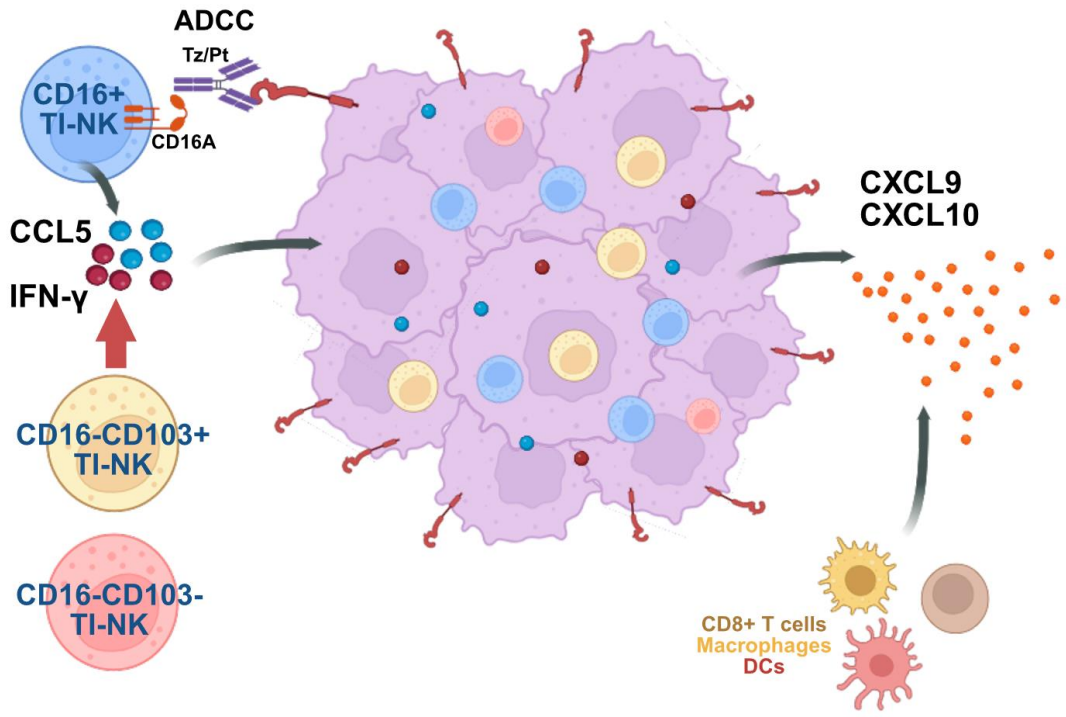

Figure 43. Modeling the influence of TI-NK cells in the clinical efficacy of anti-HER2 antibodies in breast cancer. Three different subsets of TI-NK cells were identified depending on the expression of CD16 and CD103. CD16+ NK cells arrive to the tumor and become activated through ADCC upon neoadjuvant treatment with trastuzumab and pertuzumab (Tz/Pt). Some of these cells downregulate CD16 and acquire the residency marker CD103. CD16$^+$ and CD103$^+$ cells produce CCL5 and IFN-γ. These molecules have an effect in bystander cells from the TME, which have the capacity of producing CXCL9 and CXCL10, then recruiting other effectors of the immune system, such as CD8$^+$ T cells, and potentially macrophages and dendritic cells. Created in https://BioRender.com.

In contrast, the CD16$^-$CD103$^-$ subset was characterized by a transcriptional program similar to regulatory ILC3 cells, including genes linked to angiogenesis, and immunoregulatory and protumoral functions, such as *CSF1* and *CSF2*, implicated in the recruitment of suppressor myeloid cells (MDSC) and tumor-associated macrophages (TAM) (214-216). Elevated *IL1B*, while typically associated with a proinflammatory profile, may reflect a chronic inflammatory state that supports tumor progression (217). The chemokine profile of this subset was also regulatory, with high levels of *CCL22* (associated with T-reg recruitment and immunosuppression) (218), *CXCL8* (which attracts neutrophils and promotes tumor growth and

angiogenesis) (219), *CCL2* (recruiting TAM) (220) and *CXCL10*, which can have dual roles depending on its coordination with other chemokines (203).

Together, these data highlight the multifaceted roles of TI-NK cell subsets in antitumor immunity. The overall impact of their chemokine expression depends on the balance between pro-inflammatory and immunosuppressive signals, the composition of the immune infiltrate, and the responsiveness of tumor and stromal cells to cytokine cues. This complexity underscores the importance of considering NK cell heterogeneity when designing immunotherapeutic strategies.

A notable observation from our analyses is the remarkable homogeneity in the composition of immune infiltrates across different molecular subtypes of breast cancer. Regardless of HER2 and hormone receptor status, the proportional representation and functional characteristics of these immune populations were conserved. This suggests that the mechanisms governing NK cell adaptation, tissue residency, and functional specialization are broadly applicable across breast cancer subtypes, and that patients without overexpression of HER2, but with high infiltration of NK cells, may benefit from anti-HER2 therapy or other immune-stimulatory strategies.

3. Clinical implications: biomarker discovery and predictive tools for anti-HER2 therapy

The clinical relevance of our findings is accompanied by the identification of several potential biomarkers of response to treatment, which may improve the therapeutic decision-making and cure rates in HER2-positive breast cancer patients. Notably, a coordinated increase in serum CCL5 and CXCL9 levels after anti-HER2 therapy correlates with favourable outcomes. While individual chemokine levels may not independently predict treatment response, their coordinated upregulation may reflect a heightened antitumor response, potentially driven by TI-NK cells, and could serve as a valuable biomarker for monitoring treatment efficacy in HER2-positive breast cancer (Fig. 44). Further investigation in a larger cohort is warranted to validate these findings and to explore the clinical utility of this chemokine signature as a predictive biomarker.

Predictive biomarkers are needed for the early identification of patients at high risk of relapse. The CD16A-158V/F polymorphism significantly impacts therapeutic outcomes. The CD16 receptor in individuals homozygous for phenylalanine demonstrates diminished affinity for IgG1 antibodies (68). Our research showed clear trends regarding how this genetic variant impacts the success of anti-HER2 antibodies. We found a positive correlation between carriage of at least one V allele and pCR achievement. This V allele was also linked to long-term DFS. NK cells from patients homozygous for V have a CD16 with high affinity for trastuzumab and pertuzumab, leading to enhanced activation and potentially increased capacity of recruitment of other cells. Yet CD16A is not only expressed in NK cells; other immune cells in the TME also carry the CD16A receptor, such as macrophages, DCs and some T cells (γδ T or specific αβ T cell subsets) (221-223). The improved response to anti-HER2 therapy could also involve the activation of these other immune cells. This suggests that additional immune mechanisms may contribute to the observed association, specifically FcγR-dependent antitumor immunity. A more efficient recognition of anti-HER2 antibodies by the CD16A receptor could lead to better uptake and processing of antibody-coated cancer cells by antigen-presenting cells. This, in turn, would improve the presentation of tumor antigens to T cells, promoting the development of T cell memory and creating a long-term anti-tumor "vaccine" effect (224).

Despite the lower relapse rate observed in the validation cohort compared with the discovery cohort, likely influenced by the clinical implementation of trastuzumab-emtansine (T-DM1) as adjuvant therapy for non-pCR patients after 2019, our findings support CD16A-158V/F genotyping as a valuable tool according to current standard-of-care. It can help predict whether a patient will achieve pCR and, importantly, help guide clinical follow-up for those who do not achieve a complete response to neoadjuvant anti-HER2 antibody treatment. Interestingly, even among patients in our study who did not achieve a pCR, carrying the V allele was still a good indicator of long-term prognosis. Individuals homozygous for phenylalanine who fail to achieve pCR have a higher risk of relapse and may benefit of frequent monitorization of their disease or a change in the therapeutic approach (Fig. 44).

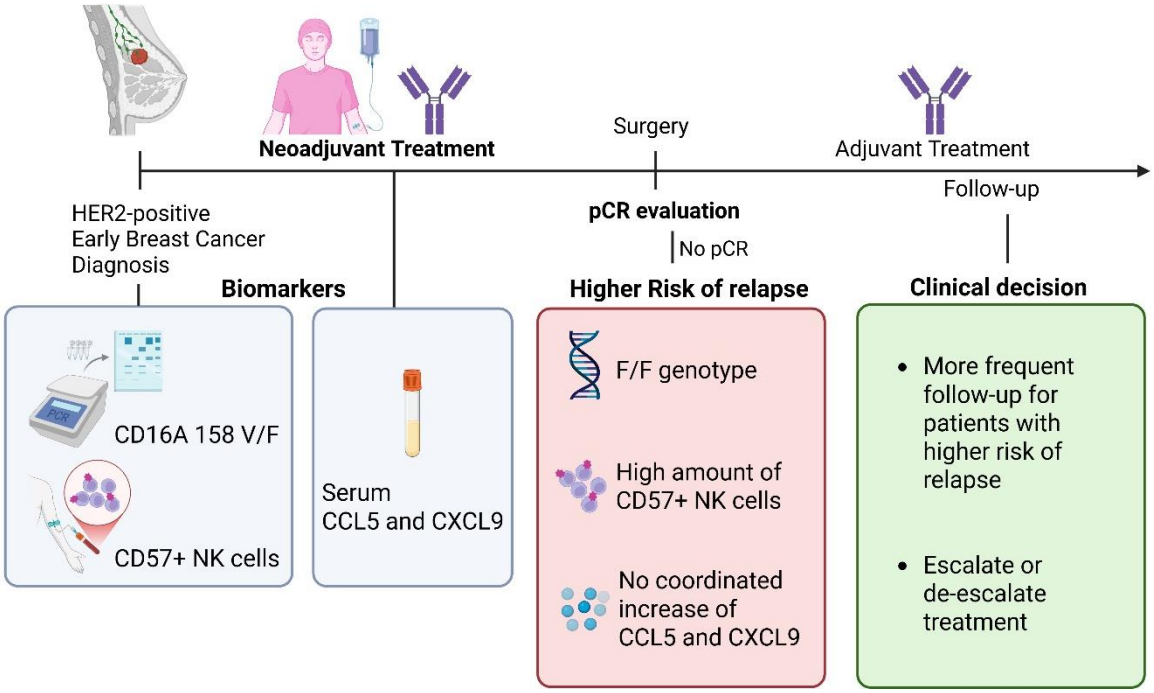

Figure 44. Possible biomarkers of response to anti-HER2 neoadjuvant treatment in HER2-positive early breast cancer patients. The CD16A-158 V/F polymorphism, the amount of circulating CD57+ NK cells, and the serum levels of CCL5 and CXCL9 are potential biomarkers described in this work that may help in the prediction of response to neoadjuvant anti-HER2 treatment. Carrying of a V allele, having low percentages of circulating $CD57^+$ NK cells, and a coordinated increase of CCL5 and CXCL9 serum levels after three cycles of chemotherapy are associated with favorable outcomes. The determination and standardization of these potential biomarkers can help to improve therapeutic decisions and cure rates. Created in https://BioRender.com.

Another potential biomarker of response to anti-HER2 antibodies is the proportions of circulating $CD57^+$ NK cells. These $CD57^+$ NK cells are highly cytotoxic but exhibit low proliferating capacity. In our previous work, a significant negative correlation between numbers of circulating $CD57^+$ NK cells and TI-NK cells was observed in HER2-positive breast cancer patients (112). Also, $CD57^+$ cells showed reduced expression of CXCR3, the receptor for CXCL9 and CXCL10, and higher expression of CXCR1 and CX3CR1 (148). Ligands of CXCR1 and CX3CR1 (fraktaline and CXCL8) have been previously associated with metastasis in breast cancer (225,226), while CXCL9 and CXCL10 were identified in our work as some of the cytokines that link TI-NK with lower risk of relapse. However, while our previous study initially reported that higher numbers of $CD57^+$ NK cells were associated to a lower likelihood of achieving pCR, this same connection has not been observed in our follow-up study. The sample size of both cohorts was small, making it difficult to

obtain robust conclusions. Further studies are needed to consider this a reliable biomarker of response to anti-HER2 antibodies in HER2-positive breast cancer (Fig. 44). Of note, only blood samples at baseline, before any treatment, were studied. The analysis of longitudinal samples could provide valuable insights about the dynamics of $CD57^+$ NK cells along treatment and their relation with patient outcomes.

4. Translational opportunities: strategies to amplify NK cell-mediated anti-tumor responses

Given the important role of TI-NK cells and the CCL5/IFN-γ-CXCL9/10 axis in mediating effective anti-tumor responses to anti-HER2 antibodies, our findings underscore the need for strategies that can increase NK cell infiltration and activation and/or induce the coordinated activation of this chemokine axis. One of the most direct approaches to overcome the scarcity of TI-NK cells is to enhance their recruitment to the tumor microenvironment. While the adoptive transfer of NK cells has shown promise in preclinical models and early-phase clinical trials (227,228), this strategy faces significant logistical and manufacturing challenges, particularly for widespread clinical application in solid tumors. Moreover, the persistence and homing of transferred NK cells to tumor sites remain limited. Genetic engineering of NK cells to express chemokine receptors is a possible strategy to improve NK cell homing. For example, NK cells genetically engineered to coexpress a CAR targeting folate receptor alpha and the chemokine receptor CXCR3 showed enhanced migration toward CXCL10 and improved antitumor activity against ovarian cancer cells, both in preclinical models *in vitro* and *in vivo* (229). Such approaches could be explored and combined with anti-HER2 antibody therapies to maximize therapeutic efficacy, although further optimization and safety evaluation are needed before clinical implementation.

Beyond cell-based therapies, pharmacological strategies to induce or amplify the CCL5/IFN-γ-CXCL9/10 axis also exist. Several clinically approved drugs, with a well-characterized safety profile, have been shown to modulate chemokine expression and may be repurposed to enhance NK cell recruitment and effector

function in tumors. Some examples include inhibitors of COX-2, STAT3, or DDP4. Cycloooxygenase-2 (COX-2) inhibitors, such as celecoxib, have been reported to increase CXCL9 and CXCL10 expression in the TME, thereby enhancing T and NK cell infiltration (230,231). Inhibition of STAT3 signaling, frequently activated in breast cancer and associated with immune exclusion, can upregulate CXCL9/10 and promote immune infiltration (232,233). Finally, dipeptidyl peptidase-4 (DDP4) inhibitors, commonly used in diabetes management, have been shown to enhance CXCL10-mediated immune cell recruitment in preclinical tumor models (234). The combination of anti-HER2 antibodies with these drugs in breast cancer patients could be a strategy to increase NK cell numbers in HER2-positive breast tumors and improve the clinical efficacy of anti-HER2 antibodies in patients with NK cell-desert tumors.

Another strategy may imply local or systemic administration of IFN-γ or agents that stimulate endogenous IFN-γ production, such as IL-12 (235,236), that could enhance the production of CXCL9 and CXCL10 by tumor and stromal cells, thereby facilitating the recruitment of NK cells and other effectors. However, the pleiotropic effects on IFN-γ on both immune and tumor cells necessitate careful evaluation of dosing, delivery, and potential adverse effects, including immune-related toxicities and the risk of inducing immune suppression or exhaustion in certain contexts, as well as the combination with current therapies (237-239). Alternatively, the intratumoral administration of recombinant chemokines (CCL5, CXCL9, CXCL10) might directly recruit effector cells without relying solely on upstream cytokine signalling. Such approaches are being explored in preclinical models and could offer a more targeted means of modulating the immune tumor landscape (240,241). Of note, intratumoral treatment has been tested in melanoma and in squamous cells carcinoma. However, future investigations are needed to translate this approach into clinical reality, especially refining the delivery technique, evaluate the potential adverse effects and the efficacy within the complex TME (242-245).

In summary, our findings highlight the critical role of TI-NK cells and the CCL5/IFN-γ-CXCL9/10 axis in orchestrating effective anti-tumor immunity. We have shown that the interplay of specific chemokine and cytokine pathways, alongside the dynamic phenotypic changes of TI-NK cell subsets, are crucial for successful

anti-HER2 therapy, paving the way for future immunotherapeutic interventions aimed at improving outcomes for HER2-positive breast cancer patients. In addition, the identification of novel biomarkers, including the coordinated increase in CCL5 and CXCL9 serum levels and the CD16A-158V/F polymorphism, offers valuable predictive and prognostic tools to guide personalized treatment.

CONCLUSIONS

1. Tumor-infiltrating NK cell activation contributes to the therapeutic efficacy of anti-HER2 antibodies, in part by inducing the CCL5/IFN-γ-CXCL9/10 chemokine axis that supports the recruitment of additional immune effectors.
2. TI-NK cells display marked heterogeneity, comprising $CD16^{+}$ cytotoxic, $CD16^{-}CD103^{+}$ pro-inflammatory, and $CD16^{-}CD103^{-}$ regulatory subsets, each modulating distinct immune microenvironments within human breast tumors.
3. Anti-HER2 therapy promotes a phenotypic shift from $CD16^{+}$ toward tissue-resident $CD16^{-}CD103^{+}$ NK cells, a subset associated with tumor growth control in preclinical models
4. Early, coordinated increases in serum CCL5 and CXCL9 levels provide dynamic biomarkers of intratumoral NK cell activation and favorable clinical responses to anti-HER2 antibodies.
5. The CD16A-158V/F polymorphism represents a robust predictive and prognostic biomarker, with the V allele conferring higher pCR rates and improved long-term survival.
6. Baseline frequencies of circulating $CD57^{+}$ NK cells may identify patients at risk of poor responses, although further validation in larger cohorts is required.
7. Patients with the CD16A-158F/F genotype who fail to achieve pCR face an increased risk of relapse, supporting its use in personalized monitoring strategies

These findings collectively establish TI-NK cells and their effector pathways as central mediators of anti-HER2 antibody activity and provide a rationale for developing NK cell-based therapeutic strategies and biomarkers in HER2-positive breast cancer.

REFERENCES

1. Carpenter S, O'Neill LAJ. From periphery to center stage: 50 years of advancements in innate immunity. Cell. 2024;187(9):2030–51.

2. Herberman RB, Nunn ME, Holden HT, Lavrin DH. Natural cytotoxic reactivity of mouse lymphoid cells against syngeneic and allogeneic tumors. II. Characterization of effector cells. Int J Cancer. 1975;16(2):230–9.

3. Kiessling R, Klein E, Wigzell H. "Natural" killer cells in the mouse. I. Cytotoxic cells with specificity for mouse Moloney leukemia cells. Specificity and distribution according to genotype. Eur J Immunol. 1975;5(2):112–7.

4. Lanier LL. Five decades of natural killer cell discovery. J Exp Med. 2024;221(8):e20231222.

5. Mebius RE, Rennert P, Weissman IL. Developing lymph nodes collect CD4+CD3- LTbeta+ cells that can differentiate to APC, NK cells, and follicular cells but not T or B cells. Immunity. 1997;7(4):493–504.

6. Satoh-Takayama N, Vosshenrich CA, Lesjean-Pottier S, Sawa S, Lochner M, Rattis F, et al. Microbial flora drives interleukin 22 production in intestinal NKp46+ cells that provide innate mucosal immune defense. Immunity. 2008;29(6):958–70.

7. Cella M, Fuchs A, Vermi W, Facchetti F, Otero K, Lennerz JK, et al. A human natural killer cell subset provides an innate source of IL-22 for mucosal immunity. Nature. 2009;457(7230):722–5.

8. Luci C, Reynders A, Ivanov II, Cognet C, Chiche L, Chasson L, et al. Influence of the transcription factor RORgammat on the development of NKp46+ cell populations in gut and skin. Nat Immunol. 2009;10(1):75–82.

9. Moro K, Yamada T, Tanabe M, Takeuchi T, Ikawa T, Kawamoto H, et al. Innate production of T(H)2 cytokines by adipose tissue-associated c-Kit(+)Sca-1(+) lymphoid cells. Nature. 2010;463(7280):540–4.

10. Fuchs A, Colonna M. Innate lymphoid cells in homeostasis, infection, chronic inflammation and tumors of the gastrointestinal tract. Curr Opin Gastroenterol. 2013;29(6):581–7.

11. Klose CSN, Flach M, Möhle L, Rogell L, Hoyler T, Ebert K, et al. Differentiation of type 1 ILCs from a common progenitor to all helper-like innate lymphoid cell lineages. Cell. 2014;157(2):340–56

12. Spits H, Artis D, Colonna M, Diefenbach A, Di Santo JP, Eberl G, et al. Innate lymphoid cells--a proposal for uniform nomenclature. Nat Rev Immunol. 2013;13(2):145–9.

13. Vivier E, Artis D, Colonna M, Diefenbach A, Di Santo JP, Eberl G, et al. Innate Lymphoid Cells: 10 Years On. Cell. 2018;174(5):1054–66.

14. Jarick KJ, Topczewska PM, Jakob MO, Yano H, Arifuzzaman M, Gao X, et al. Non-redundant functions of group 2 innate lymphoid cells. Nature. 2022;611(7937):794–800

15. Song P, Cao K, Mao Y, Ai S, Sun F, Hu Q, et al. Tissue specific imprinting on innate lymphoid cells during homeostasis and disease process revealed by integrative inference of single-cell transcriptomics. Front Immunol. 2023;14:1127413.

16. Calvi M, Di Vito C, Frigo A, Trabanelli S, Jandus C, Mavilio D. Development of human ILCs and impact of unconventional cytotoxic subsets in the pathophysiology of inflammatory diseases and cancer. Front Immunol. 2022;13:914266.

17. Vo DN, Yuan O, Kanaya M, Telliam-Dushime G, Li H, Kotova O, et al. A temporal developmental map separates human NK cells from noncytotoxic ILCs through clonal and single-cell analysis. Blood Adv. 2024;8(11):2933-51.

18. Campbell KS, Hasegawa J. Natural killer cell biology: an update and future directions. J Allergy Clin Immunol. 2013;132(3):536-44.

19. Zhou J, Tian Z, Peng H. Tissue-resident NK cells and other innate lymphoid cells. Adv Immunol. 2020;145:37-53.

20. Bozzano F, Perrone C, Moretta L, De Maria A. NK cell precursors in human bone marrow in health and inflammation. Front Immunol. 2019;10:2045.

21. Abel AM, Yang C, Thakar MS, Malarkannan S. Natural killer cells: development, maturation, and clinical utilization. Front Immunol. 2018;9:1869.

22. Inngjerdingen M, Damaj B, Maghazachi AA. Expression and regulation of chemokine receptors in human natural killer cells. Blood. 2001;97(2):367-75.

23. Berahovich RD, Lai NL, Wei Z, Lanier LL, Schall TJ. Evidence for NK cell subsets based on chemokine receptor expression. J Immunol. 2006;177(11):7833-40.

24. Lanier LL, Phillips JH. Ontogeny of natural killer cells. Nature. 1986;319(6051):269-70.

25. Prager I, Watzl C. Mechanisms of natural killer cell-mediated cellular cytotoxicity. J Leukoc Biol. 2019;105(6):1319-29.

26. Imširović V, Wensveen FM, Polić B, Jelenčić V. Maintaining the balance: regulation of NK cell activity. Cells. 2024;13(17):1464.

27. Kärre K, Ljunggren HG, Piontek G, Kiessling R. Selective rejection of H-2-deficient lymphoma variants suggests alternative immune defence strategy. Nature. 1986;319(6055):675-8.

28. Lanier LL. Up on the tightrope: natural killer cell activation and inhibition. Nat Immunol. 2008;9(5):495-502.

29. Raulet DH. Missing self recognition and self tolerance of natural killer (NK) cells. Semin Immunol. 2006;18(3):145-50.

30. Elliott JM, Yokoyama WM. Unifying concepts of MHC-dependent natural killer cell education. Trends Immunol. 2011;32(8):364-72.

31. Reth M. Antigen receptor tail clue. Nature. 1989;338(6214):383-4.

32. Aguilar OA, Fong LK, Lanier LL. ITAM-based receptors in natural killer cells. Immunol Rev. 2024;323(1):40-53.

33. Hilton HG, Guethlein LA, Goyos A, Nemat-Gorgani N, Bushnell DA, Norman PJ, et al. Polymorphic HLA-C receptors balance the functional characteristics of KIR haplotypes. J Immunol. 2015;195(7):3160-70.

34. Parham P. MHC class I molecules and KIRs in human history, health and survival. Nat Rev Immunol. 2005;5(3):201-14.

35. Vilches C, Parham P. KIR: diverse, rapidly evolving receptors of innate and adaptive immunity. Annu Rev Immunol. 2002;20:217-51.

36. Freud AG, Mundy-Bosse BL, Yu J, Caligiuri MA. The broad spectrum of human natural killer cell diversity. Immunity. 2017;47(5):820-33.

37. Houchins JP, Lanier LL, Niemi EC, Phillips JH, Ryan JC. Natural killer cell cytolytic activity is inhibited by NKG2-A and activated by NKG2-C. J Immunol. 1997;158(8):3603-9.

38. López-Botet M, Pérez-Villar JJ, Carretero M, Rodríguez A, Melero I, Bellón T, et al. Structure and function of the CD94 C-type lectin receptor complex involved in recognition of HLA class I molecules. Immunol Rev. 1997;155:165-74.

39. Braud VM, Allan DS, O'Callaghan CA, Söderström K, D'Andrea A, Ogg GS, et al. HLA-E binds to natural killer cell receptors CD94/NKG2A, B and C. Nature. 1998;391(6669):795-9

40. Zeller T, Münnich IA, Windisch R, Hilger P, Schewe DM, Humpe A, et al. Perspectives of targeting LILRB1 in innate and adaptive immune checkpoint therapy of cancer. Front Immunol. 2023;14:1240275.

41. Colonna M, Navarro F, Bellón T, Llano M, García P, Samaridis J, et al. A common inhibitory receptor for major histocompatibility complex class I molecules on human lymphoid and myelomonocytic cells. J Exp Med. 1997;186(11):1809-18.

42. Anfossi N, André P, Guia S, Falk CS, Roetynck S, Stewart CA, et al. Human NK cell education by inhibitory receptors for MHC class I. Immunity. 2006;25(2):331-42.

43. Kadri N, Wagner AK, Ganesan S, Kärre K, Wickström S, Johansson MH, et al. Dynamic regulation of NK cell responsiveness. Curr Top Microbiol Immunol. 2016;395:95-114.

44. Horowitz A, Djaoud Z, Nemat-Gorgani N, Blokhuis J, Hilton HG, Béziat V, et al. Class I HLA haplotypes form two schools that educate NK cells in different ways. Sci Immunol. 2016;1(3):eaag1672.

45. Harjunpää H, Guillerey C. TIGIT as an emerging immune checkpoint. Clin Exp Immunol. 2020;200(2):108-19.

46. Inozume T, Yaguchi T, Furuta J, Harada K, Kawakami Y, Shimada S. Melanoma cells control antimelanoma CTL responses via interaction between TIGIT and CD155 in the effector phase. J Invest Dermatol. 2016;136(1):255-63.

47. Zhang H, Liu Q, Lei Y, Zhou J, Jiang W, Cui Y, et al. Direct interaction between CD155 and CD96 promotes immunosuppression in lung adenocarcinoma. Cell Mol Immunol. 2021;18(6):1575-7.

48. Muntasell A, Ochoa MC, Cordeiro L, Berraondo P, López-Díaz de Cerio A, Cabo M, et al. Targeting NK-cell checkpoints for cancer immunotherapy. Curr Opin Immunol. 2017;45:73-81.

49. Ito M, Maruyama T, Saito N, Koganei S, Yamamoto K, Matsumoto N. Killer cell lectin-like receptor G1 binds three members of the classical cadherin family to inhibit NK cell cytotoxicity. J Exp Med. 2006;203(2):289-95.

50. Pesce S, Greppi M, Tabellini G, Rampinelli F, Parolini S, Olive D, et al. Identification of a subset of human natural killer cells expressing high levels of programmed death 1: a phenotypic and functional characterization. J Allergy Clin Immunol. 2017;139(1):335-46.e3

51. Ndhlovu LC, Lopez-Vergès S, Barbour JD, Jones RB, Jha AR, Long BR, et al. Tim-3 marks human natural killer cell maturation and suppresses cell-mediated cytotoxicity. Blood. 2012;119(16):3734-43.

52. Hosomi S, Chen Z, Baker K, Chen L, Huang YH, Olszak T, et al. CEACAM1 on activated NK cells inhibits NKG2D-mediated cytolytic function and signaling. Eur J Immunol. 2013;43(9):2473-83.

53. Ge H, Guo N, Liu Y, Lang B, Yin X, Yu X, et al. The inhibitory receptor LAG3 affects NK cell IFN-γ production through glycolysis and the PSAT1/STAT1/IFNG pathway. mBio. 2025;16(6):e0023025.

54. Dębska-Zielkowska J, Moszkowska G, Zieliński M, Zielińska H, Dukat-Mazurek A, Trzonkowski P, et al. KIR receptors as key regulators of NK cells activity in health and disease. Cells. 2021;10(7):1777.

55. Levi-Schaffer F, Mandelboim O. Inhibitory and coactivating receptors recognising the same ligand: immune homeostasis exploited by pathogens and tumours. Trends Immunol. 2018;39(2):112-22.

56. Sivori S, Vitale M, Morelli L, Sanseverino L, Augugliaro R, Bottino C, et al. p46, a novel natural killer cell-specific surface molecule that mediates cell activation. J Exp Med. 1997;186(7):1129-36.

57. Cantoni C, Bottino C, Vitale M, Pessino A, Augugliaro R, Malaspina A, et al. NKp44, a triggering receptor involved in tumor cell lysis by activated human natural killer cells, is a novel member of the immunoglobulin superfamily. J Exp Med. 1999;189(5):787-96.

58. Pende D, Parolini S, Pessino A, Sivori S, Augugliaro R, Morelli L, et al. Identification and molecular characterization of NKp30, a novel triggering receptor involved in natural cytotoxicity mediated by human natural killer cells. J Exp Med. 1999;190(10):1505-16.

59. Sen Santara S, Lee DJ, Crespo Â, Hu JJ, Walker C, Ma X, et al. The NK cell receptor NKp46 recognizes ecto-calreticulin on ER-stressed cells. Nature. 2023;616(7956):348-56.

60. Sivori S, Vacca P, Del Zotto G, Munari E, Mingari MC, Moretta L. Human NK cells: surface receptors, inhibitory checkpoints, and translational applications. Cell Mol Immunol. 2019;16(5):430-41

61. Billadeau DD, Upshaw JL, Schoon RA, Dick CJ, Leibson PJ. NKG2D-DAP10

triggers human NK cell-mediated killing via a Syk-independent regulatory pathway. Nat Immunol. 2003;4(6):557-64.

62. Campos-Silva C, Kramer MK, Valés-Gómez M. NKG2D-ligands: putting everything under the same umbrella can be misleading. HLA. 2018;91(6):489-500.

63. Bryceson YT, March ME, Ljunggren HG, Long EO. Synergy among receptors on resting NK cells for the activation of natural cytotoxicity and cytokine secretion. Blood. 2006;107(1):159-66.

64. Bruhns P, Iannascoli B, England P, Mancardi DA, Fernandez N, Jorieux S, et al. Specificity and affinity of human Fcgamma receptors and their polymorphic variants for human IgG subclasses. Blood. 2009;113(16):3716-25.

65. Watzl C, Long EO. Signal transduction during activation and inhibition of natural killer cells. Curr Protoc Immunol. 2010;11(9B).

66. Bhat R, Watzl C. Serial killing of tumor cells by human natural killer cells—enhancement by therapeutic antibodies. PLoS One. 2007;2(3):e326.

67. Srpan K, Ambrose A, Karampatzakis A, Saeed M, Cartwright ANR, Guldevall K, et al. Shedding of CD16 disassembles the NK cell immune synapse and boosts serial engagement of target cells. J Cell Biol. 2018;217(9):3267-83.

68. Koene HR, Kleijer M, Algra J, Roos D, von dem Borne AE, de Haas M. Fc gammaRIIIa-158V/F polymorphism influences the binding of IgG by natural killer cell Fc gammaRIIIa, independently of the Fc gammaRIIIa-48L/R/H phenotype. Blood. 1997;90(3):1109-14.

69. Shibuya A, Shibuya K. DNAM-1 versus TIGIT: competitive roles in tumor immunity and inflammatory responses. Int Immunol. 2021;33(12):687-92.

70. Latchman Y, McKay PF, Reiser H. Identification of the 2B4 molecule as a counter-receptor for CD48. J Immunol. 1998;161(11):5809-12.

71. Manser AR, Uhrberg M. Age-related changes in natural killer cell repertoires: impact on NK cell function and immune surveillance. Cancer Immunol Immunother. 2016;65(4):417-26.

72. Gumá M, Angulo A, Vilches C, Gómez-Lozano N, Malats N, López-Botet M. Imprint of human cytomegalovirus infection on the NK cell receptor repertoire. Blood. 2004;104(12):3664-71

73. Björkström NK, Riese P, Heuts F, Andersson S, Fauriat C, Ivarsson MA, et al. Expression patterns of NKG2A, KIR, and CD57 define a process of CD56dim NK-cell differentiation uncoupled from NK-cell education. Blood. 2010;116(19):3853-64.

74. Parham P, Moffett A. Variable NK cell receptors and their MHC class I ligands in immunity, reproduction and human evolution. Nat Rev Immunol. 2013;13(2):133-44.

75. Ong E, Yeh JC, Ding Y, Hindsgaul O, Pedersen LC, Negishi M, et al. Structure and function of HNK-1 sulfotransferase. Identification of donor and acceptor binding sites by site-directed mutagenesis. J Biol Chem. 1999;274(36):25608-12.

76. Lopez-Vergès S, Milush JM, Pandey S, York VA, Arakawa-Hoyt J, Pircher H, et al. CD57 defines a functionally distinct population of mature NK cells in the human CD56dimCD16+ NK-cell subset. Blood. 2010;116(19):3865-74.

77. Moretta L. Dissecting CD56dim human NK cells. Blood. 2010;116(19):3689-91.

78. Muntasell A, Vilches C, Angulo A, López-Botet M. Adaptive reconfiguration of the human NK-cell compartment in response to cytomegalovirus: a different perspective of the host-pathogen interaction. Eur J Immunol. 2013;43(5):1133-41.

79. López-Botet M, Muntasell A, Vilches C. The CD94/NKG2C+ NK-cell subset on the edge of innate and adaptive immunity to human cytomegalovirus infection. Semin Immunol. 2014;26(2):145-51.

80. Wu Z, Sinzger C, Frascaroli G, Reichel J, Bayer C, Wang L, et al. Human cytomegalovirus-induced NKG2Chigh CD57high natural killer cells are effectors dependent on humoral antiviral immunity. J Virol. 2013;87(13):7717-25.

81. Costa-Garcia M, Vera A, Moraru M, Vilches C, López-Botet M, Muntasell A. Antibody-mediated response of NKG2Cbright NK cells against human cytomegalovirus. J Immunol. 2015;194(6):2715-24.

82. Gotthardt D, Trifinopoulos J, Sexl V, Putz EM. JAK/STAT cytokine signaling at the crossroad of NK cell development and maturation. Front Immunol. 2019;10:2590.

83. Waldmann TA. The shared and contrasting roles of IL2 and IL15 in the life and death of normal and neoplastic lymphocytes: implications for cancer therapy. Cancer Immunol Res. 2015;3(3):219-27

84. Wagner JA, Berrien-Elliott MM, Rosario M, Leong JW, Jewell BA, Schappe T, et al. Cytokine-induced memory-like differentiation enhances unlicensed natural killer cell

antileukemia and FcγRIIIa-triggered responses. Biol Blood Marrow Transplant. 2017;23(3):398-404.

85. Müller L, Aigner P, Stoiber D. Type I interferons and natural killer cell regulation in cancer. Front Immunol. 2017;8:304.

86. Skak K, Frederiksen KS, Lundsgaard D. Interleukin-21 activates human natural killer cells and modulates their surface receptor expression. Immunology. 2008;123(4):575-83.

87. Konjević GM, Vuletić AM, Mirjačić Martinović KM, Larsen AK, Jurišić VB. The role of cytokines in the regulation of NK cells in the tumor environment. Cytokine. 2019;117:30-40.

88. Batlle E, Massagué J. Transforming growth factor-β signaling in immunity and cancer. Immunity. 2019;50(4):924-40.

89. Constantinides MG, McDonald BD, Verhoef PA, Bendelac A. A committed precursor to innate lymphoid cells. Nature. 2014;508(7496):397-401.

90. Zhang J, Marotel M, Fauteux-Daniel S, Mathieu AL, Viel S, Marçais A, et al. T-bet and Eomes govern differentiation and function of mouse and human NK cells and ILC1. Eur J Immunol. 2018;48(5):738-50.

91. Zeng B, Shi S, Ashworth G, Dong C, Liu J, Xing F. ILC3 function as a double-edged sword in inflammatory bowel diseases. Cell Death Dis. 2019;10(4):315.

92. Geremia A, Arancibia-Cárcamo CV. Innate lymphoid cells in intestinal inflammation. Front Immunol. 2017;8:1296.

93. Koprivica I, Stanisavljević S, Mićanović D, Jevtić B, Stojanović I, Miljković Đ. ILC3: a case of conflicted identity. Front Immunol. 2023;14:1271699.

94. Cella M, Otero K, Colonna M. Expansion of human NK-22 cells with IL-7, IL-2, and IL-1β reveals intrinsic functional plasticity. Proc Natl Acad Sci U S A. 2010;107(24):10961-6.

95. Bal SM, Golebski K, Spits H. Plasticity of innate lymphoid cell subsets. Nat Rev Immunol. 2020;20(9):552-65.

96. Cortez VS, Ulland TK, Cervantes-Barragan L, Bando JK, Robinette ML, Wang Q, et al. SMAD4 impedes the conversion of NK cells into ILC1-like cells by curtailing non-canonical TGF-β signaling. Nat Immunol. 2017;18(9):995-1003

97. Raykova A, Carrega P, Lehmann FM, Ivanek R, Landtwing V, Quast I, et al. Interleukins 12 and 15 induce cytotoxicity and early NK-cell differentiation in type 3 innate lymphoid cells. Blood Adv. 2017;1(27):2679-91.

98. Konjević GM, Vuletić AM, Mirjačić Martinović KM, Larsen AK, Jurišić VB. The role of cytokines in the regulation of NK cells in the tumor environment. Cytokine. 2019;117:30-40.

99. Masmoudi D, Villalba M, Alix-Panabières C. Natural killer cells: the immune frontline against circulating tumor cells. J Exp Clin Cancer Res. 2025;44(1):118.

100. Sivori S, Della Chiesa M, Carlomagno S, Quatrini L, Munari E, Vacca P, et al. Inhibitory receptors and checkpoints in human NK cells, implications for the immunotherapy of cancer. Front Immunol. 2020;11:2156.

101. Holt D, Ma X, Kundu N, Fulton A. Prostaglandin E2 (PGE2) suppresses natural killer cell function primarily through the PGE2 receptor EP4. Cancer Immunol Immunother. 2011;60(11):1577-86.

102. Tauriello DVF, Palomo-Ponce S, Stork D, Berenguer-Llergo A, Badia-Ramentol J, Iglesias M, et al. TGFβ drives immune evasion in genetically reconstituted colon cancer metastasis. Nature. 2018;554(7693):538-43.

103. Jia H, Yang H, Xiong H, Luo KQ. NK cell exhaustion in the tumor microenvironment. Front Immunol. 2023;14:1303605.

104. Liu X, Song J, Zhang H, Liu X, Zuo F, Zhao Y, et al. Immune checkpoint HLA-E:CD94-NKG2A mediates evasion of circulating tumor cells from NK cell surveillance. Cancer Cell. 2023;41(2):272-87.e9.

105. Huntington ND, Cursons J, Rautela J. The cancer-natural killer cell immunity cycle. Nat Rev Cancer. 2020;20(8):437-54.

106. Groh V, Wu J, Yee C, Spies T. Tumour-derived soluble MIC ligands impair expression of NKG2D and T-cell activation. Nature. 2002;419(6908):734-8.

107. Schlecker E, Fiegler N, Arnold A, Altevogt P, Rose-John S, Moldenhauer G, et al. Metalloprotease-mediated tumor cell shedding of B7-H6, the ligand of the natural killer cell-activating receptor NKp30. Cancer Res. 2014;74(13):3429-40.

108. Cózar B, Greppi M, Carpentier S, Narni-Mancinelli E, Chiossone L, Vivier E. Tumor-infiltrating natural killer cells. Cancer Discov. 2021;11(1):34-44

109. Böttcher JP, Bonavita E, Chakravarty P, Blees H, Cabeza-Cabrerizo M, Sammicheli S, et al. NK cells stimulate recruitment of cDC1 into the tumor microenvironment promoting cancer immune control. Cell. 2018;172(5):1022-37.e14.

110. Barry KC, Hsu J, Broz ML, Cueto FJ, Binnewies M, Combes AJ, et al. A natural killer-dendritic cell axis defines checkpoint therapy-responsive tumor microenvironments. Nat Med. 2018;24(8):1178-91.

111. Pasero C, Gravis G, Granjeaud S, Guerin M, Thomassin-Piana J, Rocchi P, et al. Highly effective NK cells are associated with good prognosis in patients with metastatic prostate cancer. Oncotarget. 2015;6(16):14360-73.

112. Muntasell A, Rojo F, Servitja S, Rubio-Perez C, Cabo M, Tamborero D, et al. NK cell infiltrates and HLA class I expression in primary HER2+ breast cancer predict and uncouple pathological response and disease-free survival. Clin Cancer Res. 2019;25(5):1535-45.

113. Nersesian S, Schwartz SL, Grantham SR, MacLean LK, Lee SN, Pugh-Toole M, et al. NK cell infiltration is associated with improved overall survival in solid cancers: a systematic review and meta-analysis. Transl Oncol. 2021;14(1):100930.

114. Wendel M, Galani IE, Suri-Payer E, Cerwenka A. Natural killer cell accumulation in tumors is dependent on IFN-gamma and CXCR3 ligands. Cancer Res. 2008;68(20):8437-45.

115. Dangaj D, Bruand M, Grimm AJ, Ronet C, Barras D, Duttagupta PA, et al. Cooperation between constitutive and inducible chemokines enables T cell engraftment and immune attack in solid tumors. Cancer Cell. 2019;35(6):885-900.e10.

116. Chow MT, Ozga AJ, Servis RL, Frederick DT, Lo JA, Fisher DE, et al. Intratumoral activity of the CXCR3 chemokine system is required for the efficacy of anti-PD-1 therapy. Immunity. 2019;50(6):1498-512.e5.

117. Dadi S, Chhangawala S, Whitlock BM, Franklin RA, Luo CT, Oh SA, et al. Cancer immunosurveillance by tissue-resident innate lymphoid cells and innate-like T cells. Cell. 2016;164(3):365-77.

118. Kim J, Kim W, Moon UJ, Kim HJ, Choi HJ, Sin JI, et al. Intratumorally establishing type 2 innate lymphoid cells blocks tumor growth. J Immunol. 2016;196(5):2410-23.

119. Chan IH, Jain R, Tessmer MS, Gorman D, Mangadu R, Sathe M, et al. Interleukin-23 is sufficient to induce rapid de novo gut tumorigenesis, independent of carcinogens,

through activation of innate lymphoid cells. Mucosal Immunol. 2014;7(4):842-56

120. Bruchard M, Geindreau M, Perrichet A, Truntzer C, Ballot E, Boidot R, et al. Recruitment and activation of type 3 innate lymphoid cells promote antitumor immune responses. Nat Immunol. 2022;23(2):262-74.

121. Gao Y, Souza-Fonseca-Guimaraes F, Bald T, Ng SS, Young A, Ngiow SF, et al. Tumor immunoevasion by the conversion of effector NK cells into type 1 innate lymphoid cells. Nat Immunol. 2017;18(9):1004-15.

122. Schuijs MJ, Png S, Richard AC, Tsyben A, Hamm G, Stockis J, et al. ILC2-driven innate immune checkpoint mechanism antagonizes NK cell antimetastatic function in the lung. Nat Immunol. 2020;21(9):998-1009.

123. Xuan X, Zhou J, Tian Z, Lin Y, Song J, Ruan Z, et al. ILC3 cells promote the proliferation and invasion of pancreatic cancer cells through IL-22/AKT signaling. Clin Transl Oncol. 2020;22(4):563-75.

124. Bray F, Laversanne M, Sung H, Ferlay J, Siegel RL, Soerjomataram I, et al. Global cancer statistics 2022: GLOBOCAN estimates of incidence and mortality worldwide for 36 cancers in 185 countries. CA Cancer J Clin. 2024;74(3):229-63.

125. Bustreo S, Osella-Abate S, Cassoni P, Donadio M, Airoldi M, Pedani F, et al. Optimal Ki67 cut-off for luminal breast cancer prognostic evaluation: a large case series study with a long-term follow-up. Breast Cancer Res Treat. 2016;157(2):363-71.

126. Li J, Chen Z, Su K, Zeng J. Clinicopathological classification and traditional prognostic indicators of breast cancer. Int J Clin Exp Pathol. 2015;8(7):8500-5.

127. Slamon DJ, Clark GM, Wong SG, Levin WJ, Ullrich A, McGuire WL. Human breast cancer: correlation of relapse and survival with amplification of the HER-2/neu oncogene. Science. 1987;235(4785):177-82.

128. Moasser MM. The oncogene HER2: its signaling and transforming functions and its role in human cancer pathogenesis. Oncogene. 2007;26(45):6469-87.

129. Loibl S, Gianni L. HER2-positive breast cancer. Lancet. 2017;389(10087):2415-29.

130. Loibl S, André F, Bachelot T, Barrios CH, Bergh J, Burstein HJ, et al. Early breast cancer: ESMO Clinical Practice Guideline for diagnosis, treatment and follow-up. Ann Oncol. 2024;35(2):159-82

131. Nami B, Maadi H, Wang Z. Mechanisms underlying the action and synergism of

trastuzumab and pertuzumab in targeting HER2-positive breast cancer. Cancers (Basel). 2018;10(10):342.

132. Cortazar P, Zhang L, Untch M, Mehta K, Costantino JP, Wolmark N, et al. Pathological complete response and long-term clinical benefit in breast cancer: the CTNeoBC pooled analysis. Lancet. 2014;384(9938):164-72.

133. Curigliano G, Burstein HJ, Gnant M, Loibl S, Cameron D, Regan MM, et al. Understanding breast cancer complexity to improve patient outcomes: The St Gallen International Consensus Conference for the Primary Therapy of Individuals with Early Breast Cancer 2023. Ann Oncol. 2023;34(11):970-86.

134. Gennari A, André F, Barrios CH, Cortés J, de Azambuja E, DeMichele A, et al. ESMO Clinical Practice Guideline for the diagnosis, staging and treatment of patients with metastatic breast cancer. Ann Oncol. 2021;32(12):1475-95.

135. Jacobs AT, Martinez Castaneda-Cruz D, Rose MM, Connelly L. Targeted therapy for breast cancer: An overview of drug classes and outcomes. Biochem Pharmacol. 2022;204:115209.

136. Hurvitz SA, Hegg R, Chung WP, Im SA, Jacot W, Ganju V, et al. Trastuzumab deruxtecan versus trastuzumab emtansine in patients with HER2-positive metastatic breast cancer: updated results from DESTINY-Breast03, a randomised, open-label, phase 3 trial. Lancet. 2023;401(10371):105-17.

137. Zhu K, Yang X, Tai H, Zhong X, Luo T, Zheng H. HER2-targeted therapies in cancer: a systematic review. Biomark Res. 2024;12(1):16.

138. O'Shaughnessy J, Gradishar W, O'Regan R, Gadi V. Risk of recurrence in patients with HER2+ early-stage breast cancer: literature analysis of patient and disease characteristics. Clin Breast Cancer. 2023;23(4):350-62.

139. Mao Y, Qu Q, Chen X, Huang O, Wu J, Shen K. The prognostic value of tumor-infiltrating lymphocytes in breast cancer: a systematic review and meta-analysis. PLoS One. 2016;11(4):e0152500.

140. Ogiya R, Niikura N, Kumaki N, Bianchini G, Kitano S, Iwamoto T, et al. Comparison of tumor-infiltrating lymphocytes between primary and metastatic tumors in breast cancer patients. Cancer Sci. 2016;107(12):1730-5.

141. Szekely B, Bossuyt V, Li X, Wali VB, Patwardhan GA, Frederick C, et al. Immunological differences between primary and metastatic breast cancer. Ann Oncol.

2018;29(11):2232-9

142. Bouzidi L, Triki H, Charfi S, Kridis WB, Derbel M, Ayadi L, et al. Prognostic value of natural killer cells besides tumor-infiltrating lymphocytes in breast cancer tissues. Clin Breast Cancer. 2021;21(6):e738-e47.

143. Muntasell A, Cabo M, Servitja S, Tusquets I, Martínez-García M, Rovira A, et al. Interplay between natural killer cells and anti-HER2 antibodies: perspectives for breast cancer immunotherapy. Front Immunol. 2017;8:1544.

144. Musolino A, Naldi N, Dieci MV, Zanoni D, Rimanti A, Boggiani D, et al. Immunoglobulin G fragment C receptor polymorphisms and efficacy of preoperative chemotherapy plus trastuzumab and lapatinib in HER2-positive breast cancer. Pharmacogenomics J. 2016;16(5):472-7.

145. Park S, Jiang Z, Mortenson ED, Deng L, Radkevich-Brown O, Yang X, et al. The therapeutic effect of anti-HER2/neu antibody depends on both innate and adaptive immunity. Cancer Cell. 2010;18(2):160-70.

146. Albanell J, Codony J, Rovira A, Mellado B, Gascón P. Mechanism of action of anti-HER2 monoclonal antibodies: scientific update on trastuzumab and 2C4. Adv Exp Med Biol. 2003;532:253-68.

147. Beano A, Signorino E, Evangelista A, Brusa D, Mistrangelo M, Polimeni MA, et al. Correlation between NK function and response to trastuzumab in metastatic breast cancer patients. J Transl Med. 2008;6:25.

148. Muntasell A, Servitja S, Cabo M, Bermejo B, Pérez-Buira S, Rojo F, et al. High numbers of circulating CD57+ NK cells associate with resistance to HER2-specific therapeutic antibodies in HER2+ primary breast cancer. Cancer Immunol Res. 2019;7(8):1280-92.

149. Musolino A, Gradishar WJ, Rugo HS, Nordstrom JL, Rock EP, Arnaldez F, et al. Role of Fcγ receptors in HER2-targeted breast cancer therapy. J Immunother Cancer. 2022;10(1):e003171.

150. Gavin PG, Song N, Kim SR, Lipchik C, Johnson NL, Bandos H, et al. Association of polymorphisms in FCGR2A and FCGR3A with degree of trastuzumab benefit in the adjuvant treatment of ERBB2/HER2-positive breast cancer: analysis of the NSABP B-31 trial. JAMA Oncol. 2017;3(3):335-41

151. Norton N, Olson RM, Pegram M, Tenner K, Ballman KV, Clynes R, et al.

Association studies of Fcγ receptor polymorphisms with outcome in HER2+ breast cancer patients treated with trastuzumab in NCCTG (Alliance) Trial N9831. Cancer Immunol Res. 2014;2(10):962-9.

152. Royce M, Osgood CL, Amatya AK, Fiero MH, Chang CJG, Ricks TK, et al. FDA approval summary: margetuximab plus chemotherapy for advanced or metastatic HER2-positive breast cancer. Clin Cancer Res. 2022;28(8):1487-92.

153. Wang L, Wang Y, Li Y, Zhou L, Du J, Wang J, et al. Resistance mechanisms and prospects of trastuzumab. Front Oncol. 2024;14:1389390.

154. Zheng G, Guo Z, Li W, Xi W, Zuo B, Zhang R, et al. Interaction between HLA-G and NK cell receptor KIR2DL4 orchestrates HER2-positive breast cancer resistance to trastuzumab. Signal Transduct Target Ther. 2021;6(1):236.

155. Collins DM, Madden SF, Gaynor N, AlSultan D, Le Gal M, Eustace AJ, et al. Effects of HER family-targeting tyrosine kinase inhibitors on antibody-dependent cell-mediated cytotoxicity in HER2-expressing breast cancer. Clin Cancer Res. 2021;27(3):807-18.

156. Berrien-Elliott MM, Jacobs MT, Fehniger TA. Allogeneic natural killer cell therapy. Blood. 2023;141(8):856-68.

157. Kamiya T, Seow SV, Wong D, Robinson M, Campana D. Blocking expression of inhibitory receptor NKG2A overcomes tumor resistance to NK cells. J Clin Invest. 2019;129(5):2094-106.

158. Innate Pharma. Study of Monalizumab and Cetuximab in Patients With Recurrent or Metastatic Squamous Cell Carcinoma of the Head and Neck. ClinicalTrials.gov Identifier: NCT02643550. 2015 Dec 16. Available from: https://clinicaltrials.gov/study/NCT02643550

159. André P, Denis C, Soulas C, Bourbon-Caillet C, Lopez J, Arnoux T, et al. Anti-NKG2A mAb is a checkpoint inhibitor that promotes anti-tumor immunity by unleashing both T and NK cells. Cell. 2018;175(7):1731-43.e13.

160. Fayette J, Licitra L, Harrington K, Haddad R, Siu LL, Liu YC, et al. INTERLINK-1: a phase III, randomized, placebo-controlled study of monalizumab plus cetuximab in recurrent/metastatic head and neck squamous cell carcinoma. Clin Cancer Res. 2025;31(13):2617-27

161. Geurts VCM, Voorwerk L, Balduzzi S, Salgado R, Van de Vijver K, van Dongen MGJ, et al. Unleashing NK- and CD8 T cells by combining monalizumab and trastuzumab

for metastatic HER2-positive breast cancer: Results of the MIMOSA trial. Breast. 2023;70:76-81.

162. Blake SJ, Stannard K, Liu J, Allen S, Yong MC, Mittal D, et al. Suppression of metastases using a new lymphocyte checkpoint target for cancer immunotherapy. Cancer Discov. 2016;6(4):446-59.

163. Xu F, Sunderland A, Zhou Y, Schulick RD, Edil BH, Zhu Y. Blockade of CD112R and TIGIT signaling sensitizes human natural killer cell functions. Cancer Immunol Immunother. 2017;66(10):1367-75.

164. Cabo M, Santana-Hernández S, Costa-Garcia M, Rea A, Lozano-Rodríguez R, Ataya M, et al. CD137 costimulation counteracts TGFβ inhibition of NK-cell antitumor function. Cancer Immunol Res. 2021;9(12):1476-90.

165. Sledge GW Jr. 4-1BB Agonist Monoclonal Antibody PF-05082566 With Trastuzumab Emtansine or Trastuzumab in Treating Patients With Advanced HER2-Positive Breast Cancer. ClinicalTrials.gov Identifier: NCT03364348. Stanford University; 2022 Oct 19. Available from: https://clinicaltrials.gov/study/NCT03364348

166. Nikkhoi SK, Li G, Eleya S, Yang G, Vandavasi VG, Hatefi A. Bispecific killer cell engager with high affinity and specificity toward CD16a on NK cells for cancer immunotherapy. Front Immunol. 2022;13:1039969.

167. Zhu A, Bai Y, Nan Y, Ju D. Natural killer cell engagers: from bi-specific to tri-specific and tetra-specific engagers for enhanced cancer immunotherapy. Clin Transl Med. 2024;14(11):e70046.

168. Munster P, Dragonfly Therapeutics. Study of DF1001 in Patients with Advanced Solid Tumors. ClinicalTrials.gov Identifier: NCT04143711. 2019 Nov. Available from: https://clinicaltrials.gov/study/NCT04143711

169. Simonetta F, Alvarez M, Negrin RS. Natural killer cells in graft-versus-host-disease after allogeneic hematopoietic cell transplantation. Front Immunol. 2017;8:465.

170. Ruggeri L, Capanni M, Urbani E, Perruccio K, Shlomchik WD, Tosti A, et al. Effectiveness of donor natural killer cell alloreactivity in mismatched hematopoietic transplants. Science. 2002;295(5562):2097-100.

171. Yi M, Li T, Niu M, Mei Q, Zhao B, Chu Q, et al. Exploiting innate immunity for cancer immunotherapy. Mol Cancer. 2023;22(1):187

172. Davis ZB, Felices M, Verneris MR, Miller JS. Natural killer cell adoptive transfer therapy: exploiting the first line of defense against cancer. Cancer J. 2015;21(6):486-91.

173. Ran GH, Lin YQ, Tian L, Zhang T, Yan DM, Yu JH, et al. Natural killer cell homing and trafficking in tissues and tumors: from biology to application. Signal Transduct Target Ther. 2022;7(1):205.

174. Fuda Cancer Hospital. Combination of Trastuzumab and Natural Killer (NK) Immunotherapy in Recurrent Breast Cancer. ClinicalTrials.gov Identifier: NCT02843126. Available from: https://clinicaltrials.gov/study/NCT02843126

175. Garralda E, Melero I. A Study of Allogenic Natural Killer Cells in Combination With Trastuzumab and Pertuzumab in Adult Patients With Refractory Metastatic HER2 Positive Breast Cancer. NK-ACT-BC_2020. ClinicalTrials.gov Identifier: NCT05385705. 2022 May 16. Available from: https://clinicaltrials.gov/study/NCT05385705

176. Graef T, Acepodia. ACE1702 in Subjects With Advanced or Metastatic HER2-Expressing Solid Tumors. ClinicalTrials.gov Identifier: NCT04319757. 2020. Available from: https://clinicaltrials.gov/study/NCT04319757

177. Yang K, Zhao Y, Sun G, Zhang X, Cao J, Shao M, et al. Clinical application and prospect of immune checkpoint inhibitors for CAR-NK cell in tumor immunotherapy. Front Immunol. 2022;13:1081546.

178. Portillo AL, Hogg R, Poznanski SM, Rojas EA, Cashell NJ, Hammill JA, et al. Expanded human NK cells armed with CAR uncouple potent anti-tumor activity from off-tumor toxicity against solid tumors. iScience. 2021;24(6):102619.

179. Xia W, Chen J, Hou W, Chen J, Xiong Y, Li H, et al. Engineering a HER2-CAR-NK cell secreting soluble programmed cell death protein with superior antitumor efficacy. Int J Mol Sci. 2023;24(7):6843.

180. Röder J, Alekseeva T, Kiefer A, Kühnel I, Prüfer M, Zhang C, et al. ErbB2/HER2-targeted CAR-NK cells eliminate breast cancer cells in an organoid model that recapitulates tumor progression. Mol Ther. 2025;S1525-0016(25)00312-0.

181. Román Alonso M, Grinyó-Escuer A, Duro-Sánchez S, Rius-Ruiz I, Bort-Brusca M, Escorihuela M, et al. Generation of chimeric antigen receptor T cells targeting p95HER2 in solid tumors. Nat Commun. 2024;15(1):9589.

182. Gergely B, Vereb MA, Rebenku I, Vereb G, Szöőr Á. Targeting HER2-positive solid tumors with CAR NK cells: CD44 expression is a critical modulator of HER2-specific CAR

NK cell efficacy. Cancers (Basel). 2025;17(5):731

183. Wolff AC, Hammond ME, Hicks DG, Dowsett M, McShane LM, Allison KH, et al.; College of American Pathologists. Recommendations for human epidermal growth factor receptor 2 testing in breast cancer: ASCO/CAP clinical practice guideline update. J Clin Oncol. 2013;31(31):3997-4013.

184. Ogston KN, Miller ID, Payne S, Hutcheon AW, Sarkar TK, Smith I, et al. A new histological grading system to assess response of breast cancers to primary chemotherapy: prognostic significance and survival. Breast. 2003;12(5):320-7.

185. Cursons J, Souza-Fonseca-Guimaraes F, Foroutan M, Anderson A, Hollande F, Hediyeh-Zadeh S, et al. A gene signature predicting natural killer cell infiltration and improved survival in melanoma patients. Cancer Immunol Res. 2019;7(7):1162-74.

186. Amir el AD, Davis KL, Tadmor MD, Simonds EF, Levine JH, Bendall SC, et al. viSNE enables visualization of high dimensional single-cell data and reveals phenotypic heterogeneity of leukemia. Nat Biotechnol. 2013;31(6):545-52.

187. Koues OI, Collins PL, Cella M, Robinette ML, Porter SI, Pyfrom SC, et al. Distinct gene regulatory pathways for human innate versus adaptive lymphoid cells. Cell. 2016;165(5):1134-46.

188. Vilches C, Castaño J, Muñoz P, Peñalver J. Simple genotyping of functional polymorphisms of the human immunoglobulin G receptors CD16A and CD32A: a reference cell panel. Tissue Antigens. 2008;71(3):242-6.

189. Vilches C, Castaño J, Muñoz P, Peñalver J. Corrigendum. Tissue Antigens. 2008;72(6):605.

190. Gianni L, Pienkowski T, Im YH, Roman L, Tseng LM, Liu MC, et al. Efficacy and safety of neoadjuvant pertuzumab and trastuzumab in women with locally advanced, inflammatory, or early HER2-positive breast cancer (NeoSphere): a randomized multicenter, open-label, phase 2 trial. Lancet Oncol. 2012;13(1):25-32.

191. Ali TH, Pisanti S, Ciaglia E, Mortarini R, Anichini A, Garofalo C, et al. Enrichment of CD56(dim)KIR+CD57+ highly cytotoxic NK cells in tumour-infiltrated lymph nodes of melanoma patients. Nat Commun. 2014;5:5639.

192. Toffoli EC, van Vliet AA, Verheul HWM, van der Vliet HJ, Tuynman J, Spanholtz J, et al. Allogeneic NK cells induce monocyte-to-dendritic cell conversion, control tumor growth, and trigger a pro-inflammatory shift in patient-derived cultures of primary and

metastatic colorectal cancer. J Immunother Cancer. 2023;11(12):e007554

193. Wiedemann GM, Santosa EK, Grassmann S, Sheppard S, Le Luduec JB, Adams NM, et al. Deconvoluting global cytokine signaling networks in natural killer cells. Nat Immunol. 2021;22(5):627-38.

194. Tassi I, Cella M, Presti R, Colucci A, Gilfillan S, Littman DR, et al. NK cell-activating receptors require PKC-theta for sustained signaling, transcriptional activation, and IFN-gamma secretion. Blood. 2008;112(10):4109-16.

195. Van Gelder RD, Gokhale NS, Genoyer E, Omelia DS, Anderson SK, Young HA, et al. Interleukin-2-mediated NF-κB-dependent mRNA splicing modulates interferon gamma protein production. EMBO Rep. 2024;26(1):16-35.

196. Luetke-Eversloh M, Cicek BB, Siracusa F, Thom JT, Hamann A, Frischbutter S, et al. NK cells gain higher IFN-γ competence during terminal differentiation. Eur J Immunol. 2014;44(7):2074-84.

197. Chung DC, Shakfa N, Vakharia J, Warner K, Jacquelot N, Sayad A, et al. CD103+CD56+ ILCs are associated with an altered CD8+ T-cell profile within the tumor microenvironment. Cancer Immunol Res. 2025;13(4):527-46.

198. Farber JM. Mig and IP-10: CXC chemokines that target lymphocytes. J Leukoc Biol. 1997;61(3):246-57.

199. Tokunaga R, Zhang W, Naseem M, Puccini A, Berger MD, Soni S, et al. CXCL9, CXCL10, CXCL11/CXCR3 axis for immune activation–a target for novel cancer therapy. Cancer Treat Rev. 2018;63:40-7.

200. Qian L, Yu S, Yin C, Zhu B, Chen Z, Meng Z, et al. Plasma IFN-γ-inducible chemokines CXCL9 and CXCL10 correlate with survival and chemotherapeutic efficacy in advanced pancreatic ductal adenocarcinoma. Pancreatology. 2019;19(2):340-5.

201. Liang YK, Deng ZK, Chen MT, Qiu SQ, Xiao YS, Qi YZ, et al. CXCL9 is a potential biomarker of immune infiltration associated with favorable prognosis in ER-negative breast cancer. Front Oncol. 2021;11:710286.

202. Szekely B, Bossuyt V, Li X, Wali VB, Patwardhan GA, Frederick C, et al. Immunological differences between primary and metastatic breast cancer. Ann Oncol. 2018;29(11):2232-9.

203. Wightman SC, Uppal A, Pitroda SP, Ganai S, Burnette B, Stack M, et al. Oncogenic

CXCL10 signalling drives metastasis development and poor clinical outcome. Br J Cancer. 2015;113(2):327-35

204. Clark AM, Heusey HL, Griffith LG, Lauffenburger DA, Wells A. IP-10 (CXCL10) can trigger emergence of dormant breast cancer cells in a metastatic liver microenvironment. Front Oncol. 2021;11:676135.

205. Kim M, Choi HY, Woo JW, Chung YR, Park SY. Role of CXCL10 in the progression of in situ to invasive carcinoma of the breast. Sci Rep. 2021;11(1):18007.

206. Zazo S, González-Alonso P, Martín-Aparicio E, Chamizo C, Luque M, Sanz-Álvarez M, et al. Autocrine CCL5 effect mediates trastuzumab resistance by ERK pathway activation in HER2-positive breast cancer. Mol Cancer Ther. 2020;19(8):1696-707.

207. Litchfield K, Reading JL, Puttick C, Thakkar K, Abbosh C, Bentham R, et al. Meta-analysis of tumor- and T cell-intrinsic mechanisms of sensitization to checkpoint inhibition. Cell. 2021;184(3):596-614.e14.

208. Pascual-García M, Bonfill-Teixidor E, Planas-Rigol E, Rubio-Perez C, Iurlaro R, Arias A, et al. LIF regulates CXCL9 in tumor-associated macrophages and prevents CD8+ T cell tumor-infiltration impairing anti-PD1 therapy. Nat Commun. 2019;10(1):2416.

209. Zhang L, Liu M, Yang S, Wang J, Feng X, Han Z. Natural killer cells: of-the-shelf cytotherapy for cancer immunosurveillance. Am J Cancer Res. 2021;11(4):1770–91.

210. Serru V, Le Naour F, Billard M, Azorsa DO, Lanza F, Boucheix C, et al. Selective tetraspan-integrin complexes (CD81/alpha4beta1, CD151/alpha3beta1, CD151/alpha6beta1) under conditions disrupting tetraspan interactions. Biochem J. 1999;340(Pt 1):103-11.

211. Gao Y, Souza-Fonseca-Guimaraes F, Bald T, Ng SS, Young A, Ngiow SF, et al. Tumor immunoevasion by the conversion of effector NK cells into type 1 innate lymphoid cells. Nat Immunol. 2017;18(9):1004-15.

212. Perez EA, Romond EH, Suman VJ, Jeong JH, Sledge G, Geyer CE Jr, et al. Trastuzumab plus adjuvant chemotherapy for human epidermal growth factor receptor 2-positive breast cancer: planned joint analysis of overall survival from NSABP B-31 and NCCTG N9831. J Clin Oncol. 2014;32(33):3744-52.

213. Mackay LK, Wynne-Jones E, Freestone D, Pellicci DG, Mielke LA, Newman DM, et al. T-box transcription factors combine with the cytokines TGF-β and IL-15 to control tissue-resident memory T cell fate. Immunity. 2015;43(6):1101-11

214. Fiordi B, Salvestrini V, Gugliotta G, Castagnetti F, Curti A, Speiser DE, et al. IL-18 and VEGF-A trigger type 2 innate lymphoid cell accumulation and pro-tumoral function in chronic myeloid leukemia. Haematologica. 2023;108(9):2396-409.

215. Buonocore S, Ahern PP, Uhlig HH, Ivanov II, Littman DR, Maloy KJ, et al. Innate lymphoid cells drive interleukin-23-dependent innate intestinal pathology. Nature. 2010;464(7293):1371-5.

216. Sielska M, Przanowski P, Pasierbińska M, Wojnicki K, Poleszak K, Wojtas B, et al. Tumour-derived CSF2/granulocyte macrophage colony stimulating factor controls myeloid cell accumulation and progression of gliomas. Br J Cancer. 2020;123(3):438-48.

217. Kiss M, Vande Walle L, Saavedra PHV, Lebegge E, Van Damme H, Murgaski A, et al. IL1β promotes immune suppression in the tumor microenvironment independent of the inflammasome and Gasdermin D. Cancer Immunol Res. 2021;9(3):309-23.

218. Curiel TJ, Coukos G, Zou L, Alvarez X, Cheng P, Mottram P, et al. Specific recruitment of regulatory T cells in ovarian carcinoma fosters immune privilege and predicts reduced survival. Nat Med. 2004;10(9):942-9.

219. Liu Q, Li A, Tian Y, Wu JD, Liu Y, Li T, et al. The CXCL8-CXCR1/2 pathways in cancer. Cytokine Growth Factor Rev. 2016;31:61-71.

220. Qian BZ, Li J, Zhang H, Kitamura T, Zhang J, Campion LR, et al. CCL2 recruits inflammatory monocytes to facilitate breast-tumour metastasis. Nature. 2011;475(7355):222–5.

221. Braakman E, van de Winkel JG, van Krimpen BA, Jansze M, Bolhuis RL. CD16 on human gamma delta T lymphocytes: expression, function, and specificity for mouse IgG isotypes. Cell Immunol. 1992;143(1):97-107.

222. Nitta T, Nakata M, Yagita H, Okumura K. Interleukin-2 activated T cells (T-LAK) express CD16 antigen and are triggered to target cell lysis by bispecific antibody. Immunol Lett. 1991;28(1):31-7.

223. Junker F, Gordon J, Qureshi O. Fc gamma receptors and their role in antigen uptake, presentation, and T cell activation. Front Immunol. 2020;11:1393.

224. DiLillo DJ, Ravetch JV. Differential Fc-receptor engagement drives an anti-tumor vaccinal effect. Cell. 2015;161(5):1035-45

225. Heo W, Lee W, Cheun JH, Lee ES, Li S, Kim HS, et al. Triple-negative breast

cancer-derived extracellular vesicles promote a hepatic premetastatic niche via a cascade of microenvironment remodeling. Mol Cancer Res. 2023;21(7):726-40.

226. Mishra A, Suman KH, Nair N, Majeed J, Tripathi V. An updated review on the role of the CXCL8-CXCR1/2 axis in the progression and metastasis of breast cancer. Mol Biol Rep. 2021;48(9):6551-61.

227. Liu E, Marin D, Banerjee P, Macapinlac HA, Thompson P, Basar R, et al. Use of CAR-Transduced Natural Killer Cells in CD19-Positive Lymphoid Tumors. N Engl J Med. 2020;382(6):545–53.

228. Vivier E, Rebuffet L, Narni-Mancinelli E, Cornen S, Igarashi RY, Fantin VR. Natural killer cell therapies. Nature. 2024;626(8000):727-36.

229. He M, Ao X, Yang Y, Xu Y, Liu T, Ao L, et al. Construction of self-driving anti-αFR CAR-engineered NK cells based on IFN-γ and TNF-α synergistically induced high expression of CXCL10. Neoplasia. 2024;58:101065.

230. Zelenay S, van der Veen AG, Böttcher JP, Snelgrove KJ, Rogers N, Acton SE, et al. Cyclooxygenase-dependent tumor growth through evasion of immunity. Cell. 2015;162(6):1257-70.

231. Pan B, Chen Z, Zhang X, Wang Z, Yao Y, Wu X, et al. 2,5-dimethylcelecoxib alleviated NK and T-cell exhaustion in hepatocellular carcinoma via the gastrointestinal microbiota-AMPK-mTOR axis. J Immunother Cancer. 2023;11(6):e006817.

232. Kortylewski M, Xin H, Kujawski M, Lee H, Liu Y, Harris T, et al. Regulation of the IL-23 and IL-12 balance by Stat3 signaling in the tumor microenvironment. Cancer Cell. 2009;15(2):114-23.

233. Zou S, Tong Q, Liu B, Huang W, Tian Y, Fu X. Targeting STAT3 in cancer immunotherapy. Mol Cancer. 2020;19(1):145.

234. Barreira da Silva R, Laird ME, Yatim N, Fiette L, Ingersoll MA, Albert ML. Dipeptidylpeptidase 4 inhibition enhances lymphocyte trafficking, improving both naturally occurring tumor immunity and immunotherapy. Nat Immunol. 2015;16(8):850-8.

235. Nguyen KG, Vrabel MR, Mantooth SM, Hopkins JJ, Wagner ES, Gabaldon TA, et al. Localized interleukin-12 for cancer immunotherapy. Front Immunol. 2020;11:575597.

236. Genentech, Inc. Interleukin-12 and Trastuzumab in Treating Patients With HER2-Positive Breast Cancer. ClinicalTrials.gov Identifier: NCT00004074. Available from:

https://clinicaltrials.gov/study/NCT00004074

237. Zaidi MR, Merlino G. The two faces of interferon-γ in cancer. Clin Cancer Res. 2011;17(19):6118-24.

238. Zibelman M, MacFarlane AW 4th, Costello K, McGowan T, O'Neill J, Kokate R, et al. A phase 1 study of nivolumab in combination with interferon-gamma for patients with advanced solid tumors. Nat Commun. 2023;14(1):4513.

239. Rosain J, Kiykim A, Michev A, Kendir-Demirkol Y, Rinchai D, Peel JN, et al. Recombinant IFN-γ1b treatment in a patient with inherited IFN-γ deficiency. J Clin Immunol. 2024;44(3):62.

240. Harlin H, Meng Y, Peterson AC, Zha Y, Tretiakova M, Slingluff C, et al. Chemokine expression in melanoma metastases associated with CD8+ T-cell recruitment. Cancer Res. 2009;69(7):3077-85.

241. Lugassy J, Abdala-Saleh N, Jarrous G, Turky A, Saidemberg D, Ridner-Bahar G, et al. Development of DPP-4-resistant CXCL9-Fc and CXCL10-Fc chemokines for effective cancer immunotherapy. Proc Natl Acad Sci U S A. 2025;122(16):e2501791122.

242. Reedy M, Jonnalagadda S, Palle K. Case report: intra-tumoral vaccinations of quadrivalent HPV-L1 peptide vaccine with topical TLR-7 agonist following recurrence: complete resolution of HPV-HR-associated gynecologic squamous cell carcinomas in two patients. Pathol Oncol Res. 2021;27:1609922.

243. Huang A, Pressnall MM, Lu R, Huayamares SG, Griffin JD, Groer C, et al. Human intratumoral therapy: linking drug properties and tumor transport of drugs in clinical trials. J Control Release. 2020;326:203-21.

244. Jiang Z, Fu Y, Shen H. Development of intratumoral drug delivery based strategies for antitumor therapy. Drug Des Devel Ther. 2024;18:2189-202.

245. Nelson BE, Naing A, Fu S, Sheth RA, Murthy R, Piha-Paul S. Potentiating intratumoral therapy with immune checkpoint inhibitors: shifting the paradigm of multimodality therapeutics. Immuno Oncol Technol. 2024;25:101040

ABBREVIATIONS

AHR – Aryl hydrocarbon receptor

ADAM-17 – A disintegrin and metalloproteinase-17

ADC – Antibody–drug conjugate

ADCC – Antibody-dependent cellular cytotoxicity

APC – Antigen Presenting Cell

ASCO – American Society of Clinical Oncology

B2M – Beta-2-microglobulin

BC – Breast cancer

Bcl11b – B-cell lymphoma/leukemia 11B

BiKEs – Bispecific killer cell engagers

CAP – College of American Pathologists

CAR – Chimeric antigen receptor

cDC1 – Conventional dendritic cell type 1

CD – Cluster of differentiation

CDI – Invasive ductal carcinoma

CLI- Invasive lobular carcinoma

CILP – Common innate lymphoid progenitor

CLP – Common lymphoid progenitor

COX-2 – Cyclooxygenase-2

CPM – Counts per million

CRAN – Comprehensive R Archive Network

CRTH2 – Chemoattractant receptor-homologous molecule expressed on Th2 cells

Cx (CXCL9/10) – C-X-C motif chemokines

DAPI – 4′,6-diamidino-2-phenylindole

DCs – Dendritic cells

DEG – Differentially expressed genes

DF – Disease-free

DFS – Disease-free survival

DIC – Ductal carcinoma in situ

DMSO – Dimethyl sulfoxide

DN – Double negative

DNAM1 – DNAX accessory molecule-1

ELISA – Enzyme-linked immunosorbent assay

EOMES – Eomesodermin

ER – Estrogen receptor

ETS1 – ETS proto-oncogene 1

FACS – Fluorescence-Activated Cell Sorting

FasL – Fas ligand

FBS – Fetal bovine serum

FcγR – Fc gamma receptor

FFPE – Formalin-fixed paraffin-embedded

FSC – Forward scatter

GATA3 – GATA-binding protein 3

GEO2R – Gene Expression Omnibus analysis tool

GFI1 – Growth factor independent 1 transcription repressor

GM-CSF – Granulocyte-macrophage colony-stimulating factor

GP6 – Glycoprotein VI

GSEA – Gene Set Enrichment Analysis

HCMV – Human cytomegalovirus

HER – Human epidermal growth factor receptor

HLA – Human leukocyte antigen

HNSCC – Head and neck squamous cell carcinoma

HPF – High-power field

HR – Hormone receptor

HR – Hazard ratio

HSC – Hematopoietic stem cell

ID2 – Inhibitor of DNA binding 2

IHC – Immunohistochemistry

IFN – Interferon

IFNAR – Interferon-alpha/beta receptor

Ig – Immunoglobulin

IL – Interleukin

ILC – Innate lymphoid cells

IPA – Ingenuity Pathway Analysis

ITAM – Immunoreceptor Tyrosine-based Activation Motif

ITIM – Immunoreceptor tyrosine-based inhibitory motif

KIR – Killer-cell immunoglobulin-like receptor

LTi – Lymphoid tissue inducer cell

Lum – Luminal subtype

MDSC – Myeloid-derived suppressor cells

MHC – Major histocompatibility complex

MICA – MHC class I chain-related protein A

MICB – MHC class I chain-related protein B

NCAM – Neural cell adhesion molecule

NCR – Natural cytotoxicity receptor

NFIL3 – Nuclear factor, interleukin 3

NFKB – Nuclear factor kappa-light-chain-enhancer of activated B cells

NGS – Next-generation sequencing

NK – Natural killer (cell)

NKP – Natural killer precursor

NSG – NOD scid gamma (mouse strain)

OR – Odds ratio

OS – Overall survival

PBMC – Peripheral blood mononuclear cell

PCNA – Proliferating cell nuclear antigen

PCR – Polymerase chain reaction

pCR – Pathological complete response

PD-1 – Programmed cell death protein 1

PD-L1 – Programmed death-ligand 1

PLZF – Promyelocytic leukemia zinc finger protein

PR – Progesterone receptor

Pt – Pertuzumab

PVR – Poliovirus receptor

rh – Recombinant human (prefix, e.g., rhIL-2)

Ritux – Rituximab

ROR – RAR-related orphan receptor

RUNX3 – Runt-related transcription factor 3

Src – Proto-oncogene tyrosine-protein kinase Src

SSC – Side scatter

STAT – Signal transducer and activator of transcription

Syk – Spleen tyrosine kinase

TAM – Tumor-associated macrophages

T-bet – T-box expressed in T cells

T-DM1 – Trastuzumab emtansine (Kadcyla)

T-Dxd – Trastuzumab deruxtecan (Enhertu)

t-SNE – t-distributed stochastic neighbor embedding

TGFβ – Transforming growth factor beta

TIGIT – T-cell immunoreceptor with Ig and ITIM domains

TIL – Tumor-infiltrating lymphocytes

TI-NK – Tumor-infiltrating NK cells

TKI – Tyrosine kinase inhibitor

TLR – Toll-like receptor

TME – Tumor microenvironment

TNBC – Triple-negative breast cancer

TNF – Tumor necrosis factor

TNFRSF – Tumor necrosis factor receptor superfamily

TOX – Thymocyte selection-associated high mobility group box protein

T-reg – Regulatory T cells

TriKEs – Trispecific killer cell engagers

Tz – Trastuzumab

ULBP / ULRB1 – UL16 binding protein 1

viSNE – Visual Stochastic Neighbor Embedding

LIST OF PUBLICATIONS

Publications included in the tesis

1. Santana-Hernández S, Suarez-Olmos J, Servitja S, Berenguer-Molins P, Costa-Garcia M, Comerma L, et al. NK cell-triggered CCL5/IFNγ-CXCL9/10 axis underlies the clinical efficacy of neoadjuvant anti-HER2 antibodies in breast cancer. J Exp Clin Cancer Res. 2024;43(1):10.

Additional publications

1. Muntasell A, Servitja S, Cabo M, Bermejo B, Pérez-Buira S, Rojo F, et al. High numbers of circulating CD57+ NK cells associate with resistance to HER2-specific therapeutic antibodies in HER2+ primary breast cancer. Cancer Immunol Res. 2019;7(8):1280-92.

2. Cabo M, Santana-Hernández S, Costa-Garcia M, Rea A, Lozano-Rodríguez R, Ataya M, et al. CD137 costimulation counteracts TGFβ inhibition of NK-cell antitumor function. Cancer Immunol Res. 2021;9(12):1476-90.

3. Rea A, Santana-Hernández S, Villanueva J, Sanvicente-García M, Cabo M, Suarez-Olmos J, et al. Enhancing human NK cell antitumor function by knocking out SMAD4 to counteract TGFβ and activin A suppression. Nat Immunol. 2025;26(4):582-94.